

Micro Electrical Discharge Machining: Axis-symmetric component manufacture and surface integrity

A thesis submitted to the University of Wales, Cardiff
for the degree of

Doctor of Philosophy

by

Andrew Rees

Cardiff School of Engineering,
Manufacturing Engineering Centre,
University of Wales, Cardiff
United Kingdom

2011

UMI Number: U585528

All rights reserved

INFORMATION TO ALL USERS

The quality of this reproduction is dependent upon the quality of the copy submitted.

In the unlikely event that the author did not send a complete manuscript and there are missing pages, these will be noted. Also, if material had to be removed, a note will indicate the deletion.



UMI U585528

Published by ProQuest LLC 2013. Copyright in the Dissertation held by the Author.
Microform Edition © ProQuest LLC.

All rights reserved. This work is protected against
unauthorized copying under Title 17, United States Code.



ProQuest LLC
789 East Eisenhower Parkway
P.O. Box 1346
Ann Arbor, MI 48106-1346

ABSTRACT

The development of micro engineering is highly dependent on the machining processes that support it. Micro Electrical Discharge Machining (μ EDM) is one of the key enabling technologies for the fabrication of micro tools and micro components. The capabilities of this machining technology have to be studied to determine the process capabilities and constraints.

The present work investigates factors that influence the process of μ EDM and the components that can be produced by applying this technology. Chapter 2 reviews the current state of the art in this field. In addition, different aspects related to the process capabilities are discussed, especially, the factors that affect the quality of electrodes produced on-the-machine, surface roughness optimisation/prediction and the effect of material micro structure on resultant surface integrity.

In Chapter 3 factors affecting the quality of electrodes produced on the machine through the process of Wire Electro-Discharge Grinding (WEDG) are investigated. The effects that electrode material, machining strategy and machine accuracy have on the electrode re-generation are studied.

Then, in Chapter 4, the effects of process parameters on the resulting surface finish after performing WEDG are investigated in order to identify an optimum processing window. In addition, a method for predicting the resulting surface finish is proposed.

In Chapter 5 a comparative study is carried out to investigate the effects of material

microstructure refinement on the resulting surface integrity of samples machined by Micro Wire Electrical Discharge Machining (μ WEDM). In particular, the process-material interactions on the resulting micro hardness, phase content changes, Heat Affected Zone (HAZ), surface roughness, micro cracks, recast layers formation, Material Removal Rate (MRR) and element spectrum after both rough and finishing μ WEDM cuts are studied.

Finally, in Chapter 6 the main contributions to knowledge as a result of the carried out research are presented. They can be summarised as follows:

- The choice of electrode material used when applying the process of WEDG has a significant effect on achievable aspect ratio and surface roughness.
- The application of specially developed dressing strategies has a major impact on the quality of the electrode.
- Due to the inherent process errors related to machine accuracy and repeatability of the WEDG process, specialised “adaptive control” systems need to be developed and implemented to increase the process accuracy.
- Technological parameters that are optimised for conventional μ WEDM are not directly applicable for use with the WEDG process as they do not provide comparable results in respect to surface finish.
- The application of inductive learning algorithms is a simple and cost-effective method for identifying patterns in the process behaviour and thus to create models for on-the-machine prediction of the surface roughness.
- Material microstructure refinement does not only provide superior mechanical properties to workpiece materials but also leads to favourable machining

“footprints” during μ WEDM machining and a lower surface roughness.

- Surface contamination due to the alloying of the tool electrode with the workpiece material is always present regardless of material microstructure, and thus can limit the application areas of this technology.

ACKNOWLEDGMENTS

Initially I would like to express my gratitude to Cardiff University for the acceptance of my application for pursuing postgraduate education, obtained via the Manufacturing Engineering Centre, Cardiff School of Engineering.

During my time at the Manufacturing Engineering Centre it has been my privilege to work under the guidance of my supervisors Professor S.S. Dimov and Professor D.T. Pham. My enthusiasm towards my research stems from the high standard of work ethic and technical knowledge gained through my supervisors. I am deeply indebted to them for giving me the opportunity to fulfil one of my life ambitions.


Thanks also to my colleagues within the Manufacturing Engineering Centre. I would like to express my sincere appreciation to Chris, Samuel, Emmanuel, Roussi, Steffen, Hassan and Eleri for their assistance throughout my research.

My deepest gratitude goes to my wife Emily, her love and support over the years has been pivotal in allowing me to reach my goals. Thanks also to my beautiful daughter Lili Gwen for always putting a smile on Daddy's face.

Finally, I would like to thank my Father for his support and encouragement throughout my career and for showing so much belief in me. In recognition of his support I dedicate this research to him.


DECLARATION

This work has not previously been accepted in substance for any degree and is not concurrently submitted in candidature for any degree.

Signed.......... (Candidate) Date ...1|9|2011.....

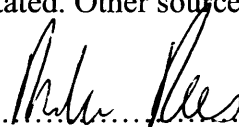
Statement 1

This thesis is being submitted in partial fulfilment of the requirements for the degree of PhD.

Signed.......... (Candidate) Date ..1|9|2011.....

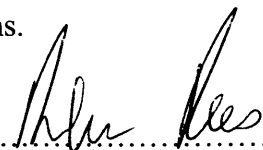
Statement 2

This thesis is the result of my own independent work/investigation, except where otherwise stated. Other sources are acknowledged by explicit references.

Signed.......... (Candidate) Date ..1|9|2011.....

Statement 3

I hereby give consent for my thesis, if accepted, to be available for photocopying and for inter-library loan, and for the title and summary to be made available to outside organisations.

Signed.......... (Candidate) Date ..1|9|2011.....

CONTENTS

ABSTRACT	ii
ACKNOWLEDGMENTS	v
DECLARATION	vi
CONTENTS	vii
LIST OF TABLES	xii
LIST OF FIGURES	xiii
NOTATION	xvii
CHAPTER 1 INTRODUCTION	1
1.1 Motivation.....	1
1.2 Research objectives.....	4
1.3 Thesis organisation.....	6
CHAPTER 2 LITERATURE REVIEW	8
2.1 Micro manufacturing.....	8
2.2 Micro machining.....	12
2.2.1 Micro milling.....	12
2.2.2 Micro electro discharge machining.....	14
2.2.3 Laser milling.....	14
2.2.4 Ion beam machining.....	15

2.3 Micro electrical discharge machining.....	16
2.3.1 The electrical discharge machining process.....	17
2.3.2 Electrode wear.....	23
2.3.3 Electrode discharge grinding.....	24
2.3.4 Sacrificial block.....	25
2.3.5 Wire electro discharge grinding.....	26
2.3.6 Rotating sacrificial block.....	29
2.3.7 Micro-EDM generators.....	31
2.4 Hybrid EDM Processes.....	35
2.4.1 WEDG in combination with μ -die sinking	35
2.4.2 WEDG in combination with μ WEDM.....	37
2.4.3 Surface Integrity.....	40
2.5 Summary and conclusions.....	43

CHAPTER 3 FACTORS AFFECTING THE QUALITY OF ELECTRODES PRODUCED BY WIRE ELECTRO-DISCHARGE GRINDING

3.1 Motivation.....	46
3.2 Factors affecting electrode quality.....	47
3.3 Experimental set-up.....	49
3.4 Experimental results.....	54
3.4.1 Electrode material.....	54
3.4.2 Machining strategy.....	57
3.4.3 Machine accuracy.....	61

3.4.4 Process improvements.....	75
3.5 Summary and conclusions.....	83

CHAPTER 4 SURFACE FINISH OPTIMISATION AND PREDICTION FOR WIRE ELECTRO DISCHARGE GRINDING.....85

4.1 Motivation.....	85
4.2 WEDG and μ WEDM.....	86
4.3 Experimental set-up.....	89
4.4 Experimental results.....	95
4.4.1 Workpiece preparation.....	95
4.4.2 Experimental design.....	101
4.4.3 Machining response evaluation.....	109
4.4.4 Optimal parameters.....	114
4.4.5 Confirmation experiment.....	119
4.4.6 Comparison with μ WEDM.....	119
4.5 Inductive model for in-process surface roughness predictions.....	122
4.5.1 Data pre-processing.....	125
4.5.2 Model generation and discussion.....	129
4.6 Summary and conclusion.....	143

CHAPTER 5 THE EFFECTS OF MATERIAL GRAIN STRUCTURE ON SURFACE INTEGRITY OF COMPONENTS PROCESSED BY

μWEDM.....	146
5.1 Motivation.....	146
5.2 μWEDM process.....	147
5.3 Material, equipment and experimental design.....	149
5.4 Results and Discussion.....	160
5.4.1 Micro hardness.....	160
5.4.2 Surface morphology.....	162
5.4.3 Surface roughness.....	164
5.4.4 Micro cracks and recast layer.....	167
5.4.5 Material removal rates.....	171
5.4.6 Material composition.....	175
5.5 Summary and conclusions.....	177

CHAPTER 6 CONTRIBUTIONS AND FUTURE

WORK.....	180
6.1 Contributions.....	180
6.2 Future work.....	182

APPENDIX A:	184
--------------------------	------------

APPENDIX B:	186
--------------------------	------------

APPENDIX C:	188
APPENDIX D:	191
APPENDIX E:	194
APPENDIX F:	204
REFERENCES	206

LIST OF TABLES

Table 3.1	Technology parameters used on the AGIE machine.....	52
Table 3.2	Technology parameters applied on the Sarix machine.....	53
Table 4.1	Set-up parameters.....	92
Table 4.2	Monitoring parameters.....	94
Table 4.3	Set-up parameters for conventional μ WEDM.....	102
Table 4.4	Machining parameters and their levels.....	106
Table 4.5	L27 orthogonal array.....	108
Table 4.6	ANOVA for Surface Roughness.....	110
Table 4.7	Response table for signal to noise ratios Larger is better.....	116
Table 4.8	Optimum factor levels.....	116
Table 4.9	ANOVA for S/N ratios.....	116
Table 4.10	An example of a training instance.....	128
Table 4.11	An example of a generic rule set.....	132
Table 4.12	The rule set when 9 membership functions were used for the output.	139
Table 5.1	Finish and rough machining parameters.....	152
Table 5.2	Mechanical properties of the Al5083 samples.....	153

LIST OF FIGURES

Figure 2.1	Classification of technologies according to process ‘dimension’ and material relevance	11
Figure 2.2	Ignition phase of a discharge (OEL-HELD GmbH publication).....	20
Figure 2.3	Melting phase of a discharge (OEL-HELD GmbH publication).....	21
Figure 2.4	Ejection phase of a discharge (OEL-HELD GmbH publication).....	22
Figure 2.5	Electrode generation through sacrificial block (Lim 2003).....	27
Figure 2.6	Dressing electrodes through WEDG (Rees et al., 2007).....	28
Figure 2.7	Dressing electrodes through rotating sacrificial disk (Lim 2003).....	30
Figure 2.8	Transistor type pulse generator (Han 2004).....	33
Figure 2.9	RC pulse generator (Han 2004).....	34
Figure 3.1	Experimental set-up.....	51
Figure 3.2	Electrode dressing operation.....	56
Figure 3.3	Relationship between electrode material, process deviation (D_2) and the repeatability of high aspect ratio electrodes.....	59
Figure 3.4	A $\varnothing 120\ \mu\text{m}$ rod ground to $\varnothing 20\ \mu\text{m}$ with an aspect ratio of 250.....	60
Figure 3.5	The surface roughness of the two electrodes (a) W – Electrode Ra 0.95 (b) WC – Electrode Ra 1.35.....	63
Figure 3.6	Machining strategies.....	64
Figure 3.7	Electrodes produced during the three experiments..... (a) Experiment 1: a one cut machining strategy (b) Experiment 2: a two cuts’ machining strategy (c) Experiment 3: a four cuts’ machining strategy	65

Figure 3.8	The electrode machined in the repeated first experiment.....	67
Figure 3.9	Reference position set-ups.....	69
	(a) A running wire	
	(b) A WC block	
Figure 3.10	Variations in setting up the ‘dressing position’	70
Figure 3.11	Dressing procedure.....	72
Figure 3.12	The profile of the dressed electrode.....	74
Figure 3.13	Variations of the diameter of the dressed electrodes.....	76
Figure 3.14	Flowchart of the compensation procedure.....	77
Figure 3.15	Optical measurement set-up.....	79
Figure 3.16	Variations of the diameter of the dressed electrodes.....	80
Figure 3.17	Diameters of dressed electrodes with and without optical verification on the Sarix machine.....	82
Figure 4.1	WEDG in combination with μ WEDM.....	90
Figure 4.2	Slicing operation.....	96
Figure 4.3	(a) Test piece 1 (b) Cross section of X-X.....	98
Figure 4.4	Factors affecting the WEDG operation.....	100
Figure 4.5	Surface profiles resulting after (a) conventional μ WEDM and (b) WEDG.....	104

Figure 4.6	Figure 4.6. Normal plot of residuals.....	112
Figure 4.7	Residuals versus fitted values.....	113
Figure 4.8	Main effects on the S/N ratio.....	117
Figure 4.9	Interaction plot.....	118
Figure 4.10	Surface roughness comparison of two test pieces machined by μ WEDM	121
Figure 4.11	Voltage profiles of WEDG and conventional μ WEDM.....	123
Figure 4.12	Illustration of steady state machining regime.....	127
Figure 4.13	Prediction accuracy of the generated models.....	130
Figure 4.14	Triangular fuzzy set.....	134
Figure 4.15	Predicted and measured Ra when 3 fuzzy output sets were used.....	136
Figure 4.16	Nine membership functions for the output.....	138
Figure 4.17	Predicted and measured Ra when 9 fuzzy output sets were used.....	140
Figure 4.18	An approach for searching on the machine for an optimum processing window.....	142
Figure 5.1	Test piece configuration.....	150
Figure 5.2	Micrographs of AR (a) and CP (c) samples and their corresponding statistical analysis.....	156
Figure 5.3	‘Ultrafine Grained’(UFG) Al5083 sample morphology.....	157
Figure 5.4	‘Ultrafine Grained’ (UFG) Al5083 TEM micrograph.....	157
Figure 5.5	Pulse discrimination system showing three voltage pulse states.....	159
Figure 5.6	Micro hardness of the AR (a), CP (b) and UFG (c) samples.....	161
Figure 5.7	Metallographic images.....	163
Figure. 5.8	Roughness of the μ WEDM samples: (a) rough and (b) finish.....	166

Figure 5.9 Machined surfaces of AR (a), CP (b) and UFG (c) workpieces after the μ WEDM finishing cuts.....168

Figure 5.10 Recast layer thickness of the μ WEDM samples: (a) rough and (b) finish.....170

Figure 5.11 Pulse characteristics for the three studied materials.....172

Figure 5.12 MRR of the μ WEDM samples.....174

Figure 5.13 The EDX spectrums of the workpiece surfaces after μ WEDM.....176

NOTATION

A	Amperage
AD	Anderson-Darling statistics
Adj	MS adjusted mean square
Adj SS	Adjusted sum of squares
Al	Aluminium
Al5083	5083 series aluminium alloys
ANOVA	Analysis of variance
AR	As received
Au	Gold
C	Capacitor
C	Carbon
CAD	Computer aided design
CNC	Computer numerical control
Co	Cobalt
CP	Conventionally processed
Cu	Copper
D.F.	Degrees of freedom
D_1	Initial diameter of the electrode
D_1	Target diameter
D_2	Diameter of the dressed electrode
DC	Direct current
D_2^M	Diameter of measured electrode
D_w	Running wire diameter
ECAP	Equal Channel Angular Pressing

EDM	Electrical discharge machining
F	Variance ratio
Fe	Iron
FET	Field effect transistor
FIB	Focussed ion beam
Ghz	Giga hertz
GmbH	Gesellschaft mit beschraenkter Haftung
GPa	Giga pascals
HAZ	Heat affected zone
IBM	Ion beam machining
Iso	International organisation for standardisation
K	Potassium
kHz	Kilo Hertz
MEMS	Micro electromechanical systems
MEW	Machine-electrode-wire
Mg	Magnesium
mm/s	Millimetres per second
Mn	Manganese
MNMT	Micro and nano manufacturing technologies
MNT	Micro and nano-technology
MPa	Mega pascal
MRR	Material removal rate
MST	Micro-system technology
N	Number of samples
NC	Numerical control

N_f	Number of membership functions for the output
nF	Nano farad
nm	Nano metre
ns	Nano second
NSF	National science foundation
p	P-value (appropriateness of rejecting the null hypothesis)
PhD	Doctor of philosophy
Pt	Platinum
Pw	Pulse frequency
R	Resister
R & D	Research and development
R	Number of replications
Ra	Arithmetic mean value
RC	Relaxation circuit
RPM	Revolutions per minute
S_{profile}	Square cross-section
S/N	Signal-to-noise
SEM	Scanning electron microscope
Seq SS	Sequential sum of squares;
Servo ist	Real value of the servo control parameter
S_g	Spark gap
Si	Silicon
S_{pos}	Part run-out error
STD	Standard deviation
StDev	Standard deviation

TEM	Transmission electron microscopy
Ti	Titanium
Tr	Triangular fuzzy set
U.S.	United States
UFG	Ultrafine grained
Ufs	Average voltage between the electrode wire and the work piece
UTS	Ultimate tensile strength
UWM	Uniform wear method
V	Voltage
V _x	Cutting speed along the x axis
W	Tungsten
W300	Ferritic steel
WC	Tungsten carbide
WEDG	Wire electro-discharge grinding
WTEC	World technology evaluation centre
Y_i	Response value (Surface Roughness)
Y_{pos}	Machine movement coordinate
Zn	Zinc
%	Percentage
°C	Degrees centigrade
∞	Infinite
μ	Micron
μ EDM	Micro electrical discharge machining
μ J	Micro joule

μm	Micro metre
μs	Micro second
μWEDM	Micro wire electrical discharge machining
2.5D	Two and a half dimensional
3D	Three dimensional
4M	Multi-material micro manufacture
ΔC	Compensation corrections introduced
ΔD_2	Deviation of the electrode diameter from its target value after the dressing
ΔD_w	Variation of the wire diameter from their nominal values
ΔS_g	Variations of the spark gap
$\Delta\text{Y}_{\text{pos}}$	Accuracy of machine movement coordinate

CHAPTER 1

INTRODUCTION

1.1 Motivation

It has been recognised for several years that Microsystems-based products will be an important part of Europe's industrial manufacturing future, exploring the possibilities for functionality, mobility and intelligence in devices that a new generation of materials and processes will offer (Matthews and Dimov, 2008). During 2007 the market sales in the Micro Electro Mechanical Systems (MEMS) industry reached \$6.9 billion showing a growth in the market of 11% (Eloy, 2008). Indeed, by 2012 the predicted sales in the MEMS industry is expected to reach \$12 billion (Eloy, 2008). To support this growth multi functional, multi-material products, must advance from the laboratory to low-cost volume manufacture.

Europe has an excellent research competence and the required system knowledge to capture a good proportion of the new expanding Micro and Nano Manufacturing Technologies (MNMT) market. However to explore this opportunity, there is a need for more applied Research and Development (R & D) and faster transfer from R & D results and innovation into the market (Ratchev and Turitto, 2008). There is a clear trend for both research institutions and companies to dedicate significant resources to developing the operational capabilities for a range of Micro-System Technology (MST) based products.

With consumer awareness of the new high resource and knowledge-intensive capabilities for micro and nano manufacturing, micro product development offers great economic potential. However, to capitalise on and develop this potential, it is paramount that production platforms underpinning the design and serial manufacture of MST-based products are created and characterised to reduce uncertainties associated with the “translation” of micro-engineering ideas into commercial opportunities. Downscaling of traditional manufacturing processes to deliver MST based products is one way for broadening the functionality for existing manufacturing processes, and at the same time to develop new capabilities.

With the decrease of size, cost reductions can be achieved through the use of less material, energy, storage space, and transport. There are also environmental incentives with the potential for reduction in carbon emissions. However, there are many challenges associated with such downscaling. One of them is the length scale integration. To resolve this problem new technologies need to be developed that converge new and existing technologies to create new hybrid machining platforms.

An important area of development in micro engineering is the creation of the necessary capabilities for micro tooling and master making that can underpin cost effective mass production of micro components employing high throughput replication technologies, e.g. micro-injection moulding and thermal imprinting. Especially, the micro tool-making industry can benefit from the existing trend for technology convergence and the opportunities that the development of hybrid micro manufacturing processes offers. To meet the growing demands for micro manufacturing it is necessary to understand and

characterise the capabilities and limitations of available micro machining technologies.

Micro Electrical Discharge Machining (μ EDM) is a complex process with many factors affecting its capabilities; these constraints have to be investigated systematically in order to establish it as a viable platform for machining miniaturised components and tools. In particular, this necessitates significant advances in our knowledge in the areas of micro machining, micro tooling and micro fabrication. The process designers have to be equipped with this knowledge in order to reduce uncertainties at the product development stage when it is required to select the most appropriate production route for a given product by “mapping” product technical requirements with capabilities of the available micro machining techniques.

The engineering challenges tackled in this research are centred on broadening our understanding of μ EDM technology and also in developing it further to address specific requirements for producing functional micro features in existing and new emerging products. This PhD research investigates the current limitations of this technology, and thus to reduce the machining uncertainties when applying it for the manufacture of miniaturised products and micro tools.

In this research empirical knowledge is used to improve the process design, by quantifying the technical requirements and limitations of the technology, and developing new processing solutions. In particular, the aim is to characterise this developing manufacturing platform for the production of micro components and tooling such as micro measurement probes, micro punch and micro replication tooling masters.

In order to keep the investigation focused the research of the μ EDM process is extensively supported by a state-of-the-art survey of latest research and developments in the field.

1.2 Research Objectives

The overall aim of this research was to investigate the manufacture of components and characterise process/material interactions of μ EDM when used in combination with μ die-sink EDM and μ WEDM from a range of both traditional and novel materials. To carry out the empirical part of this research test parts were designed and then machined through the development of different methods of μ EDM to investigate:

- Factors affecting the quality of electrodes produced on the machine through the process of wire electro discharge grinding;
- Surface finish optimisation and prediction for the process of wire electro discharge grinding;
- The effect of material micro structure on the surface integrity of components produced through the process of μ WEDM.

After identifying the fundamental issues related to each of the above, a selection of process conditions were used to evaluate the μ EDM process and characterise their impact on component quality, surface finish optimisation and surface integrity. Further to this, methods were developed to improve the accuracy and quality of components as well as proposing an inductive learning algorithm to generate a rule set for assessing the resulting surface roughness after WEDG machining. To achieve the overall aims of

the research the following objectives were set:

- To investigate the factors that affect the quality of electrodes produced on-the-machine. With a focus on the affect of the electrode material, machining strategy and machine accuracy on the electrode re-generation process, when the WEDG process is used in combination with μ EDM.
- To perform a comprehensive analysis of the process capability of the WEDG system when used in combination with the μ WEDM. To assess the effects of spindle speed, flushing pressure, discharge interval, open circuit voltage and pulse ON time on the resulting surface finish after performing the main cut in WEDG. In addition, to develop a method for predicting the resulting surface finish through the use of an inductive learning technique for data processing.
- To investigate and characterise the effects of material microstructure on the resulting surface integrity of samples machined by μ WEDM. In particular, the process-material effects on the resulting micro hardness, phase content changes, Heat Affected Zone (HAZ), surface roughness, micro cracks, recast layers formation, material removal rate (MRR) and element spectrum after both rough and finishing μ WEDM cuts.

1.3 Thesis Organisation

The research is presented in six chapters, of which Chapters 3 to 5 encompass the main investigations, and Chapters 2 and 6 are a literature review and a summary of the main contributions of this work, respectively.

Chapter 2, includes three sections. In the first section the available micro machining processes are introduced. Then, the state-of-the-art, main characteristics and fundamental principles of the μ EDM process are presented and critically analysed. The third section describes the specific focus of this research including the main concepts identified and how they are investigated.

Chapter 3 establishes an understanding of the factors that affect the quality of electrodes produced on-the-machine when the process of WEDG is used in combination with the μ EDM process. In particular, the focus is on the effects that electrode material, machining strategy and machine accuracy have on the electrode re-generation process. The chapter starts with a discussion of the factors affecting the quality of on-the-machine dressed electrodes. Then, the research methods adopted to investigate experimentally the factors that affect the quality of the dressed electrodes are discussed. Finally, the empirical results are analysed and conclusions are made about the affects that electrode material, machining strategy and machine accuracy have on the quality of electrodes produced on-the-machine, and a solution is proposed to improve the accuracy of the process.

Chapter 4 investigates the technological capabilities of a hybrid micro machining

process for performing WEDG. In particular, μ WEDM is employed in combination with a rotating submergible spindle. Initially, the chapter proposes a machining strategy for workpiece preparation. Then, a Taguchi design of experiment method is applied to identify and optimise the most statistically significant main cut parameters on the achievable surface roughness. Following this, a simple and cost-effective method for on-the machine prediction of surface roughness is presented. The chapter concludes by analysing the capability of WEDG to produce a level of surface finish comparable to that achievable with μ WEDM.

Chapter 5 investigates the machining response of metallurgically and mechanically modified materials when they are processed by μ WEDM. The chapter commences, by introducing the research methods adopted to investigate experimentally the effects of the material microstructure on resulting surface integrity of Al5000 series aluminium alloys after μ WEDM processing. In particular, the process-material effects on the resulting micro hardness, phase content changes, heat affected zone, surface roughness, micro cracks, recast layer, material removal rate and element spectrum after both rough machining and finishing. The chapter concludes by analysing the empirical results and commenting on the surface integrity and machining response of each test piece.

In Chapter 6 the main contributions of the research are summarised. Some possible directions for further investigations are also suggested.

CHAPTER 2

LITERATURE REVIEW

Overview

In this chapter an overview of the available micro machining processes is provided. In the second section the chapter continues with a description of the state of the art, where the main characteristics and fundamental principles of the μ EDM process are presented and critically analysed. The third section concludes the chapter with a summary of the open research issues that constitute the core of this work.

2.1 Micro Manufacturing

Evidence of product miniaturisation can be seen as far back as the 1960's. The first experiments on the miniaturisation of a hole drilling by EDM were performed at 'Philips Research Lab' in the Netherlands in the mid 1960's (Osenbruggen et al., 1965). However, in recent years there has been an increase in the interest in micro manufacturing research and development activities (Ehmann, 2007). In 2006 under the U.S. National Science Foundation (NSF) the World Technology Evaluation Centre (WTEC) initiated an international technology assessment study focused on the emerging global trend towards the miniaturisation of manufacturing equipment, and systems for micro scale components and products. Some of the outcomes of the report were that micro manufacturing is an important technology because:

- It is an enabling technology for the widespread exploitation of nano science and nano technology developments – it bridges the gap between nano and macro worlds.
- It is a disruptive technology that will completely change our thinking as to how, when and where products will be manufactured e.g. onsite, on demand in the hospital operating room or on board a warship.
- It is a transforming technology that will redistribute manufacturing capability from the hands of a few to the hands of many – micro machining becomes a cottage industry.
- It is a strategic technology that will enhance competitiveness, reduce capital investment, reduce space and energy costs, increase portability and increase productivity.

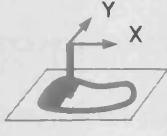
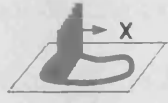
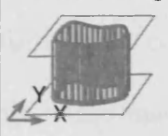
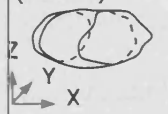
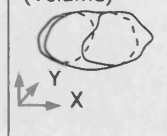
The opportunities associated with micro manufacturing were identified in the following three categories:

- Scientific challenges and needs.
- Technological challenges and needs.
- Environmental and social challenges and needs.

Whilst the late 20th century has seen a silicon based micro electronics revolution, the 21st century looks forward to the broader use of Micro and Nano-Technology (MNT) in many products (Dimov, 2005). It was recognised that applications of MNT into product platforms such as micro fluidics, micro-optics and micro sensors, require each constituent part of such miniaturised devices to be manufactured cost effectively in

high volumes in a range of materials. Business needs are the driving force behind the development of such novel product platforms. To create the necessary pre-requisites, manufacturing capabilities have to be created that are well characterised to minimise the risks associated with the development of MNT enabled products.

To address these technology and application challenges, and at the same time to capitalise on the opportunities that they represent for European industry a network of excellence in Multi-Material Micro Manufacture (4M) was established as an instrument for integration of European research. The 4M community proposed a classification of available micro manufacturing technologies (Figure 2.1) and also most significant market sectors that these technologies underpin. Especially, these sectors are: medical/surgical, automotive and transport, biotechnology, consumer products, information and communication, energy/chemical, scientific/academic community, and pharmaceutical (Dimov et al., 2006). In order for these industry sectors to capitalise on existing and emerging market opportunities the requirement for low cost / volume production is paramount.

Dimension capabilities	1D Processing 	Multiple 1D Processing 	2D Processing 	3D Processing (Surface) 	3D Processing (Volume) 
Metals	LH, EDM, ECM, Grinding	MF, Grinding	Lap, Pol, MF	Lap, Pol, ECP, EF, EP	EDM, MF
Polymers	3DL	3DP	EBL, IBL, LL, PUL, XL		HUE, NIL, NI, R2RE, IM
Ceramics	3DL, Grinding	3DP	IBL, LL,	Lap, Pol	NIL, NI, R2RE
Any material	EBM, FIB, LA, PM, AWJ, Drilling, Milling, Turning, SLS		Etch, PMLP, SP	PVD, CVD, SC, SA	Casting, MCIM, PIM

Key:

3DL	3D Lithography	Lap	Lapping
3DP	3D Printing	LH	Laser hardening
AWJ	Abrasive water jet	LL	Laser lithography
Casting	Casting	MCIM	Multi-component injection moulding
CVD	Chemical vapour deposition	MF	Metal Forming
DL	Direct LIGA	Milling	Milling
Drilling	Drilling	NI	Nano-imprinting
EBM	Electron beam machining	NIL	Nano-imprint lithography
EBL	Electron beam lithography	PIM	Powder injection moulding
ECM	Electrochemical machining	PUL	Photo / UV lithography
EDM	Electrical discharge machining	PM	Plasma machining
EF	Electroforming	PMLP	Projection mask-less nanopatterning
ECP	Electro-chemical polishing	Pol	Polishing
EP	Electroplating	PVD	Physical vapour deposition
Etch	Etching	R2RE	Reel to reel embossing
FIB	Focused ion beam	SA	Self assembly
Grinding	Grinding	SC	Spin coating
HUE	Hot/UV embossing	SLS	Selective laser sintering
IBL	Ion beam lithography	SP	Screen printing
IM	Injection moulding	Turning	Turning / Diamond turning
LA	Laser ablation	XL	X-ray lithography

Figure 2.1 Classification of technologies according to process 'dimension' and material

relevance (Dimov et al., 2006)

2.2 Micro Machining

To create the necessary micro tool-making capabilities for cost effective manufacture it is necessary to study the capabilities of available micro machining technologies. The diversity of existing machining processes is large, and the use of available equipment for producing micro features/structures represents many challenges. The technologies that can be used for micro tool-making can be categorised into two main types, mechanical and energy assisted processes (Dimov et al., 2006). Some of these processes are downscaled versions of existing conventional macro manufacturing technologies, while others are novel methods that apply various physical and chemical effects (Uhlmann et al., 2005; Asad et al., 2007; Amer et al., 2002; Brecher et al., 2010).

2.2.1 Micro milling

Micro milling originates from the watch making industry for manufacturing small parts. With new achievements in computer numerical control (CNC) control systems, powder metallurgy for sintering small super hard cutters and new spindles capable of over 100 000 rev/min (Weule et al., 2001), micro milling has become an important technology for producing micro moulds and dies (Schaller et al., 1999; Rahnama et al., 2009; Uhlmann et al 2005). With controlled and dedicated tool paths, the tool in interaction with the workpiece removes the unwanted material. Mechanically this is only possible when the tool material is sufficiently harder than the material being cut. Dimov et al., (2004) found that the step over movements, the depth of cut, feed-rates per tooth, cutting speeds, cutting tool wear, and the use of cutting fluid/air/oil mist are

important for their influence on the cutting behaviour. Popov et al., (2006) also found that interfacial interaction between the cutter and the workpiece material was very important, in particular it was found that the microstructure of the workpiece can play a fundamental role in the cutting process. For tool life expectancy, mechanical loading and thermal diffusion between the materials should be at a minimum. Tool fabrication is another important issue, especially to have a proper cutting it is necessary the depth of cut to be set by taking into account the tool edge radius. Currently sintered carbide end mill tools and drills of 100 μ m are commercially available. These tools have the capability to machine plastics, metal and composite materials but hard or very brittle materials are difficult to machine. Unpredictable tool life and premature tool failure are major problems in micro-machining, and there are on going research efforts to develop new systems for detecting tool breakage during micro-milling and drilling (Gandarias et al., 2006; Newby et al., 2007). Another important pre-requisite for performing micro cutting is the availability of ultra precision milling and turning machines. There are a number of such machines on the market that have advanced CNC controllers for the machining of micro 3D structures with high aspect ratio and high geometrical complexity. However, to achieve the necessary accuracy and repeatability in machining parts at micro scale the cutting process should take place in temperature controlled environment. For example, every 0.1 $^{\circ}$ C change of the spindle temperature can lead to an additional 1 μ m (or more) enlargement error. There are also other sources of errors such as the potential for dust on the tool holder, and chips of cut material (up to 25 μ m size) present on the tool during calibration and measurement. Setups and tool changeovers also require a controlled procedure that includes a 15 minute temperate run-in of the machine spindle. With such influences known and controlled to a minimum, the machine is adept to producing tool inserts for moulding purposes.

2.2.2 Micro electrical discharge machining

Micro electrical discharge machining (μ EDM) is one technology widely used for the manufacture of microstructures and tooling inserts for micro-injection moulding. With the workpiece and electrode submerged in a dielectric fluid, material is removed by melting and vaporization by high frequency electrical sparks generated by high voltage pulses between the cathode tool and a workpiece anode (Madou, 2001). After the initial pioneering research work interest in Micro-EDM was fading until, in the late 1980's, the Japanese rediscovered this technique again (Masuzawa et al., 1985). Due to the flexibility of the EDM process and its capability to produce complex 3D structures, currently the technology is employed in a number of applications including fabrication of micro parts for watches, keyhole surgery, housings for micro-engines, tooling inserts for fabrication of micro-filters and micro fluidics devices (Rees et al., 2007). Typical μ EDM technologies include μ WEDM, μ die-sinking, μ EDM Drilling, μ EDM milling and Wire Electrode Discharge Grinding (WEDG). A detailed description of the fundamentals of EDM can be seen in section 2.3.1

2.2.3 Laser milling

Laser machining has been applied to various industrial applications (Meijer et al., 2002; Campanelli et al., 2007). Due to the absence of an electrode or cutting tool during machining it is an ideal candidate for performing micro machining. Commercially available laser systems compete successfully with conventional manufacturing methods in a number of applications where the latter methods have reached the limits of their

capabilities. Lasers can also be easily integrated into CNC machines and thus turning them into flexible and efficient material removal machines. Especially, the laser milling process allows complex parts and tooling inserts to be fabricated directly from computer aided design (CAD) data in a wide range of advanced engineering materials such as ceramics, hardened steel, titanium and nickel alloys (Pham et al., 2001). The type of laser source chosen to carry out such machining depends on the workpiece material, and especially on the specific laser-material interactions. There are already many different laser sources on the market, with different wavelengths and pulse durations, suitable for integration into machine tools for many 2.5D laser machining applications (Gower, 2000; Dobrev et al., 2005, Petkov et al., 2008; Pham et al., 2002; Pham et al., 2005, Karnakis et al., 2006 ; Knowles et al., 2006; Knowles et al., 2007).

2.2.4 Ion Beam Machining (IBM)

Ion beam machining is considered a non-conventional method of machining. In IBM a stream of charged atoms (ions) of an inert gas, such as argon, is accelerated in a vacuum by high energies and directed toward a solid workpiece. The beam removes atoms from the workpiece by transferring energy and momentum to atoms on the surface of the object, when an atom strikes a cluster of atoms on the workpiece, it dislodges between 1 and 10 atoms from the workpiece. Focussed ion beam (FIB) systems are designed to structure nano and micro features in silicon or non-silicon materials by either 3D sputtering or deposition (Ochiai et al., 1999; Lalev et al., 2008; Loeschner et al., 2003; Platzgummer et al., 2006). Ions extracted from a plasma source, normally liquid gallium, are accelerated and then by “bombarding” the workpiece to sputter surface atoms. If organic gases are also applied in the vicinity of the surface, the

resulting collisions can give rise to the deposition of neutral species (Pt, W, C, Au, etc) on the surface. FIB systems can also be operated in two modes; direct writing and projection mode where the latter is considered to be much faster than the former by utilising a programmable aperture to structure a uniform broad beam (Loeschner et al., 2003; Platzgummer et al., 2006).

2.3 Micro Electrical discharge machining

Many micro fabrication techniques such as lithography, etching, laser milling and micro milling are suitable to produce micro components and micro tooling masters (Rajurkar and Yu, 2000). However, these processes in general lack the ability of machining three-dimensional shapes, or are limited in the surface finish achievable. μ EDM is one process that represents a viable alternative.

Micro EDM was initially used for the purpose of producing small holes in metal sheets. The holes were in the range of diameters larger than 200 μ m. The electrodes that were used came in the form of tubular rods and dielectric fluid was pumped through to enhance the flushing within the working gap (Meeusen, 2003). In 1985, Masuzawa et al. introduced a technique of on-the-machine electrode generation through a device, which was baptised WEDG (Masuzawa et al., 1985). The device was developed with a view to create very thin electrodes. The thin electrodes could then be used as micropins or as tool electrodes to produce micro holes. The WEDG technique developed quickly, resulting in cylindrical tool electrodes with a diameter less than 3 μ m being achieved. The result of the development of electrode dressing, has now made electrical discharge machining one of the most extensively used non-conventional material removal

processes. Its unique feature of using thermal energy to machine electrically conductive parts regardless of hardness has been its distinctive advantage in the manufacture of mould, die, automotive, aerospace and surgical components (Valentincic et al., 2006; Heeren et al., 1997; Ho and Newman, 2003). The electrode generation and re-generation is considered a key enabling technology for stimulating the revival of the μ EDM process, as it does not only allow the process scale down but it also represents a method for minimising the effects of electrode wear.

2.3.1 The electrical discharge machining process

The Electrical Discharge Machining process is an electro-thermal machining technology which removes workpiece material by the erosive action of electrical discharges. The discharges are created between a tool electrode and a workpiece electrode. Both the electrode and the workpiece are immersed in a dielectric fluid and separated by a small working gap. When a voltage is applied between the electrode and the workpiece, the corresponding electric field in the working gap exceeds the dielectric breakdown level, a discharge is then created. The applied voltage is generally pulsed at a predefined frequency, creating successive discharges. Each discharge melts and evaporates a small amount of material on both tool and workpiece electrodes (Toren et al., 1975; Abbas et al., 2007). The evaporated material and a portion of the melted material are removed by the dielectric fluid. The remaining material re-solidifies and creates a crater like surface on both the electrode and workpiece. By applying a large number of sparks, large material volumes can be achieved. The material removal on the tool electrode can be kept an order of magnitude lower than the

material removal on the workpiece by an appropriate selection of electrode materials and by appropriate machine parameter settings.

Figure 2.2, 2.3 and 2.4 illustrate the three main phases of a discharge. The first ignition phase (Figure 2.2) is the preparation phase of the discharge channel which is initiated at the moment the generator applies the necessary voltage between the workpiece and electrode. When a critical electric field is exceeded between a spot on the tool and a spot on the workpiece, conduction paths grow at microsecond speeds through the dielectric fluid, in the form of branch trees, called streamers. These streamers are precursors of the effective dielectric breakdown. In a second melting phase (Figure 2.3) the electrode and the workpiece are locally melted by the discharging spark. The discharge consists of a plasma channel surrounded by a gaseous mantle. The plasma channel, consisting of free electrons and positively charged ions, is characterised by high pressure and high temperature. The free electrons accelerate towards the anode and heat up the anode during the impact, while the ions strike and heat up the cathode. On both the electrode and workpiece, material is melted and evaporated by the high power concentration of the plasma channel. It is found that the diameter of the plasma channel at the cathode side remains constant, while the plasma channel enlarges at the anode side. This means that the current density at the cathode side remains constant, while the current density at the anode side decreases. While the generator cuts the electric current at the end of the discharge pulse, the plasma channel disappears and the corresponding pressure drop causes a sudden and intense boiling locally on the workpiece and electrode surfaces. During the third ejection phase (Figure 2.4) the proportion of the melted electrode material is ejected into the surrounding dielectric fluid. With this action the cycle of a single discharge is finished. When the dielectric

fluid is sufficiently deionised, another pulse can be applied in order to produce the next discharge (Meeusen, 2003; Kunieda et al., 2005; Rajurkar et al., 2006; Yeo et al., 2008;).

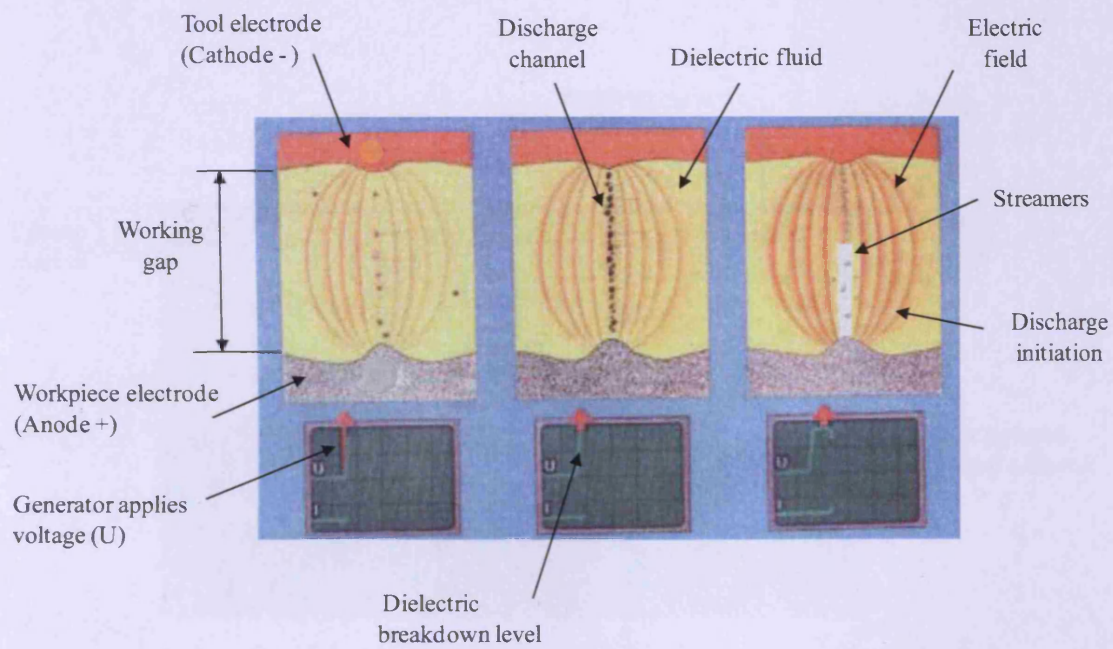


Figure 2.2. Ignition phase of a discharge (OEL-HELD GmbH publication)

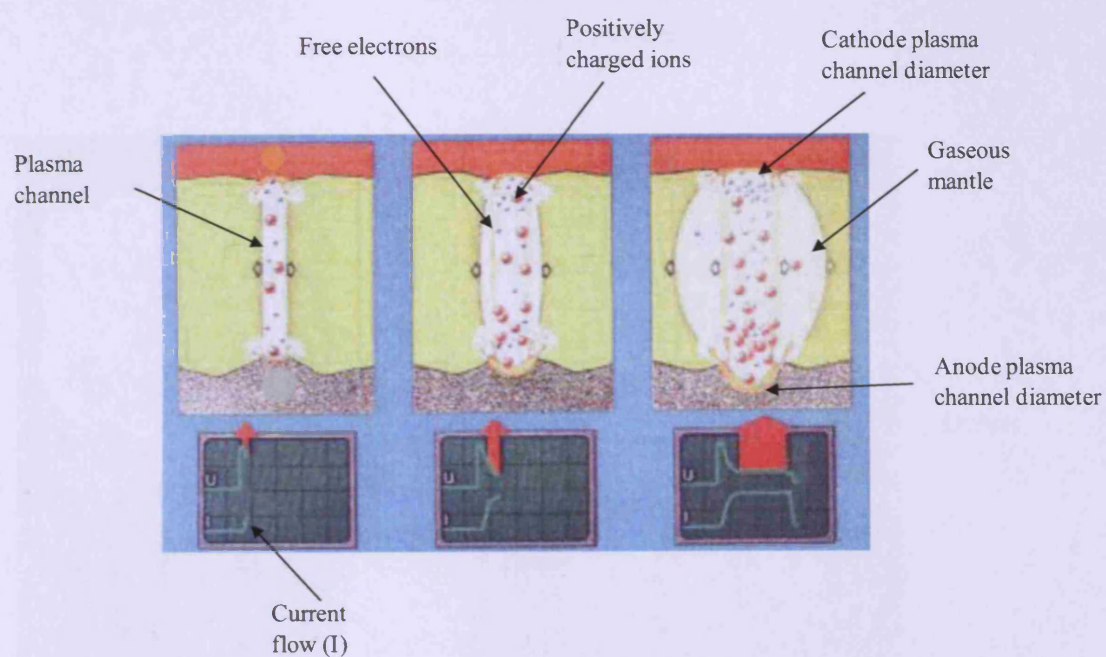


Figure 2.3. Melting phase of a discharge (OEL-HELD GmbH publication)

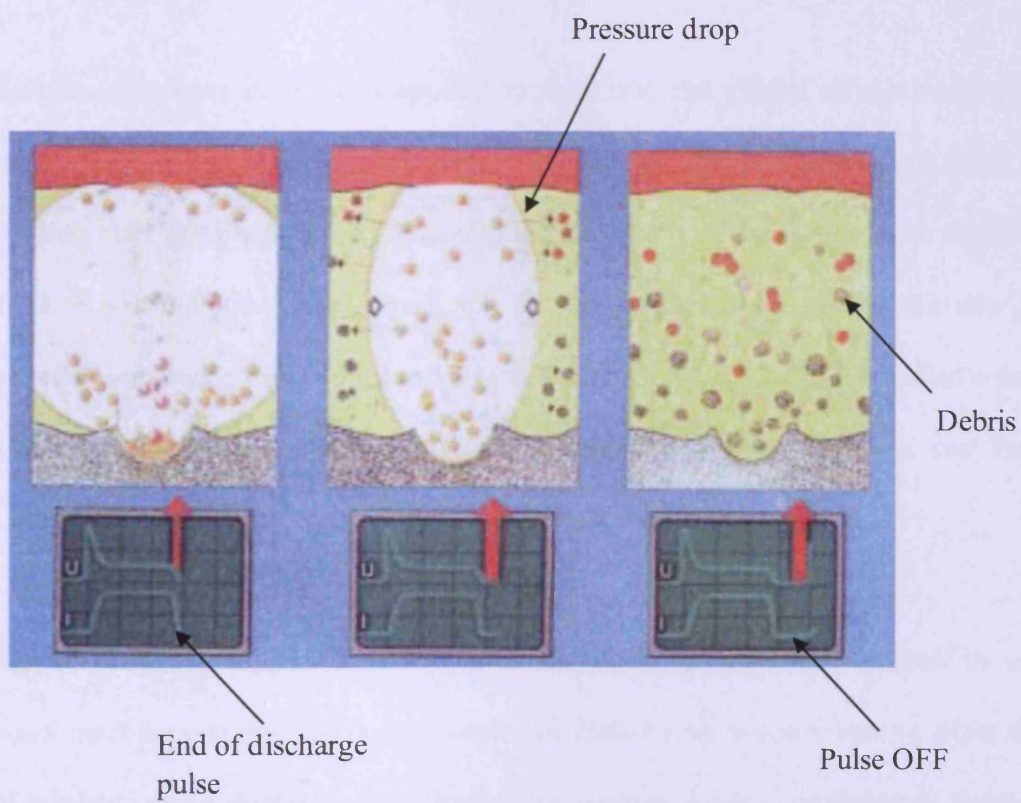


Figure 2.4. Ejection phase of a discharge (OEL-HELD GmbH publication)

2.3.2 Electrode Wear

The electrode wear becomes an important issue when employing μ EDM as the volumetric wear, defined as the ratio between electrode and workpiece wear, is relatively high and cannot be considered negligible (Yu et al., 1998a; Bigot et al., 2005). The volumetric wear modifies the process as the sparking area will change as the electrode wears, which will affect the accuracy and quality of the machined part.

Several techniques have been applied to minimise the effects of electrode wear. In micro EDM drilling, the electrode wears when producing blind holes. As a result, when eroding material down to a fixed depth, the real depth of the hole will be significantly smaller. One solution is to repeat the process a number of times with new or re-generated microelectrodes until the required depth is obtained. This is called a multiple electrode strategy (Meeusen, 2003). The main drawback is that it can be time consuming and difficult to predict the number of electrodes required.

The problems associated with the electrode wear become more difficult to address when machining complex 3D micro cavities. Either wear is too severe to allow the use of complex-shape electrodes in a classical die-sinking process, or electrode geometry is difficult to produce. Thus, for the production of micro 3D cavities, the use of micro EDM milling with simple shape-electrodes was proposed as an alternative machining strategy. In this case, a basic method called the Uniform Wear Method (UWM) can be applied (Yu et al., 1998a; Yu et al., 1998b). A layer-by-layer machining strategy is applied that based on estimation of the wear ratio compensates the wear during the machining of each layer by a constant electrode feeding in the Z-axis. For this

technique very accurate estimation of wear is required, because any error in the estimation would have a cumulative effect through the layers.

Many researchers have focused on the difficult problem of wear estimation (Yu et al., 2003; Mohri et al., 1995; Narasimhan., 2005) but the accuracy of the proposed models still needs to be verified and improved for use in micro EDM milling (Bissacco et al., 2010). As the sparking conditions in μ EDM can be application/material dependant and generally do not remain constant, the adoption of machining strategies to counter act electrode wear completely is difficult to implement in practise. The main drawback in applying the previously presented wear compensation methods is that they rely highly on the accuracy of the wear estimation models they employ. Thus, with these methods the under or over-estimating the degree of wear would result in machining inaccuracies.

With improvements in wear estimation models, further developments in compensation methods should be expected. Therefore, until such a time the generation and re-generation of electrode on-the-machine remains a key enabling technology for the successful use of μ EDM.

2.3.3 Electro-Discharge Grinding

As stated previously, during the μ EDM process the volumetric wear, the ratio between electrode and workpiece wear, is relatively high and cannot be considered negligible (Yu, et al., 1998a; Bigot et al., 2005). Thus, to manufacture microstructures there is often a need to compensate the wear by replicating electrodes or to apply specialist machining techniques. To support this requirement, techniques for on-the-machine

electrode generation were developed (Masuzawa et al., 1985).

The phenomenon of electrode dressing draws away from conventional EDM process whereby the user would strive to protect the electrode, by holding wear to a minimum. To achieve electrode dressing the operator intentionally ‘wears out’ the electrode. To wear out the electrode, adjustments are made to the EDM control settings to provide the highest wear conditions possible. The conditions for creating the highest wear conditions for μ EDM are negative polarity, excessive amperage, high frequencies and high capacitance (Guitrau, 1997).

Several researchers have developed techniques for generating electrodes. Generally, for the purposes of μ EDM electrodes are formed through one or a combination (Wong et al., 2003; Ho and Newman, 2003; Masuzawa et al., 1985; Mohri et al., 2003) of the following processes:

- Sacrificial block dressing or sometimes referred to as reverse EDM
- Wire electro-discharge grinding (WEDG)
- Rotating sacrificial disk

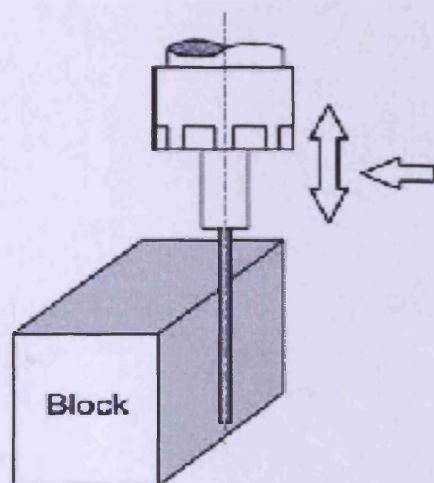
2.3.4 Sacrificial Block

During ‘Sacrificial block dressing or sometimes referred to as reverse EDM’ (Figure 2.5) a sacrificial conductive block is used to intentionally wear the electrode out. Both the electrode and block are immersed in a dielectric fluid. The electrode is then rotated at approximately 500 RPM. The machine CNC control then brings the electrode into

contact with the electrode block, creating a discharge which in-turn, allows dressing to occur. In essence what the user is actually doing is transforming the sacrificial conductive block into the electrode and transforming the electrode into the workpiece. To intentionally wear out the electrode, adjustments are made to the EDM control settings to provide the highest wear conditions possible (Guitrau, 1997). Another iteration of this process was investigated by (Yamazaki et al., 2004) whereby the electrodes were dressed through self-drilled holes. With this method, a rod electrode with negative polarity is rotated and fed into a plate electrode to make a hole. After the rod returns to its initial position, the axis of the rod electrode is off-centred from the centre of the hole at a certain distance. The polarity of the rod electrode is then reversed, and the rod electrode is either, with or without rotation fed into the plate electrode. A straight rod electrode can be achieved with this process if the outlet hole does not wear (Yamazaki et al., 2004).

2.3.5 Wire electro-discharge grinding (WEDG)

During WEDG a continuously running wire moving at a speed of approximately 3 – 5mm/s is used to intentionally wear the electrode out (Lim et al., 2003). Both the electrode and running wire are immersed in a dielectric fluid. Figure 2.6 illustrates a typical set-up. The electrode is then rotated at approximately 500 RPM. The machine CNC control then brings the electrode into contact with the running wire, this then creates a discharge which in-turn, allows dressing to occur.



(a) Stationary sacrificial block

Figure 2.5 Electrode generation through sacrificial block (Lim et al., 2003)

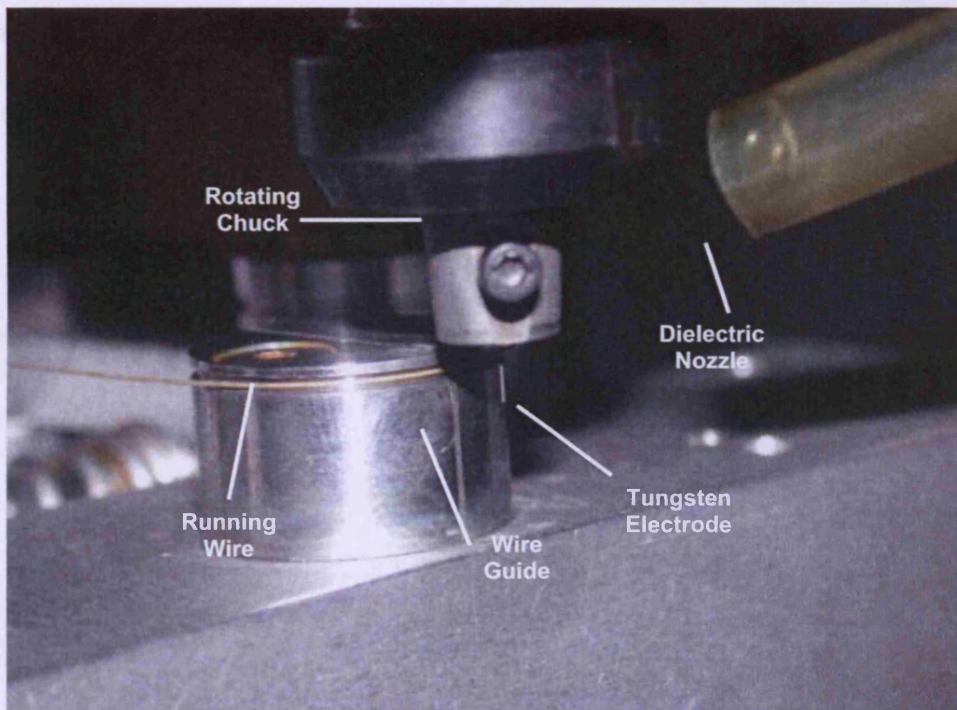
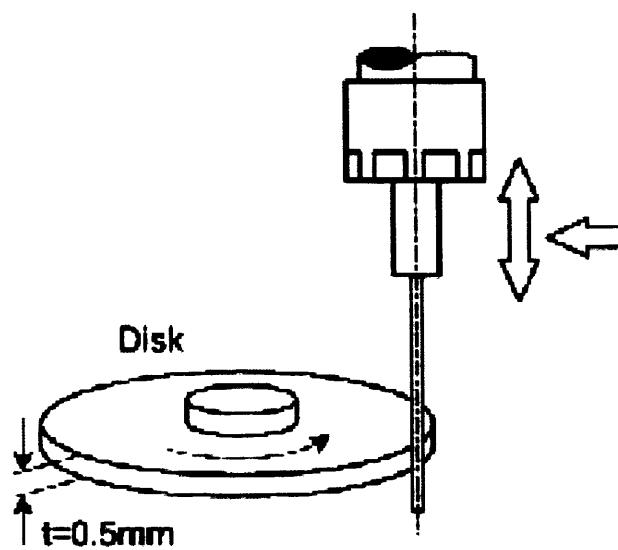


Figure 2.6 Dressing electrodes through WEDG (Rees et al., 2007)

2.3.6 Rotating sacrificial disk

During 'Rotating sacrificial disk dressing' a continuously rotating cylindrical, (60mm by 0.5mm thick) sacrificial disk (Lim et al., 2003), is used to intentionally wear the electrode out. Both the electrode and sacrificial disk are immersed in a dielectric fluid. Figure 2.7 illustrates a typical set-up. The electrode is then rotated at approximately 500 RPM, whilst the sacrificial disk is rotated at about 90 RPM. The machine CNC control then brings the electrode into contact with the rotating disk, this then creates a discharge which in-turn, allows dressing to occur.



(b) Rotating sacrificial disk

Figure 2.7 Dressing electrodes through rotating sacrificial disk (Lim et al., 2003)

2.3.7 Micro-EDM generators

Historically, μ EDM experiments were executed using sinking-EDM techniques and equipment. However, progressively the equipment and techniques have evolved and in addition to micro die-sink machines, μ WEDM and WEDG processes now fall into the category of μ EDM application. For μ EDM application generators with minimised discharge energy of $1\mu\text{J}$ have been developed (Masuzawa, 2000).

In conventional EDM, two types of pulse generators are generally used; Relaxation circuit (RC) pulse generators and transistor type pulse generators, shown in Figures 2.8 and 2.9 respectively (Han et al., 2004). The fabrication of parts smaller than several micro metres requires minimisation of the pulse energy ($<1\mu\text{J}$) supplied into the gap between the workpiece and electrode (Masuzawa, 2000). This means that finish machining by micro EDM requires pulse durations of several nano second durations (Juhr et al., 2004). Since the RC pulse generator can generate such smaller discharge energies simply by minimising the capacitance in the circuit it is widely employed in μ EDM. Smaller discharge energies generally result in better quality surface finish obtainable with this type of generator (Jahan et al., 2009). However, machining using the RC pulse generator is known to have the following demerits:

- extremely low removal rate from its low discharge frequency due to the time needed to charge the capacitor,
- uniform surface finish is difficult to obtain because the discharge energy varies depending on the electrical charge stored in the capacitor before dielectric breakdown,

- thermal damage occurs easily on the workpiece if the dielectric strength is not recovered after the previous discharge as current will continue to flow through the same plasma channel in the gap without charging the capacitor.

The transistor type pulse generator on the other hand widely used in conventional EDM has some advantages. Compared with the RC pulse generator, it provides a higher removal rate due to its high discharge frequency because there is no need to charge a capacitor. Moreover, the pulse duration and discharge current can arbitrarily be changed depending on the machining characteristics required. This indicates that the application of the transistor type pulse generator to micro-EDM can provide dramatic improvements in the removal rate due to the increase in the discharge frequency by more than several dozen times.

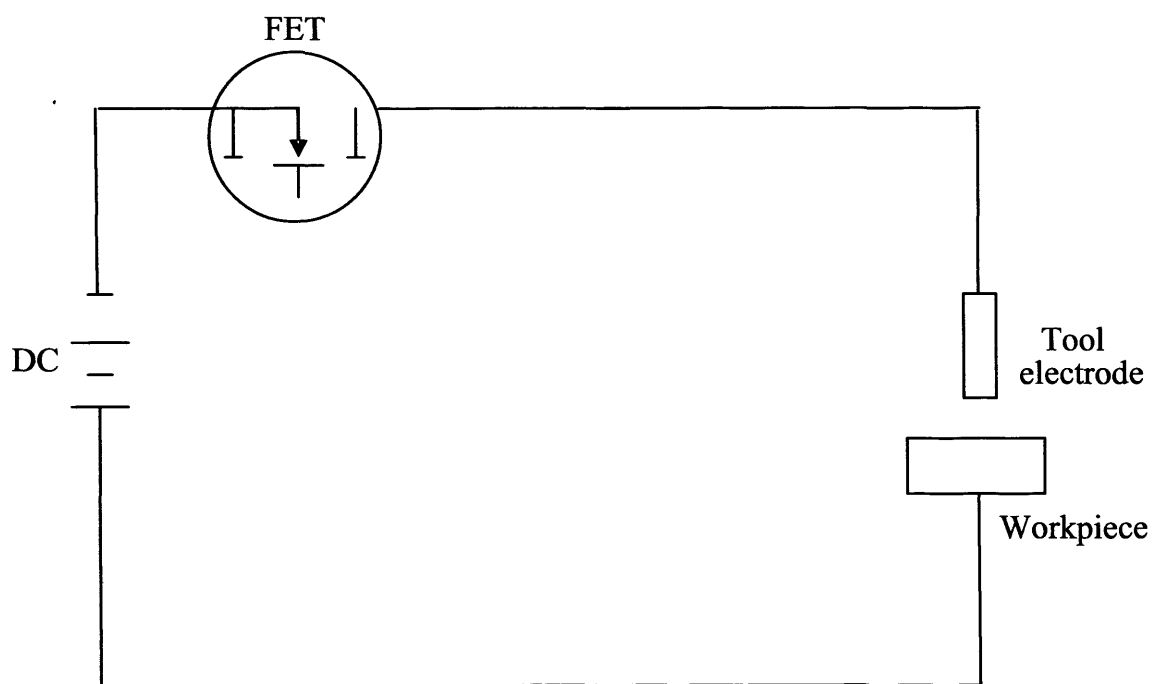


Figure 2.8. Transistor type pulse generator

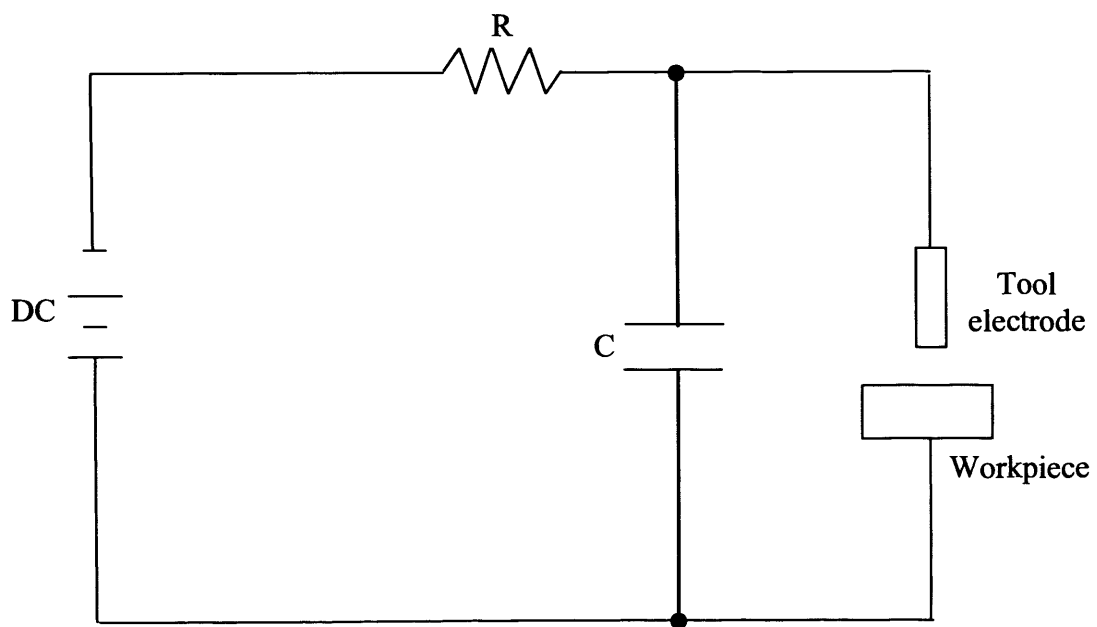


Figure 2.9. RC pulse generator

2.4 Hybrid EDM Processing

μ EDM is flexible technology widely used for the manufacture of complex 3-D microstructures, and tooling inserts for micro-injection moulding and hot embossing. Originally μ EDM was applied predominantly for producing small holes in metal foils. Due to the flexibility of the EDM process and its capability to produce complex 3D structures, the technology is currently employed in a number of applications. To broaden the application area of this technology WEDM can be combined with other technologies as it is the case with WEDG, and it is considered a hybrid machining process (Ho et al., 2004).

2.4.1 WEDG in combination with μ -die sinking

To broaden the application of μ EDM, electrodes can be manufactured on-the-machine when the WEDG process is used in combination with the μ -die sinking process. This method of electrode generation and re-generation is considered a key enabling technology for improving the performance of the μ EDM process (Masuzawa, 2001). However, several factors that affect the quality of the dressed electrodes need to be investigated, namely:

- Electrode material;
- Machining strategy;
- Machine accuracy.

The electrodes that are commonly used for machining during the μ EDM process are

manufactured from tungsten (W) or cemented tungsten carbide (WC) (Kawakami and Kunieda, 2005). The effect that the material microstructure has on the achievable minimum fracture sizes in EDM has been studied (Kawakami and Kunieda, 2005). The relationship between surface roughness and fracture strength of electrodes has also been investigated (Huang et al., 2004). However, the effects that the material has on the quality of electrodes produced by applying the WEDG process has not been investigated.

Generally, when machining strategies are studied in μ EDM, the main focus of such investigations is on the technological parameters and their optimisation. For example, Kawakami and Kunieda (2005) studied the influence of open voltage, capacitance and polarity on the process performance. Lim et al. (2003) investigated the characteristics of the dressing process, however the effects that depth of cut and the number of passes have on the quality of the machined electrodes have not been analysed.

Pham et al. (2004) investigated the accumulation of errors in the μ EDM drilling process and also factors affecting the accuracy of the machined holes. Although the accuracy of the electrode dressing technique was considered, the effects of electrode material and machining strategies on the electrode quality were not studied. In addition, it is important to investigate the dressing process independently from the machine on which it is implemented.

To develop the process of WEDG further there is a requirement to investigate the effects of electrode material, machining strategy, and machine accuracy on process repeatability, achievable aspect ratios, electrode surface quality, and process accuracy.

In addition, a method for improving the accuracy of the dressing process would be advantageous.

2.4.2 WEDG in combination with μ WEDM

In the field of micro machining, the surface finish achievable by applying a given technology is an important factor determining its processing capabilities, and also an important criterion for performing a process optimisation. To extend the capabilities of existing micro technologies, a number of non conventional and also “hybrid” machining processes were proposed that combine the capabilities of different complementary techniques. WEDG is a typical example of such a process (Masuzawa et al., 1985; Yu et al., 1998b).

Although many groups investigated the WEDG process (Masuzawa et al., 1985; Yu et al., 1998b; Masuzawa et al., 2005), the research was mainly focused on removing a relatively small volume of material in order to produce electrodes for performing drilling and milling operations on die-sinking μ EDM machines. In particular, typical electrodes would be dressed from 150 μ m down to 5 μ m in diameter (Masuzawa et al., 2005). The work by Rees et al. (2007) investigated the effect that the machining strategy has on the quality of electrodes produced through the process of WEDG. However, these machining strategies are not directly applicable when combining WEDG with μ WEDM as the volume of material to be removed is generally much higher. Therefore, it is required to develop dedicated machining strategies, and thus to adapt the WEDG process to specific processing conditions during μ WEDM.

Piltz and Uhlmann, (2006) investigated the effect of three different approaches for producing cylindrical components by employing die-sinking μ EDM and μ WEDM. In particular, the process behaviour in terms of pulse stability, hydrodynamic behaviour of dielectrics, machine dependent gaps and feed controls were investigated. However, this research did not study the effects of these process characteristics on the resulting surface finish, and also the optimisation issues associated with μ WEDM (Piltz and Uhlmann, 2006).

Another implementation of the WEDG process for the machining of free form cylindrical parts was investigated by Qu et al. (2002a; 2002b). The objective of this research was to extend the capabilities of the conventional WEDM technology by introducing an additional rotary axis to the machine set-up. In particular, the effects of pulse on-time, part rotational speed and wire feed rate on surface integrity and roundness of produced parts were analysed. However, the process was studied in the context of machining macro-components and thus, its findings were not directly applicable to cylindrical WEDM at micro scale.

In a study conducted by Jühr et al. (2004), the importance of selecting correct process parameters for performing the main cut during WEDM was highlighted. The research concluded that the material properties and surface finish resulting after the main cut could be improved only marginally by performing follow up cuts. Therefore, when machining micro components employing the WEDG process, special attention should be paid to the surface quality obtained after the main cut because it determines to a larger extent the achievable final surface roughness.

The exact mechanism of WEDG is not reported clearly in the literature. The conducted review of the research concerning the production of cylindrical components by EDM revealed that the focus was mostly on macro-size components, and the process effects on material removal rates (MRR) opposed to surface roughness were investigated by applying statistical methods and mathematical models (Mohammadi et al., 2008; Haddad et al., 2008; Matorian et al., 2008).

The process information obtained by using a data acquisition system provides an insight into the EDM process and its “footprint”. Once gathered and interpreted this process data can be used to develop predictive models and judge about the process performance. The acquired data once pre-processed can be used to generate a predictive model for estimating the resulting surface roughness, and thus potentially to minimise the necessary and time consuming optimisation tasks and find the causal relationship between the process footprint and surface quality.

Many machine learning techniques are available for the creation of such predictive models. However, few attempts have been made to employ such techniques in the field of EDM. One such study was described by Tsai et al. (2001) where satisfactory results were reported in applying neural networks to estimate the surface finish of parts produced by EDM. In particular, their research compared the capabilities of various neural networks for creating models for predicting the resulting surface finish as a function of the work material and electrode polarity.

However, the drawback of applying neural networks is that the created models represent a “blackbox” and are therefore almost impossible to interpret by human

experts. It would be beneficial for machine operators to be able not only to estimate the resulting surface roughness but also to understand the logic of the underlying model, and thus to allow them to comprehend the causal relations between process parameters and the resulting process performance.

2.4.3 Surface Integrity

Characterising the resulting surface integrity after machining with various micro manufacturing technologies is becoming a very important factor in broadening their application areas, and especially in satisfying the constantly growing requirements for miniaturisation, function integration, longevity and reliability of existing and emerging MST based products. Particularly, it is very important to study the influence of materials' microstructure and processing conditions on the mechanical properties of the machined surfaces.

Field and Kahles (1964) were the first to introduce the concept of surface integrity in a technical sense by defining it as the inherent or enhanced condition of a surface produced by machining processes or other surface generation operations. Their subsequent comprehensive review of surface integrity, encountered in machined components, is among the first in the published literature on this topic and this work emphasized the study of the nature of metallurgical alterations occurring in the surface layers of various alloys in material removal processes (Fields et al., 1971). Typical surface alterations were identified as plastic deformation, micro-cracking, phase transformations, hardness variations, tears and laps related to built-up edge formation,

and residual stress distribution. Field et al. (1972) subsequently presented a detailed description of measuring methods available for surface integrity inspection along with an experimental procedure for assessing surface integrity parameters. This involved three different levels of surface integrity data sets to study and evaluate the characteristic features of machined surfaces. Their pioneering contributions gained worldwide recognition and timeless value, leading to the subsequent establishment of an American National Standard for surface integrity (American National Standard on Surface Integrity 1986; Jawahir IS, et al 2011).

The sparks and plasma channels, generated during the EDM process create craters on the surface and a thermal wave propagates through the material resulting in a heat affected zone (HAZ) on the sub surface and the formation of a recast layer on the surface of the components produced through EDM (Qu et al., 2002b) thereby modifying the surface integrity of work piece surfaces. Considering the process-material interactions as a result of the plasma channel generated between the electrode and the workpiece (Wong et al., 2003), at the end of the pulse ON time, the molten material is partially ejected and vaporized from the surface by the vapour and plasma pressure, but a part of the molten material remains near the surface, held by surface tension forces. The heat quickly dissipates into the bulk of the material and a recast layer is formed by the re-solidification of the remaining liquid material on the surface. This re-solidification/recast layer is typically very fine grained and for some W300 ferritic steels found to be twice higher than that of the bulk material (Cusanelli et al., 2004). Normally this layer is subjected to a surface tensile stress regime, localised hardening microcracking, porosity and grain growth. Also it may be alloyed with carbon as a side product of dielectric ionization during the sparks, or with the material transferred from the tool (Ramasawmy et al., 2005). Immediately beneath the recast or

white layer as it is sometimes referred to is a HAZ. This is where the heat is not high enough to cause melting but is sufficiently high to induce micro-structure transformation in the material (Rebelo et al., 1998). Generally, the recast layer that is formed on the surface as a result of EDM is considered as a major flaw, thus preventing the use of EDM for some critical applications, such as aerospace components (Aspinwall et al., 2008).

In the work carried out by Lee et al. (2004) the process-material interaction were investigated, and the surface alloying effects of Ti-based materials during WEDM processing and EDM texturing were analysed. The effects of the recast layer and resulting micro hardness of components after WEDM were reported. The investigation was mostly focused on the effects of different Ti alloying compositions and did not analyse the influence of varying material microstructure.

In the work reported by Rebelo et al. (1998) the crack formation on EDM surfaces was investigated. It was concluded that cracks were associated with the development of high thermal stresses that exceeded the ultimate tensile strength of the material. For ultrafine grained (UFG) materials, the Ultimate Tensile Strength (UTS) is usually higher than that for materials with a coarse grain microstructure (Popov et al., 2006). Therefore, it is important to investigate the crack formation on WEDM surfaces of workpieces with different crystalline microstructure, especially with different grain sizes and varying UTS.

In micro machining, size effect has a major influence on the material response (Mian et

al., 2009). This is attributed to the fact that the unit or physical size of material removal can be in the same order of magnitude as the feature or the grain size of the material being processed. In the study carried out by Mian et al. (2009) it was observed that in the micro machining of multi-phase ferrite–pearlite steel, the micro tool edge radius and variation of material grain size affected milling conditions especially the resulting surface finish and burr size. The findings of this investigation although not directly applicable to the process of μ WEDM, clearly show the importance of material microstructure when performing material removal at the micro scale.

Although electrical discharge machining is essentially a material removal process, there is also a transfer of material between the electrode and work piece (Kumar et al., 2009). Kumar et al. (2009) studied the chemical composition of AISI H13 die steel after EDM. However, this research did not analyse the effect that material micro structure has on the material transfer between the electrode and the work piece.

2.5 Summary and conclusions

In the first section of this chapter, a review of the micro manufacturing process is provided. The necessity and requirements of non-silicon micro manufacturing led research and development activities are discussed, and subsequently the available micro machining platforms are presented and an overview of their capabilities is provided.

In the second section, the chapter continues with a general description of the state of the art in micro electrical discharge machining, where the main characteristics and fundamental principles are presented. In addition, within the context of the necessity

for micro electrical discharge machining and the current state of the art, the chapter concludes by identifying open research issues.

In particular, it has been shown that during the μ EDM process the volumetric wear, the ratio between electrode and workpiece wear, is relatively high and cannot be considered negligible. Thus, to manufacture microstructures there is often a need to compensate the wear by replicating electrodes. To address this requirement, a technique for on-the-machine electrode generation can be utilised called WEDG. The electrode generation and re-generation through WEDG is considered a key enabling technology for improving the performance of the μ EDM process. Consequently, it is necessary to investigate the affects that electrode material, machining strategy and machine accuracy have on the quality of electrodes produced on-the-machine.

The literature review highlighted that to broaden the application area of μ WEDM and the range of components manufactured by applying this technology, a rotary submersible spindle can be added to the equipment set-up to allow the machining of cylindrical components. To further develop this technology, new machining strategies are required together with a better understanding of the effects that spindle speed, flushing pressure, discharge intervals, open circuit voltage and pulse ON time have on the resulting surface roughness and process footprints during WEDG. Furthermore, the applicability of inductive learning models for the prediction of the resulting surface finish should be investigated. The model results have to be validated against physical field data and thus to judge better about their accuracy.

Material microstructure refinement has a significant impact on materials' machining

response and this should be explored if micro machining is to meet the constantly growing requirements for miniaturisation, functional integration, longevity and reliability of existing and new emerging MST based products. Consequently, characterising the effect that material microstructure has on the resulting surface integrity after μ WEDM machining is required to broaden the application areas of micro machining. In particular the process-material effects on the resulting micro hardness, phase content changes, heat affected zone, surface roughness, micro cracks, recast layer, material removal rate and element spectrum after both rough and finishing μ WEDM have to be investigated and characterised.

CHAPTER 3

FACTORS AFFECTING THE QUALITY OF ELECTRODES PRODUCED BY WIRE ELECTRO- DISCHARGE GRINDING

3.1 Motivation

During the μ EDM process the volumetric wear, the ratio between electrode and workpiece wear, is relatively high and cannot be considered negligible. Thus, to manufacture microstructures there is often a need to compensate the wear by replicating electrodes. To address this requirement, a technique for on-the-machine electrode generation was developed that had utilised a technology called WEDG. In spite of the development of different machining strategies, for example the uniform wear method, the multiple electrode strategy, and the wear compensation method, the accuracy and repeatability the μ EDM process is still highly dependent on the WEDG process. Thus, the electrode generation and re-generation is considered a key enabling technology for improving the performance of the μ EDM process. The investigation aims to establish an understanding of the effects that electrode material, machining strategy and machine accuracy have on the quality of electrodes produced on-the-machine.

This chapter is organised as follows. In Section 3.2 factors affecting the quality of on-the-machine dressed electrodes are discussed. Then, the research method adopted to investigate experimentally the factors that influence the quality of the dressed electrodes is described in Section 3.3. Next, section 3.4 presents the experimental results and analyses the factors that affect that electrode material, machining strategy and machine accuracy have on the quality of electrodes produced on-the-machine and a solution is proposed to improve this process. Finally, Section 3.5 summarises the research and gives conclusions.

3.2 Factors affecting electrode quality

As it was stated in the previous section the electrode generation and re-generation is considered a key enabling technology for improving the performance of the μ EDM process (Masuzawa, 2001). Some of the factors affecting the quality of the dressed electrodes are discussed below.

- Electrode material;
- Machining strategy;
- Machine accuracy.

The electrodes that are commonly used for machining during the μ EDM process are manufactured from W or cemented WC. The effect that the material micro structure has on the achievable minimum fracture sizes in EDM has been studied by Kawakami and Kunieda (2005). The relationship between surface roughness and fracture strength of

electrodes has also been investigated by Huang et al., (2004). However, the effects that the material has on the quality of electrodes produced by applying the WEDG process has not been investigated.

Generally, when machining strategies are studied in μ EDM, the main focus of such investigations is on the technological parameters and their optimisation. For example, Kawakami and Kunieda (2005) studied the influence of open voltage, capacitance and polarity on the process performance. Lim et al., (2003) investigated the characteristics of the dressing process, however the effects that depth of cut and the number of passes have on the quality of the machined electrodes have not been analysed.

Pham et al., (2004) investigated the accumulation of errors in the μ EDM drilling process and also factors affecting the accuracy of the machined holes. Although the accuracy of the electrode dressing technique was considered, the effects of electrode material and machining strategies on the electrode quality were not studied. In addition, it is important to investigate the dressing process independently from the machine on which it is implemented.

In this study the same experimental set-up as in Pham et al. (2004) is used to assess the capabilities of the on-the-machine electrode dressing process. In particular, this research investigates the effects of electrode material, machining strategy, and machine accuracy on process repeatability, achievable aspect ratios, electrode surface quality, and process accuracy. Also, a method is proposed for improving the accuracy of the dressing process.

3.3 Experimental Set-up

To study the factors affecting the quality of on-the-machine dressed electrodes, a WEDG system (APPENDIX A) was designed and manufactured similar to that design proposed by Masuzawa et al. (1985) is employed. Figure 3.1 shows the system design and its working principle. The continuously running wire of a copper and zinc alloy is fed from a retaining spool into the system at a speed of 3 – 5 mm/s. The retention of the wire spool ensures that a constant tension is applied to the Ø 0.3 mm running wire throughout the dressing process. Then, the running wire goes through a vibration damper. Next it travels around a fixed guide that ensures wire stability during the process. This is also the position where the electrode dressing takes place. Finally the wire progresses further through one more guides before it is deposited. The dressing set-up is also shown in Figure 2.6.

In this research the same grinding unit is used on two μ EDM machines, Agietron Compact 1 Micro die sink (APPENDIX B) and Sarix SX-100 HPM Micro Hole Drilling machine (APPENDIX C). For all experiments the machine programmes were generated manually.

The electrodes employed in this study are W and WC rods, commonly used in μ EDM machining. On both machines the rods are clamped in rotating spindles. The technological parameters applied in the dressing processes are given in Table 3.1 and Table 3.2

To examine the surface quality of the dressed electrodes, 3D profiles were generated, by scanning the test pieces using a surface mapping system, Micro-XAM. In addition, an optical measuring system, Quick Vision Accel, was employed to measure the machined electrodes.

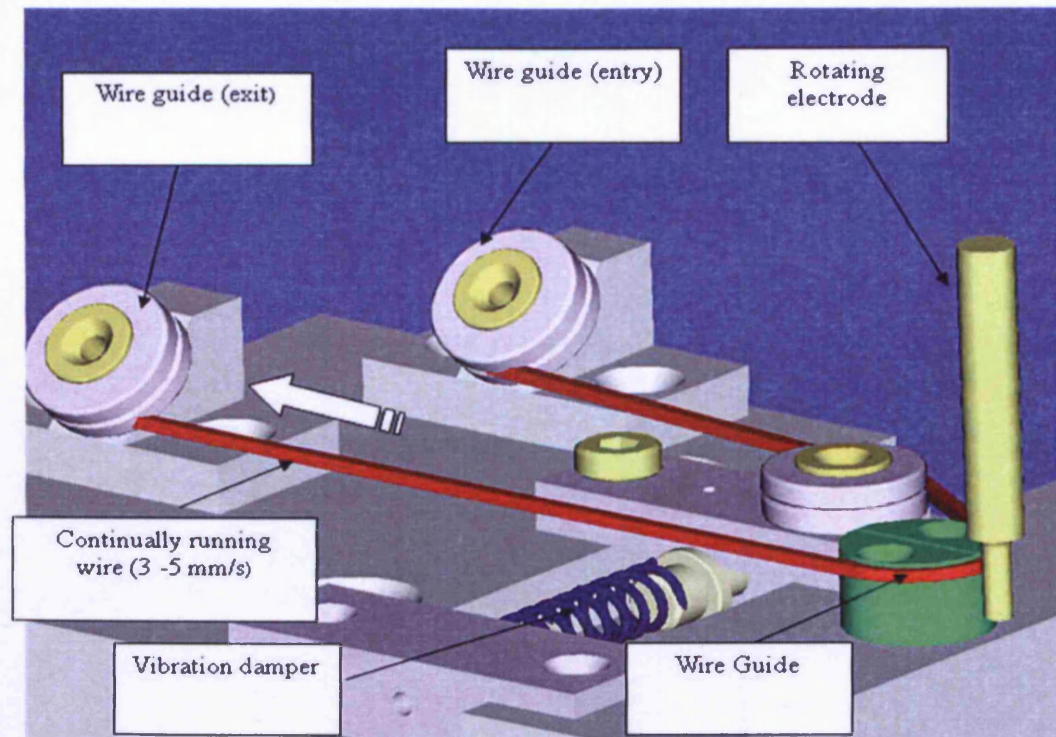


Figure 3.1 Experimental set-up

Table 3.1 Technology parameters used on the AGIE machine

Technological parameter	Value
Polarity	Positive
Open voltage	60 V
Discharge current	0.8 A
Time ON	1.3 μ s
Time OFF	1.8 μ s
Discharge voltage	20 V
Capacitance	15 nF
Discharge energy	1.2 μ J

Table 3.2 Technology parameters applied on the Sarix machine

Technological parameters	Value
Polarity	Positive
Open voltage	90 V
Discharge current	2 A
Time ON	5 μ s
Time OFF	3.3 μ s
Discharge voltage	35 V
Capacitance	33 nF
Discharge energy	2.02 μ J

3.4 Experimental Results

3.4.1 Electrode material

In this research, the influence of the electrode material on the WEDG process behaviour in regard to its repeatability and achievable aspect ratio is investigated. A set of experiments were conducted where electrodes were dressed from a diameter of $150\mu\text{m}$, D_1 , down to $20\mu\text{m}$, D_2 to a length of 3mm. The technological parameters for performing this dressing operation are shown in Table 3.1. The electrodes were manufactured by applying a three passes machining strategy as illustrated in Figure 3.2. In particular, the electrode diameters were reduced by $50\mu\text{m}$ in the first machining pass and then by $40\mu\text{m}$ during the second and the third passes.

Figure 3.3 shows that WC electrodes with high aspect ratios were produced consistently in all tests and their diameters varied in the range of $17\mu\text{m}$ to $23\mu\text{m}$. However, only 6 out of the 10 tests were successful when the W electrodes were dressed. One possible explanation of these results is the relatively high Young's Modulus of Elasticity of WC, 713 GPa (Shackelford and Alexander, 2001), in comparison with that of W, 344 GPa (Van Vlack, 1970). The experiments also showed that WC was less prone to fracture, and thus high aspect ratio electrodes were produced repeatedly.

To analyse the process limitations when producing high aspect ratio electrodes, ten consecutive experiments were carried out whereby WC electrodes were dressed to an aspect ratio of 250 (see Figure 3.4). All ten WC electrodes were successfully produced.

However, when the same test was performed on W electrodes, it was not possible to achieve such high aspect ratios in any of the ten consecutive trials. The highest aspect ratio that could be achieved with the W electrodes was 150 in 6 out of 10 experiments.

To assess the effects that the electrode material has on the surface finish achievable during the dressing process, the roughness of one W and one WC electrodes were analysed. Both electrodes were dressed to a diameter of 20 μ m with a length of 1mm using the technology in Table 3.1. The electrodes were cut applying a one pass machining strategy.

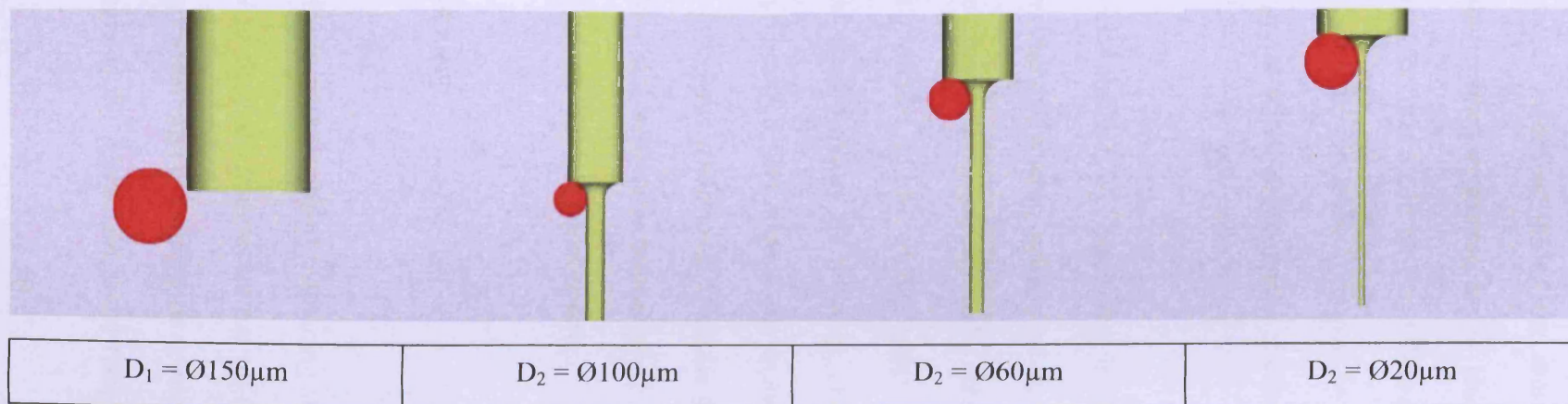


Figure 3.2 Electrode dressing operation

A lower surface finish was achieved on the W electrode, Ra 0.95, than on the WC electrode, Ra 1.35, as shown in Figure 3.5. A possible explanation of this result could be found in the process behaviour during the dressing. In particular, the dressing process was more stable when machining the W electrodes which were produced by extrusion. The reason for this could be the different microstructure of W and WC electrodes. The WC sintered electrode is formed by 'cementing' very hard tungsten monocarbide (WC) grains into a binder matrix of cobalt (Co) by liquid phase sintering (Tao et al., 2006).

Thus, the erosion behaviour of WC electrodes is determined by its microstructure. Compared to W, the thermodynamic stability of the WC particles in a Co binder is relatively low, which has a direct impact on the electrode surface quality during the dressing process. In particular, in case of WC composites, the melting temperatures of the WC particles and the Co binder are different, 2800°C (Janmanee and Muttamara, 2010) and 1492°C (Higgins, 1994) respectively in atmospheric pressure, compared to 3422°C for W under the same conditions. Thus, the melting of the WC grains and the Co binder take place at different temperatures which could explain a relatively higher roughness witnessed on the WC in Co electrodes.

3.4.2 Machining strategy

In this section the effects of the applied machining strategies on the electrode surface finish are discussed. In the research carried out by (Allen et al., 1999) tapering and ovality was witnessed when high machining rates were used. As the WC rods showed no signs of form errors in the performed initial tests only the resulting surface finish

was investigated. The WC rods were dressed from D_1 of $150\mu\text{m}$ to D_2 of $20\mu\text{m}$ with a length of 2mm . Each electrode was produced using a range of cutting depths as shown in Figure 3.6 using 1, 2 or 4 cut machining strategies. The dressing operation was carried out applying the sparking conditions in Table 3.1.

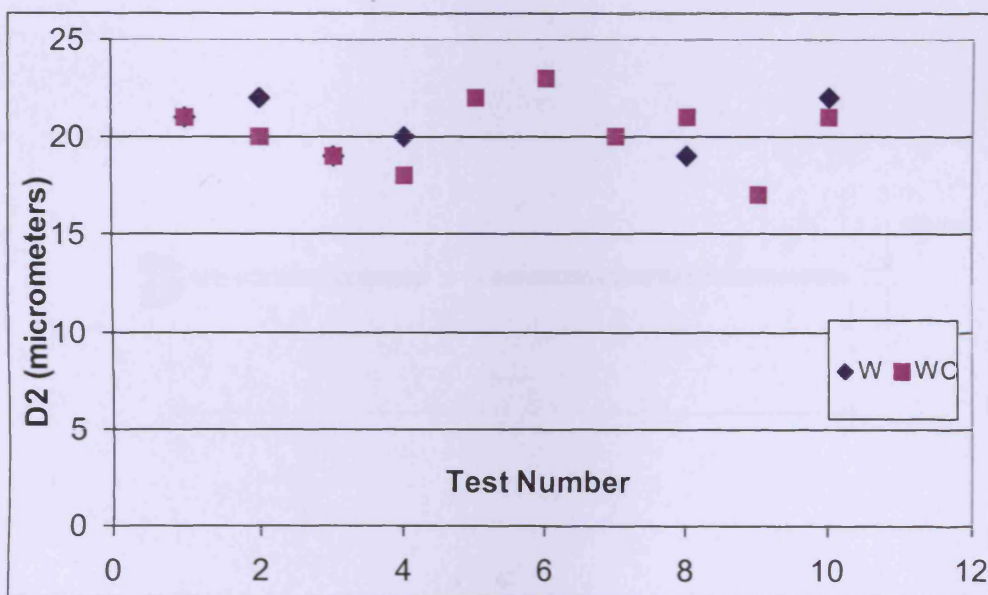


Figure 3.3 Relationship between electrode material, process deviation (D_2) and the repeatability of high aspect ratio electrodes

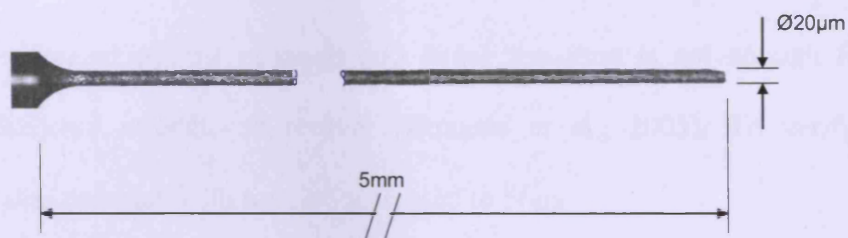


Figure 3.4 A Ø120 µm rod ground to Ø20 µm with an aspect ratio of 250

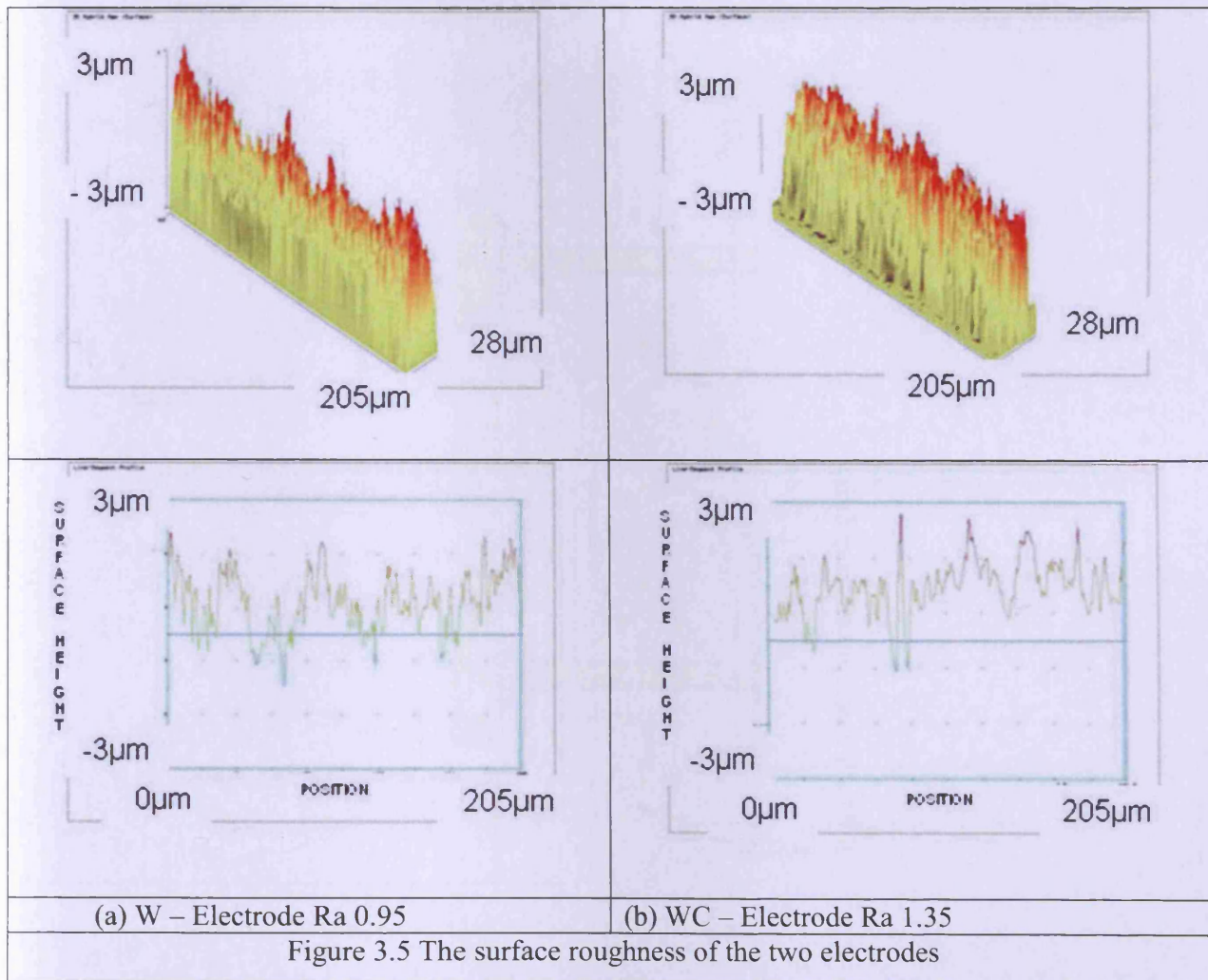
Figure 3.7 shows that the volume of material removed during the dressing process has a major effect on the resulting surface quality. The surface finish improves considerably with the reduction of the depth of the cut. The relatively poor surface quality when the dressing was performed in one and two cuts, could be attributed to a combination of two factors, a vibration of the running wire, and the technology parameters used on the machine. When trying to remove large amounts of material with a single cut, in Experiment 1, it is possible that the selected time OFF of $1.8\ \mu\text{s}$ was not suitable. Also, the poor surface finish could be explained with the large number of false discharges caused by the relatively short time off. As a result of this, there is not sufficient time to extinguish the created plasma channels and hence the time is not enough for the dielectric breakdown strength to recover (Kunieda et al., 2005). To verify this, Experiment 1 was repeated with time off increased to $56\mu\text{s}$.

Figure 3.8 shows the results of this repeated experiment. As can be seen, the modifications to the sparking conditions have little effect on the electrode surface quality. The time taken to dress the electrode increased from 6 minutes and 13 seconds to 16 minutes and 34 seconds. Thus, it could be concluded that the relatively poor surface quality achieved in Experiment 1 and 2 was due to vibration of the running wire and also due to some variations of its diameter (ΔD_w).

3.4.3 Machine accuracy

Before electrode dressing can start, the reference position of the running wire on the dressing device needs to be determined. During the initial setting up of the process an electrical contact occurs between the electrode and the running wire, and this contact

signal is registered by the machine CNC system. However, when the electrode approaches the dressing entity, the check for the existence of a contact is not carried out continuously and thus there is a time delay in its registering. Pham et al. (2004) have investigated methods to improve this referencing procedure. In particular, the machine positional accuracy and repeatability can be improved by using a unidirectional approach when bringing the electrode into contact with the running wire and also through optimising the approaching speed to minimise the time delay in registering the contact. It is important to note that the specific design of the WEDG unit affects also the accuracy of the dressing operation. To investigate the errors introduced by the adopted method for setting up the 'dressing position', experiments were conducted on a continuously running wire and on a WC block as shown in Figure 3.9.



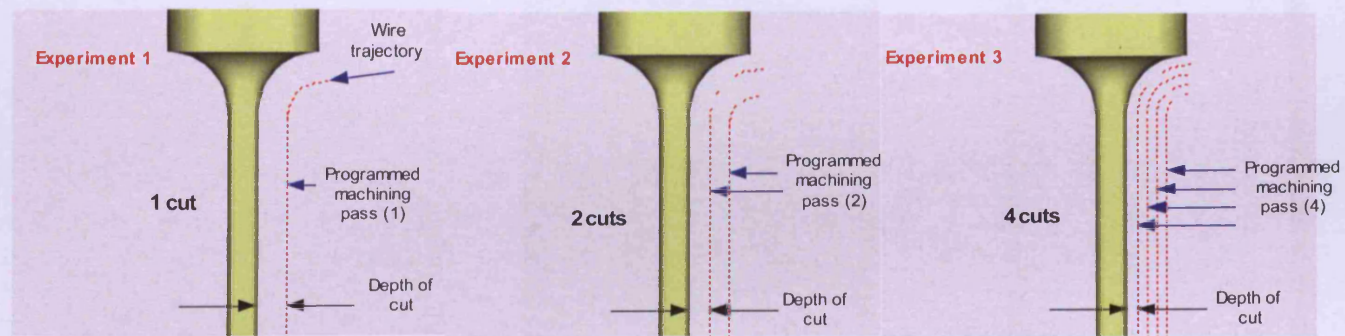
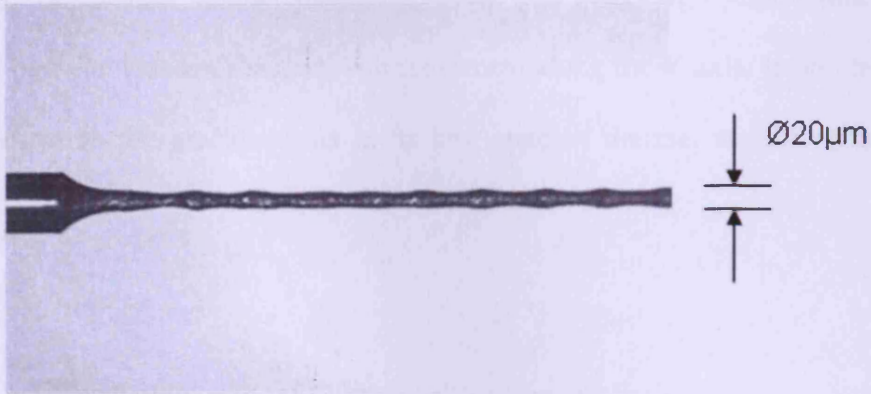
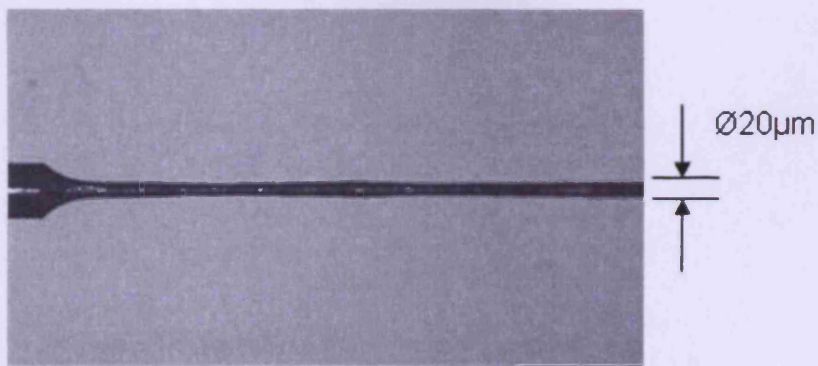


Figure 3.6 Machining strategies



(a) Experiment 1: a one cut machining strategy



(b) Experiment 2: a two cuts' machining strategy



(c) Experiment 3: a four cuts' machining strategy

Figure 3.7 Electrodes produced during the three experiments

20 tests were carried out using the same experimental set-up as in Pham et al. (2004). Whereby, the lowest contact detection speed was selected, 1 mm/minute, and the dressing position was approached with movement along the Y axis. In addition, during the experiments the machine was in its best state of thermal stability (Pham et al., 2004).

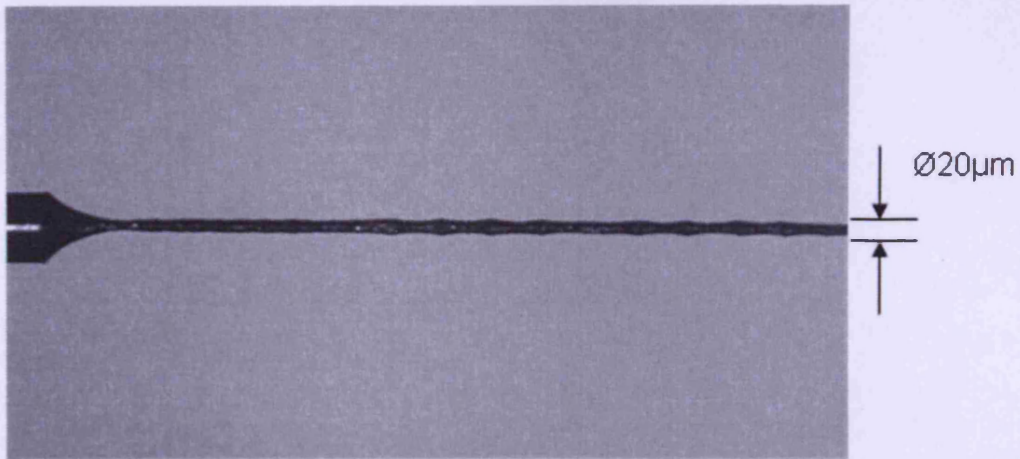
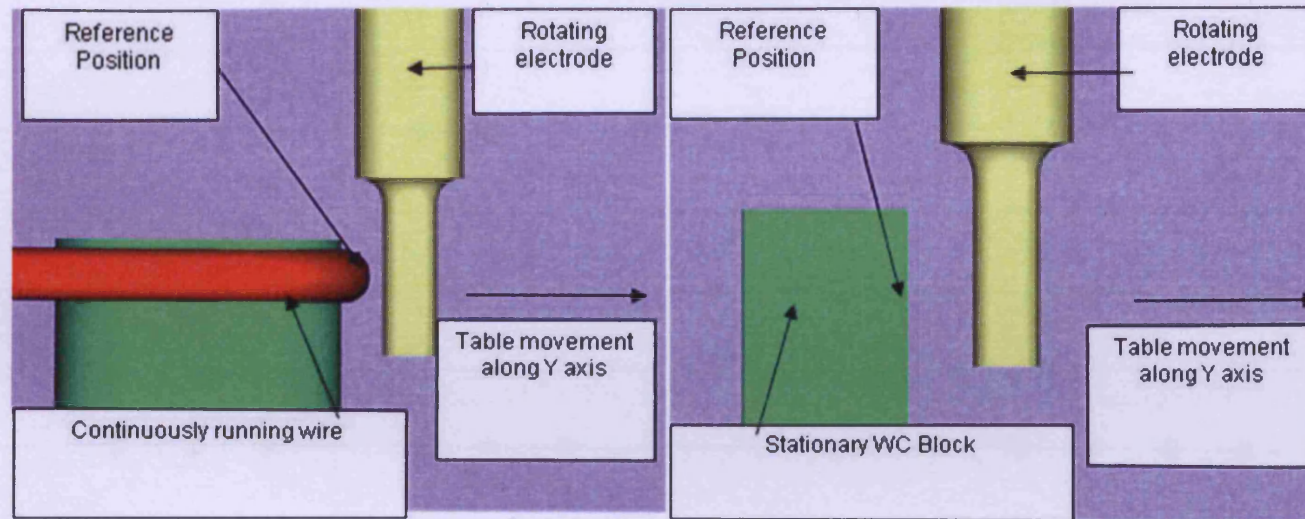


Figure 3.8 The electrode machined in the repeated first experiment

Errors in setting up the 'dressing position' occurred as illustrated in Figure 3.10, due to the machine positioning accuracy and repeatability, ΔY_{pos} . Although the machine temperature was stabilised before the machining, some degree of thermal deformation occurred during the process. The continuously running wire used on the WEDG unit had also introduced some errors, ΔD_w (Kawakami and Kunieda, 2005). In particular, the variations observed during the setting up process could be a result of the wire vibrations. In addition, the diameter of the dressing wire is prone to a degree variation due to the tolerance of the wire used.



(a) A running wire

(b) A WC block

Figure 3.9 Reference position set-ups

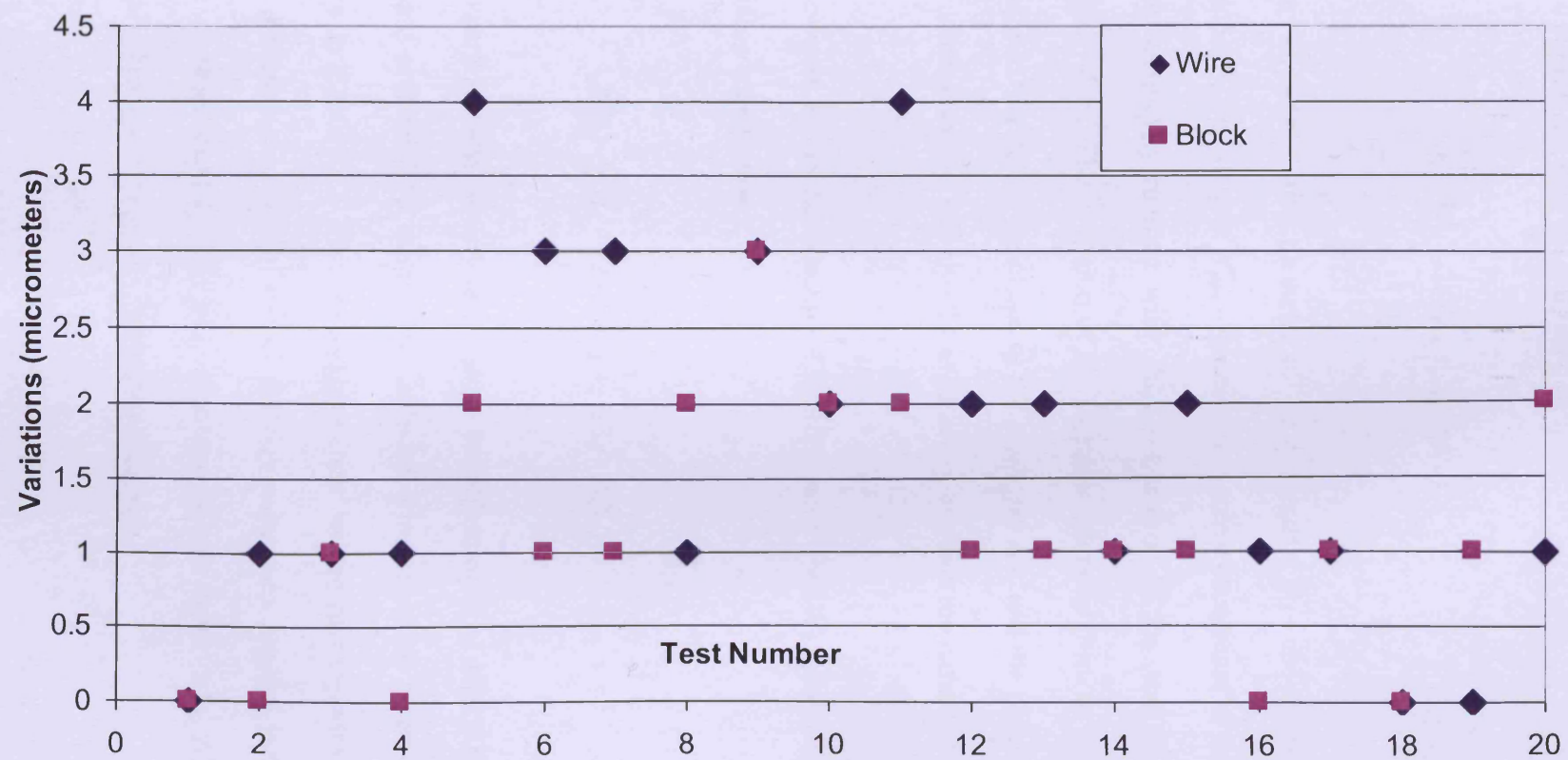


Figure 3.10 Variations in setting up the 'dressing position'

Figure 3.11 shows the dressing procedure used in this research. The dressing movement can be expressed using the following equation:

$$D_2 = D_1 - 2(Y_{pos} + S_g + D_w) \quad (1)$$

where: D_1 is the initial diameter of the electrode; D_2 - the diameter of the dressed electrode; S_g - spark gap; Y_{pos} - machine movement coordinate of the electrode relative to the continually running wire; ΔD_w – variation of the wire diameter from their nominal values. The deviation of the electrode diameter from its target value after the dressing ΔD_2 is due to variations of the spark gap ΔS_g and the wire diameter ΔD_w from their nominal values, and also the accuracy of machine movement, ΔY_{pos} .

These errors within the ‘Machine-Electrode-Wire’ (MEW) system can be expressed by the following equation:

$$\Delta D_2 = \Delta D_1 + 2 (\Delta Y_{pos} + \Delta S_g + \Delta D_w) \quad (2)$$

An experiment was carried out to assess the effects of ΔD_1 , ΔS_g , ΔY_{pos} and ΔD_w on the dressing process. The experiment included dressing of 10 electrodes to the profile shown in Figure 3.12. The ‘dressing position’ on the running wire was set-up before each electrode machining. The technology parameters applied in the tests were the same as those used in the other experiments (see Table 3.1). All electrodes were produced using a ‘three cuts’ machining strategy.

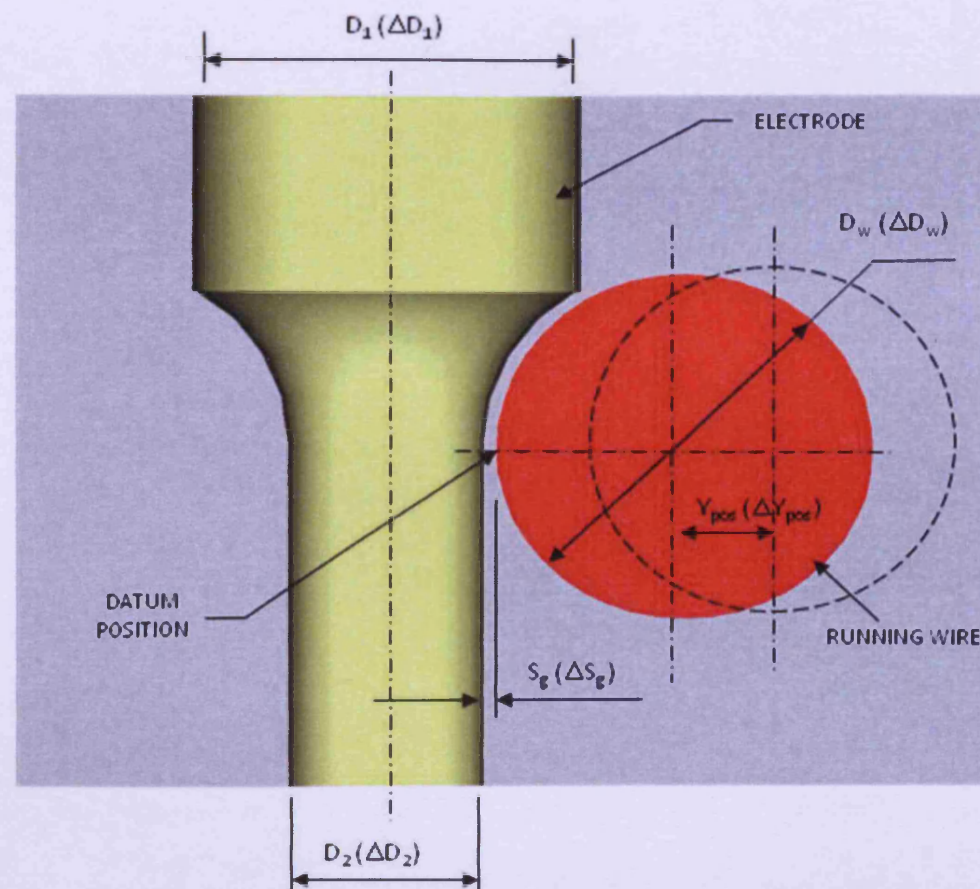


Figure 3.11 Dressing Procedure

The results of the tests are shown in Figure 3.13. The variations of the electrode diameter, ΔD_2 , are caused by several factors. In particular, the errors during the dressing process are due to machine positional accuracy and repeatability, ΔY_{pos} , spark gap variations, ΔS_g , thermal instability, and a dressing position detection error. According to this experiment, ΔD_2 could be up to $21\mu\text{m}$ that is not acceptable for many applications. Therefore, an approach to improve the accuracy of the dressing process is discussed in the next section.

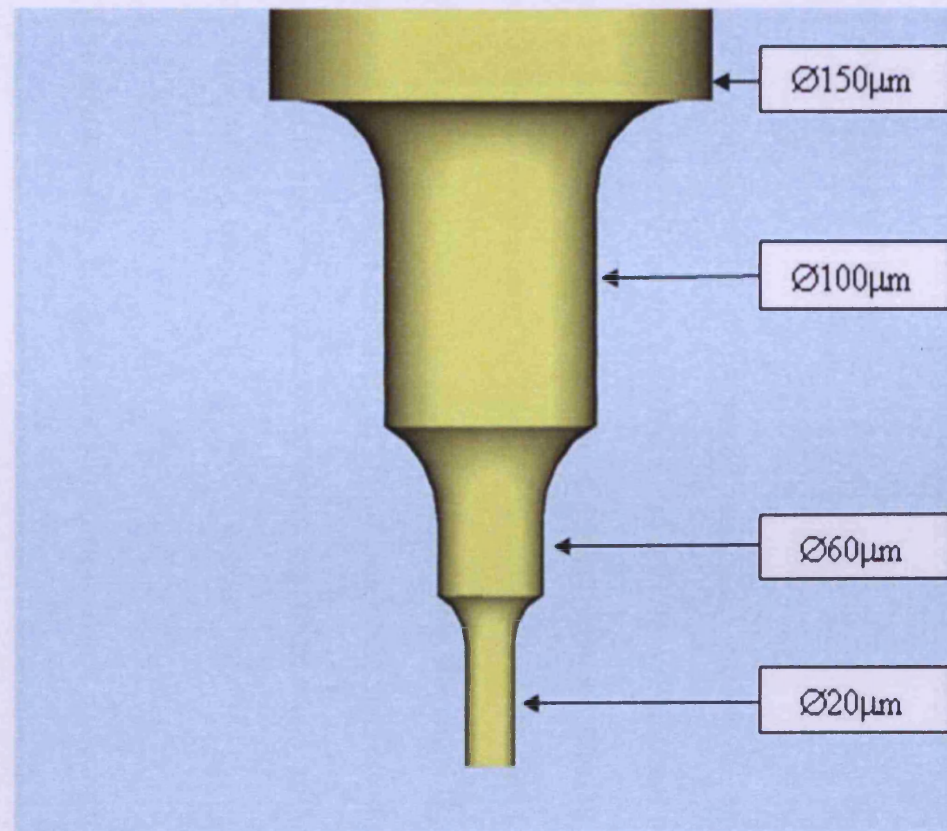


Figure 3.12 The profile of the dressed electrode

3.4.4 Process Improvements

To improve the accuracy of the dressing process, it is required to compensate some of the errors within the MEW system. In this research the process improvements that could be achieved by utilising an optical verification method are discussed. The flow chart describing the compensation process utilising such an optical measuring device is presented in Figure 3.14. In particular, the device applied in this study is an Erowa x80 microscope as shown in Figure 3.15.

To assess the capabilities of the proposed verification method, the optical device was fitted to the Agietron Compact 1 Micro die sink EDM machine and the compensation procedure in Figure 3.14 applied. The experiment included dressing sequentially 10 electrodes to the profile shown in Figure 3.12 and applying the technology parameters in Table 3.1. The electrodes were initially dressed to a diameter, $D_2 + \Delta D_2$, which is bigger than the final target diameters of D_2 for each of the steps, $\varnothing 100 \mu\text{m}$, $\varnothing 60 \mu\text{m}$ or $\varnothing 20 \mu\text{m}$, respectively. This was done to ensure that there was a sufficient material left to compensate for any errors within the MEW system.

After the initial dressing, the electrodes were measured and if required, corrections, ΔC , were introduced. This procedure is interactive and continues until $D_2 - D_2^M$ is within acceptable limits. Due to the machine accuracy and repeatability and errors in optical measurements there will always be some deviation ΔD_2 . The results of the experiment are given in Figure 3.16.

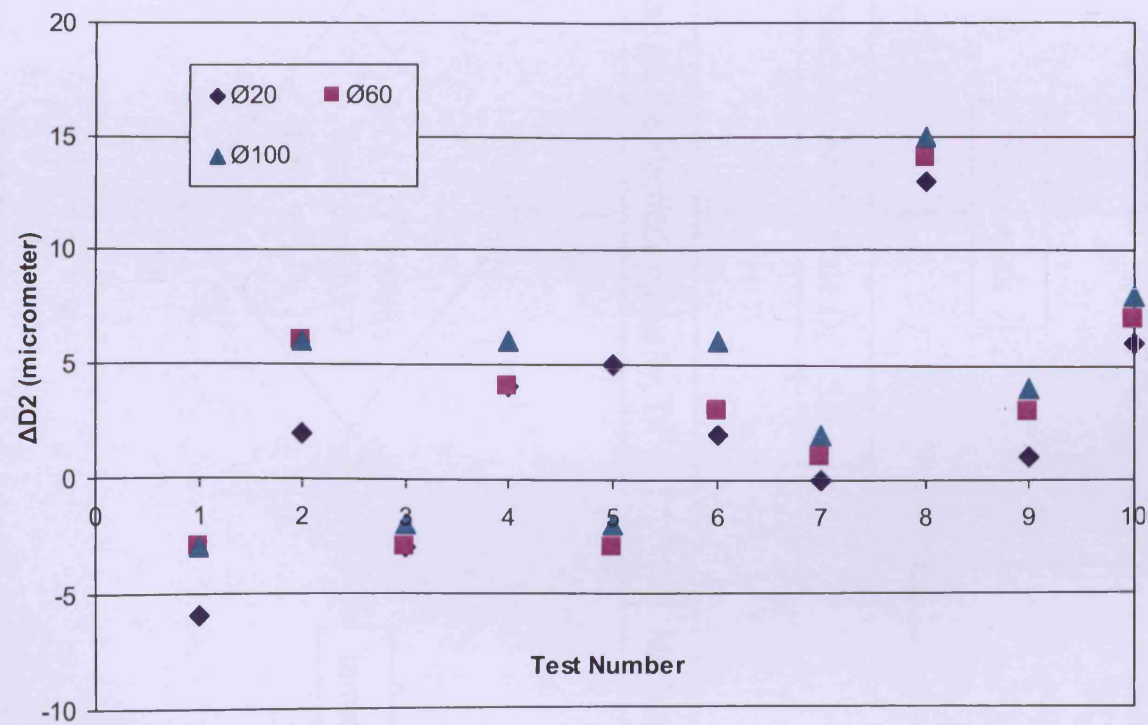


Figure 3.13 Variations of the diameter of the dressed electrodes

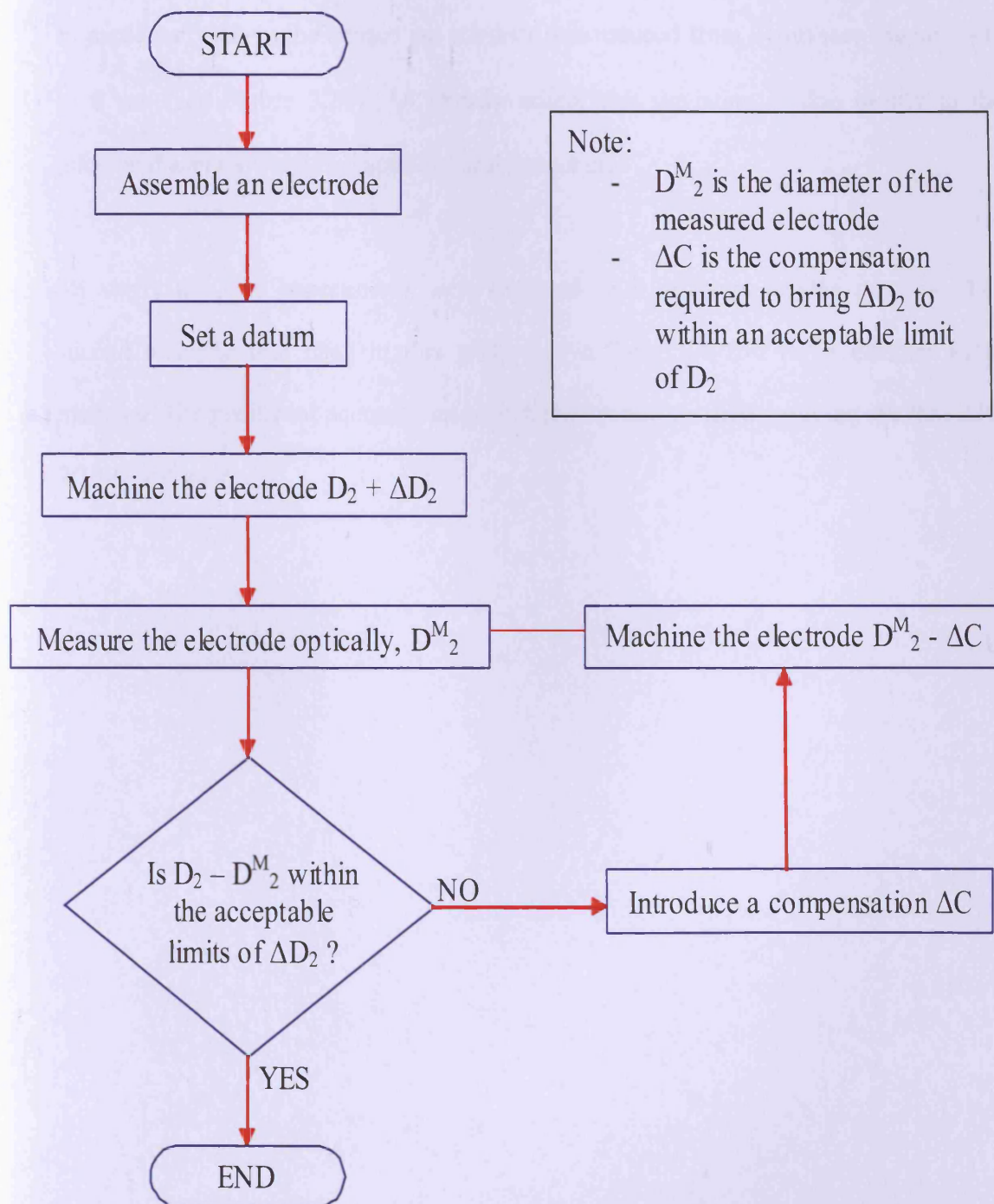


Figure 3.14 Flowchart of the compensation procedure

The variability previously witnessed in the dressing process was considerably reduced. In particular, ΔD_2 in the carried out ten tests was reduced from 21 μm (see Figure 3.13) to 8 μm (see Figure 3.16). As already stated, this deviation is due mostly to the positional accuracy and repeatability of the machine.

To verify this, the experiments were repeated on a different μEDM machine. The second machine tool used in this study was a Sarix SX-100 HPM desktop EDM machine. The positional accuracy and repeatability was verified applying the ISO 230-2:1997 test code.

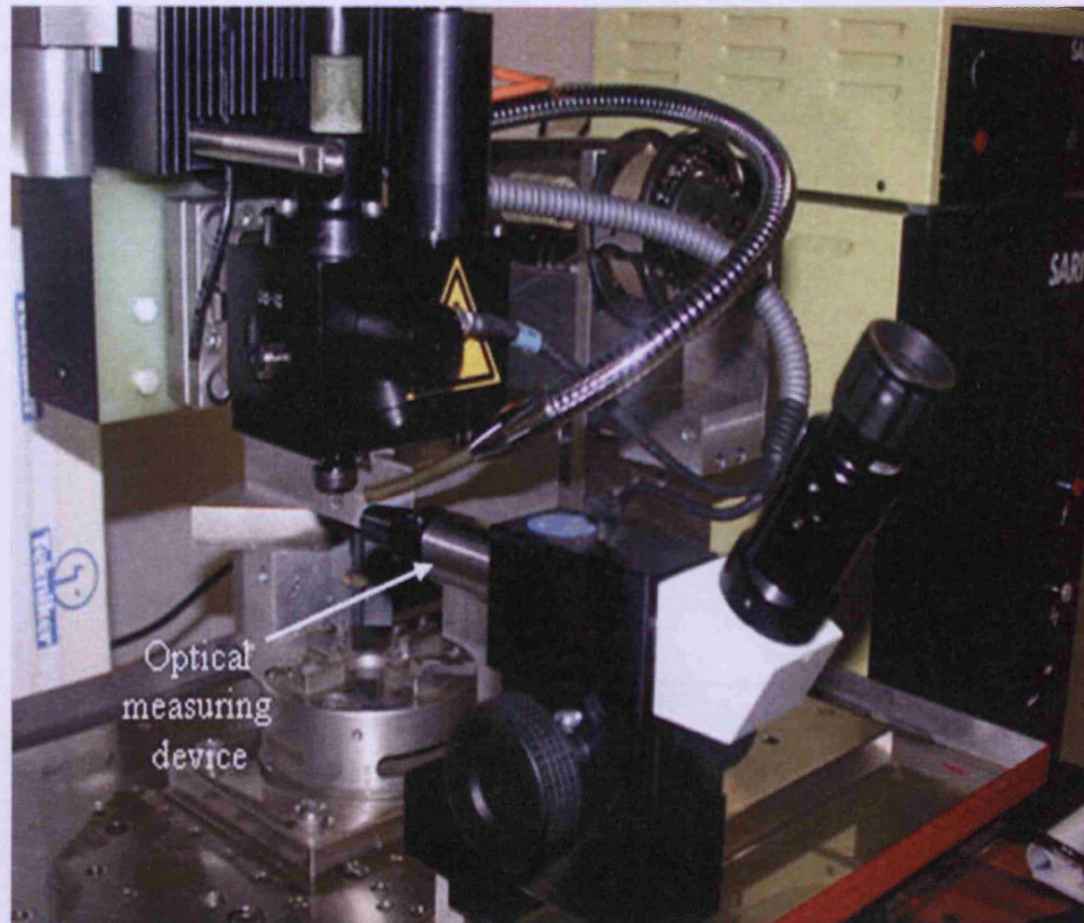


Figure 3.15 Optical measurement set-up

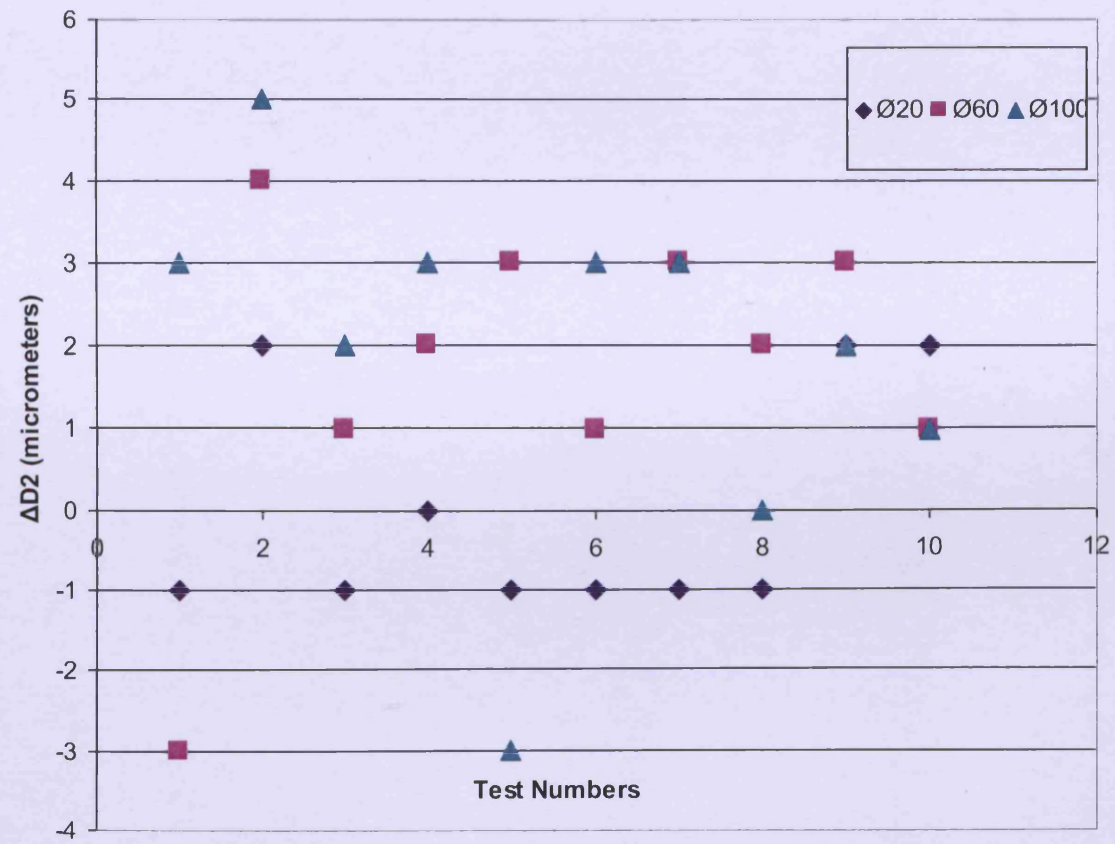


Figure 3.16 Variations of the diameter of the dressed electrodes

Once again the experiment included dressing 10 electrodes from diameters of 150 μm to 10 μm applying the same WEDG set-up as that on the first machine and also the technology parameters in Table 3.2. Initially, 10 electrodes were produced without using the optical verification process. Then a further 10 electrodes were dressed following the procedure in Figure 3.14.

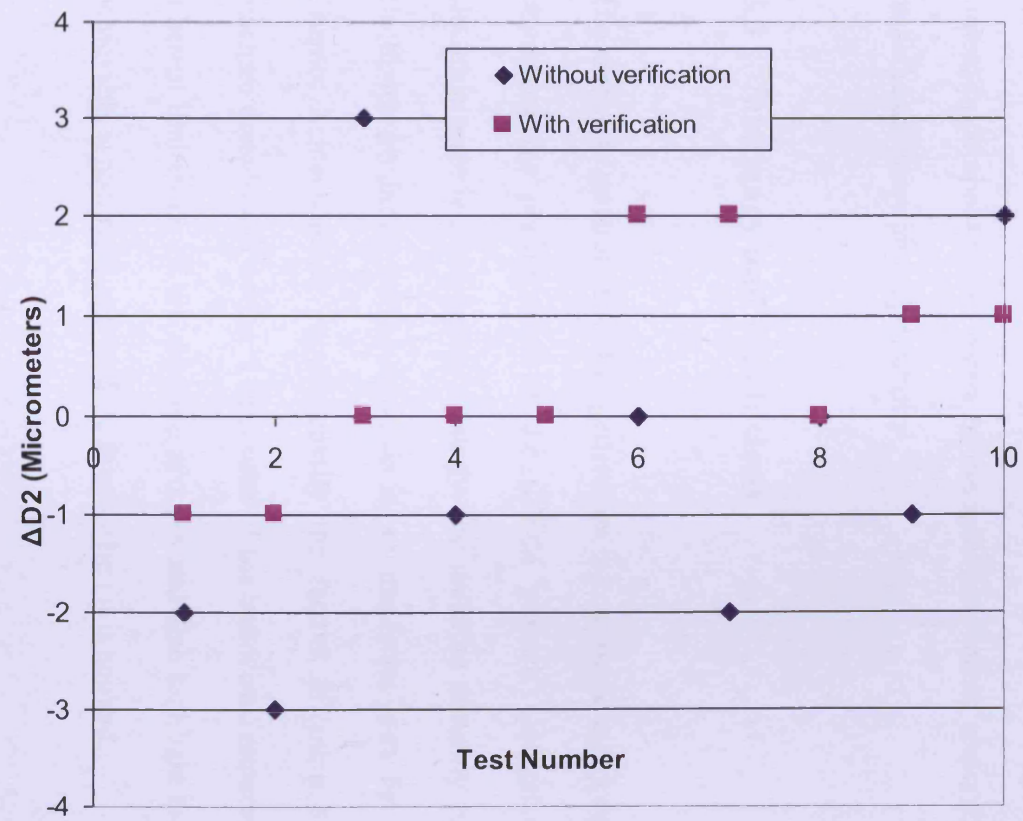


Figure 3.17 Diameters of dressed electrodes with and without optical verification on the Sarix machine

The results of the experiments are provided in Figure 3.17. As expected the accuracy of the dressing process is very much dependent on the machine accuracy. The deviation of ΔD_2 decreased significantly when the proposed verification procedure was applied. In particular, ΔD_2 decreases from 9 to 3 μm . The high accuracy of the dressing process is directly linked to the machine high accuracy. This demonstrates that the proposed compensation method is highly effective and could be used as an adaptive control system to compensate for many of the inherent process errors except those related to machine accuracy and repeatability.

3.5 Summary and conclusions

The electrode generation and re-generation is considered a key enabling technology for improving the performance of the μEDM process. Understanding the affect that electrode material, machining strategy and machine accuracy have on the quality of electrodes produced on-the-machine is an important area for further investigation. Chapter 3 investigated experimentally the factors effecting the quality of on-the-machine dressed electrodes. The results of the conducted experiments demonstrate the inherent limitations of the dressing process and also highlight the factors affecting the achievable aspect ratio and surface finish when it is applied.

The following conclusions could be drawn from this experimental study.

- To produce high aspect ratio electrodes WC is more appropriate than W. An aspect ratio of 250 was achieved repeatedly when dressing WC electrodes in comparison to aspect ratios of 150 in the case of W.

- A lower surface finish can be achieved on W electrodes in comparison with that on WC electrodes. This could be attributed to the thermodynamic stability of WC that is relatively low compared to W.
- The applied dressing strategy has a major effect on the quality of the electrode. A high number of machining passes leads to a higher standard of surface finish. To a lesser extent vibration and variation in the diameter of the continually running wire affect also the surface quality.
- Variations in the setting of the 'dressing position' occur due to the positioning accuracy and the repeatability of EDM machines. In addition, the running wire is also prone to a dimensional variation when the electrodes are brought into contact with it during the dressing process.
- By employing an optical verification system, many of the factors that affect the accuracy of the machined electrode can be compensated. A compensation method is proposed to allow adaptive control of the dressing process that significantly increases the accuracy of the dressing process. The method proved to be highly effective and could be used to reduce many of the inherent process errors except those related to machine accuracy and repeatability.

CHAPTER 4

SURFACE FINISH OPTIMISATION AND PREDICTION FOR WIRE ELECTRO DISCHARGE GRINDING

4.1 Motivation

To broaden the application area of μ WEDM and the range of components manufactured by applying this technology, a rotary submergible spindle can be added to the equipment set-up to allow the machining of cylindrical components. This type of machining is termed WEDG. To develop this technology further requires the development of new machining strategies, and to gain a further understanding of the effects that spindle speed, flushing pressure, discharge interval, open circuit voltage and pulse ON time in particular their effects on the resulting surface roughness after performing the main cut in WEDG. Through process optimisation this study will evaluate the possibility of producing axis-symmetric components with surface roughness comparable to that achievable when performing conventional μ WEDM. In addition, the study investigates the development of predictive models for accessing the resulting surface finish by employing inductive learning techniques for data processing.

This chapter is organised as follows. In Section 4.2 some of the limitations and processing capability of the WEDG system when used in combination with either the μ EDM or μ WEDM are discussed. Then an experimental study employing the Taguchi

parameter design method is conducted to identify the most statistically significant main cut set-up parameters that affect the surface roughness through analysis of variance (ANOVA) as described in Section 4.3. The next section 4.4 presents a signal-to-noise (S/N) ratio analysis to optimise the technological parameters for performing WEDG and analysis the difference between the fundamental voltage pulse profiles in WEDG and μ WEDM. Section 4.5 explores the use of an inductive learning algorithm to generate a model for on-the-machine prediction of the surface roughness. Finally, Section 4.6 summarises the research carried out and gives conclusions.

4.2 WEDG and μ WEDM

In the field of micro machining, the surface finish achievable by applying a given technology is an important factor determining its processing capabilities, and also an important criterion for performing a process optimisation. To extend the capabilities of existing micro technologies, a number of non conventional and also “hybrid” machining processes were proposed that combine the capabilities of different complementary techniques. WEDG is a typical example of such a process (Masuzawa et al., 1985; Yu et al., 1998b; Weng et al., 2003).

Although many groups investigated the WEDG process (Masuzawa et al., 1985; Yu et al., 1998b; Masuzawa et al., 2005), the research was mainly focused on removing a relatively small volume of material in order to produce electrodes for performing drilling and milling operations on die-sinking μ EDM machines. In particular, typically the electrodes would be dressed from 150 μ m down to 5 μ m in diameter (Masuzawa et

al., 2005). The work by Rees et al. (2007) investigated the effect that the machining strategy has on the quality of electrodes produced through the process of WEDG. However, these machining strategies are not directly applicable when combining WEDG with μ WEDM as the volume of material to be removed is generally much higher. Therefore, it is required to develop dedicated machining strategies, and thus to adapt the WEDG process to specific processing conditions during μ WEDM.

Piltz and Uhlmann, (2006) investigated the effect of three different approaches for producing cylindrical components by employing die-sinking μ EDM and μ WEDM. In particular, the process behaviour in terms of pulse stability, hydrodynamic behaviour of dielectrics, machine dependent gaps and feed controls were investigated. However, this research did not study the effects of these process characteristics on the resulting surface finish, and also the optimisation issues associated with μ WEDM (Piltz and Uhlmann, 2006).

Another implementation of the WEDG process for the machining of free form cylindrical parts was investigated by Qu et al. (2002a; 2002b). The objective of this research was to extend the capabilities of the conventional WEDM technology by introducing an additional rotary axis to the machine set-up. In particular, the effects of pulse on-time, part rotational speed and wire feed rate on surface integrity and roundness of produced parts were analysed. However, the process was studied in the context of machining macro-components and thus, its findings were not directly applicable to cylindrical WEDM at micro scale.

In a study conducted by Juhr et al. (2004), the importance of selecting correct process parameters for performing the main cut during WEDM was highlighted. The research concluded that the material properties and surface finish resulting after the main cut could be improved only marginally by performing follow up cuts. Therefore, when machining micro components employing the WEDG process, a special attention should be paid to the surface quality obtained after the main cut because it determines to a larger extent the achievable final surface roughness.

The exact mechanism of WEDG is not reported clearly in the literature. The conducted review of the research concerning the production of cylindrical components by EDM revealed that the focus was mostly on macro-size components, and the process effects on material removal rates (MRR) as opposed to surface roughness were investigated by applying statistical methods and mathematical models (Mohammadi et al., 2008; Haddad et al., 2008; Matoorian et al., 2008).

In this context, the effects of spindle speed, flushing pressure, discharge interval, open circuit voltage and pulse ON time on the resulting surface roughness after performing the main cut in WEDG were investigated experimentally in this investigation. Prior to conducting the machining experiments a method was devised for workpiece preparation in order to overcome the limitations of existing machining strategies. Then, by employing the Taguchi parameter design method a set of experiments was conducted. Analysis of variance (ANOVA) was then employed to identify the most statistically significant factors affecting the surface quality. Next, a signal-to-noise (S/N) ratio analysis was conducted to optimise the technological parameters for

performing WEDG. Furthermore, voltage pulse waveforms were studied to quantify the fundamental differences between WEDG and μ WEDM. Finally, an on-the-machine prediction method was proposed to create a rule set for assessing the resulting surface roughness after WEDG.

4.3 Experimental set-up

In this experimental study, a 50 μ m brass coated steel wire was used as an electrode and the test pieces employed were 3 mm in diameter and composed of 94% tungsten carbide and 6% cobalt. In particular, the workpiece material was produced through sintering powder with an average grain size of 0.3 μ m. In the proposed experimental set-up, the test piece was fixed on the machine utilising the collet of the submergible rotating spindle as shown in Figure 4.1.

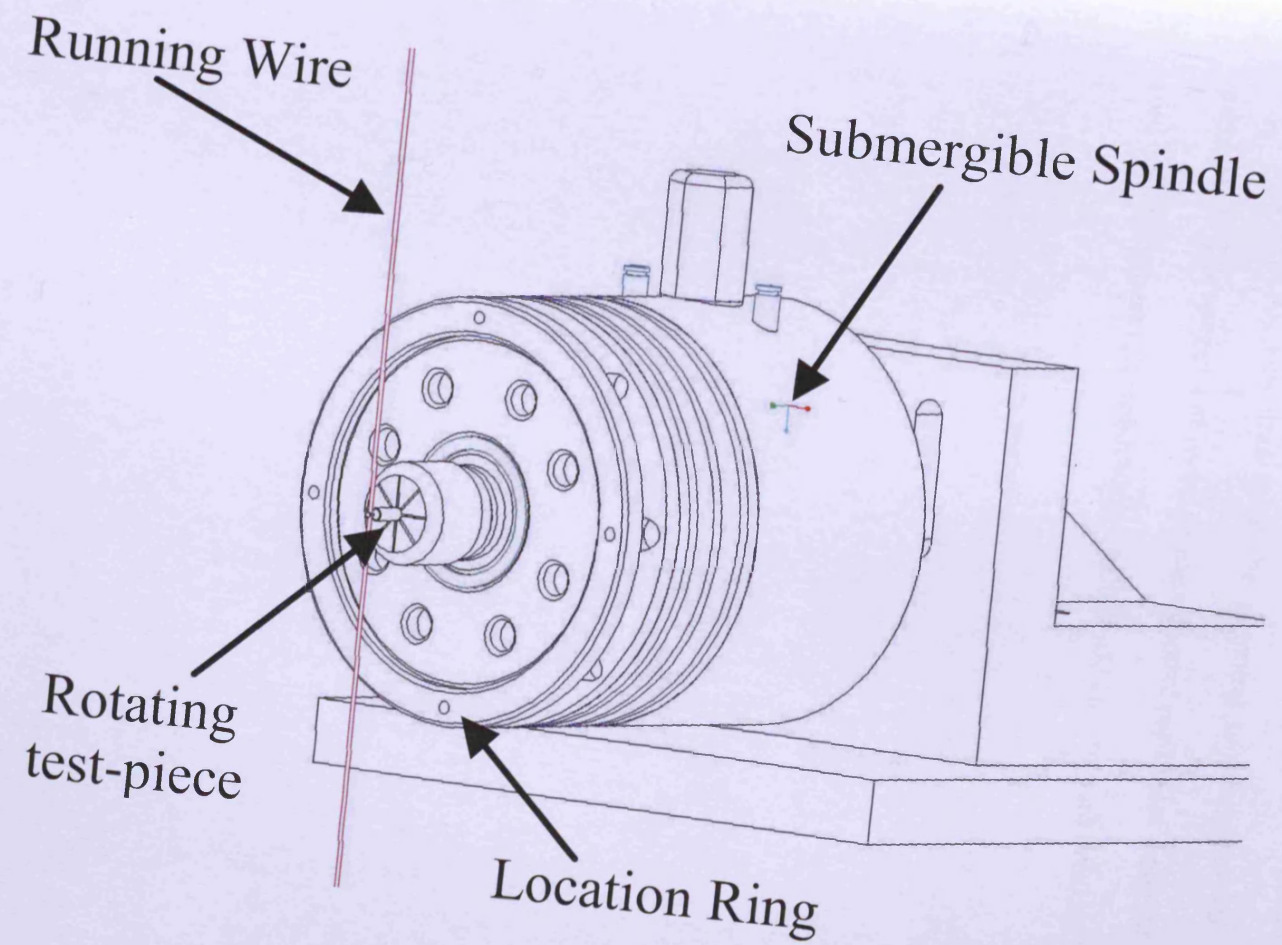


Figure 4.1. WEDG in combination with μ WEDM

A series of experiments were conducted to optimise the WEDG process in regards to resulting surface roughness applying the Taguchi parameter design method. In Table 4.1 the five control parameters with the three levels used in this study are provided. They were selected because their values can be varied by the machine operator when performing WEDG, and thus have the potential to realise on-the-machine process optimisation. The ranges and levels of each control parameter were carefully selected to avoid unstable processing conditions which could lead to wire breakages.

Table 4.1. Set-up parameters

Parameter	Process Range	Description
Spindle Speed	500 to 1500 [RPM]	Spindle rotational speed
Flushing	0 to 0.2 [MPa]	Flushing provided from both the upper and lower heads of the machine
Discharge Intervals	12.5 to 42.5 [μ s]	Time duration between pulses
Open circuit voltage	100 to 200 [volts]	Voltage between the electrode and the workpiece when the distance between them is too great to allow ionisation of the dielectric fluid
Pulse ON time	4.5 to 52.4 [μ s]	Pulse duration

In addition, four process parameters were continuously monitored during the experiments. They are given in Table 4.2. During the machining five data points per second for each parameter were recorded using a data acquisition system. This relatively low data acquisition rate was selected in order to capture the process “footprint” over long machining periods and thus to make the volume of acquired data manageable, in particular the size of the formed data files over an average time slot of 3.5 min were 180 MB. Then, the data was pre-processed using the ‘Lab VIEW’ software. In this research, the data was processed further employing inductive learning techniques to create predictive models for performing on-the-machine assessment of the resulting surface finish after WEDG.

Table 4.2. Monitoring parameters

Symbol	Description	Unit
V _x	Cutting speed along the x axis	mm/min
U _{fs}	Average voltage between the electrode wire and the work piece	Volts
Servo ist	Indicates the real value of the servo control parameter	%
P _w	Pulse frequency	kHz

Finally, after the experiments, the surface roughness of each cylindrical component after their machining was measured employing a white light interferometer microscope. The parameter used to evaluate the surface roughness was the arithmetic mean roughness (Ra) because relative heights in micro topographies are more representative. In particular, Ra measurements were obtained by analysing the scanned profiles along a sampling length of 250 μm , and by applying a high-pass filter to remove their waviness characteristics.

4.4 Experimental Results

4.4.1 Workpiece preparation

In this research, the workpieces were initially machined to prepare them for the follow-up WEDG operation. Especially, test pieces with a diameter of 3 mm were machined down to 100 μm in diameter (D_1) and 2 mm in length. Initially, an attempt was made to WEDG these D_1 cylindrical sections directly, by applying conventional μWEDM technological parameters while rotating the workpiece. However, the result was not satisfactory as the volume of material that had to be removed was very high and led to continuous wire breakage.

To tackle this problem a machining strategy was developed whereby the test pieces were initially sliced to square cross-sections by applying a conventional μWEDM machining. Thus, by performing this pre-WEDG machining the majority of material was removed. Figure 4.2 illustrates these slicing operations which involved machining the test piece at four different angular positions with 90° off-sets between them. After this preparatory step WEDG with a continuously rotating spindle was performed.



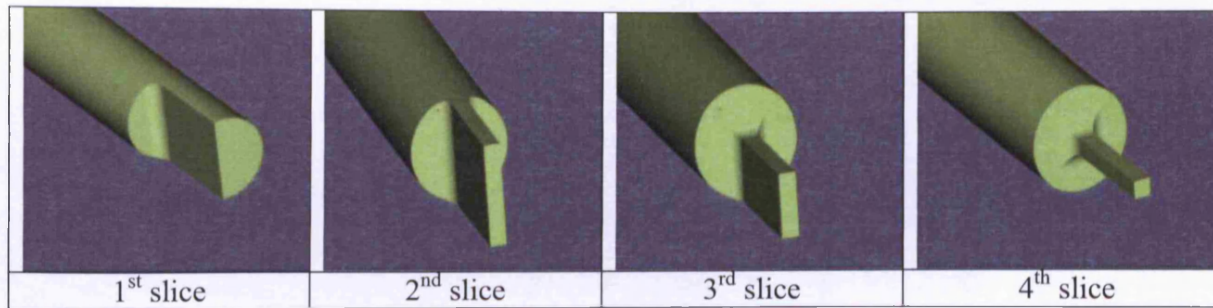


Figure 4.2. Slicing operation

Furthermore, the material allowance requirements after the four slicing cuts were investigated. Given that the final parts should be machined down to 100 μm in diameter, an initial test piece with a 110 μm square cross-section and 2 mm in length was produced.

The machining result after the WEDG operation is provided in Figure 4.3(a) while Figure 4.3(b) shows a cross section of the resulting 2 mm section. It is apparent that the machining conditions had been changing when the test piece was rotating, which led to a change in surface finish along the test piece, e.g. sides 'A' & 'B' in Figure 4.3(a). The reason for this inconsistency is the varying amount of material that had to be removed along the square profile, the workpiece run-out error and the spark gap required to have a stable WEDG machining. In particular, side 'A' of the 2 mm section was produced during the slicing stage because the run-out error plus the spark gap had exceeded the necessary WEDG allowance of 10 μm .

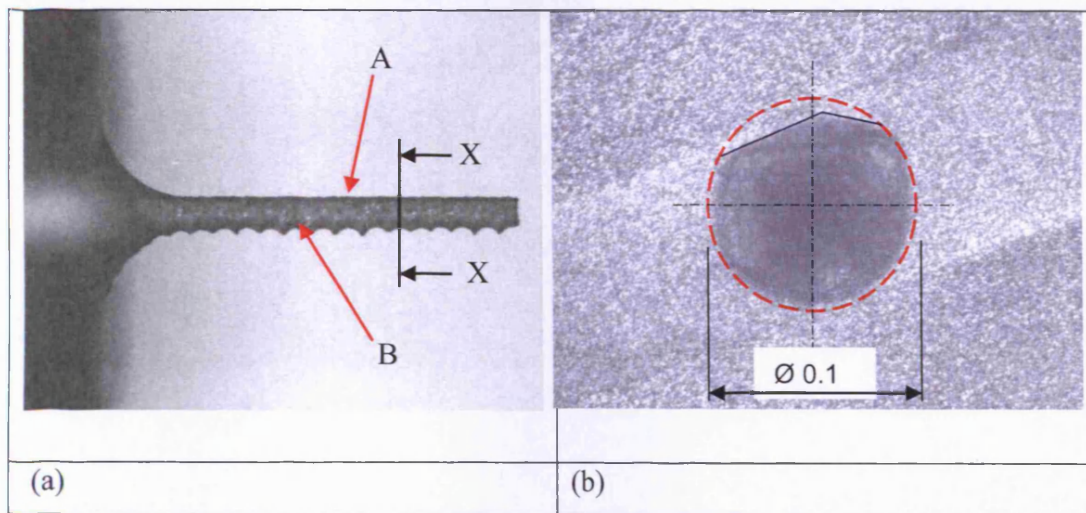


Figure 4.3 The machining result after the WEDG operation: (a) 2 mm section of the test piece and (b) X-X cross section.

Based on this initial trial it was not difficult to conclude that the machining allowance after the slicing operations was insufficient. Figure 4.4 shows the factors that should be taken into account when calculating the allowance for the WEDG operation. Especially, the dimensions of the workpiece after the slicing operations can be calculated using the following equation:

$$S_{\text{profile}} = D_1 + S_{\text{pos}} + S_g \quad (1)$$

where: D_1 is the target diameter; S_{pos} is the part run-out error and S_g - the spark gap.

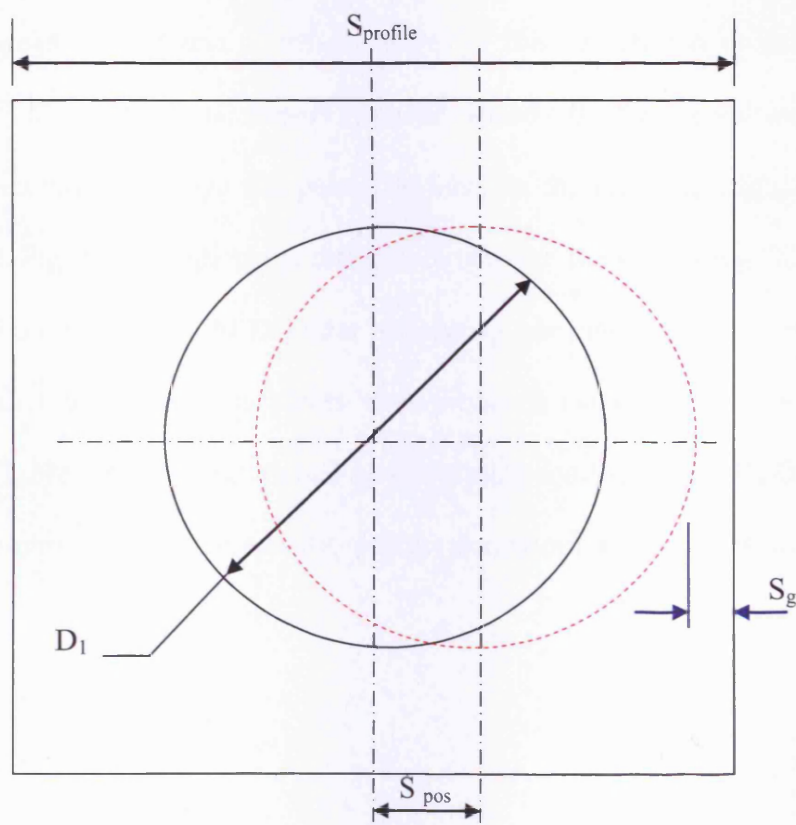


Figure 4.4 Factors affecting the WEDG operation

For this study, the sum of S_g and S_{pos} was considered to be $80\text{ }\mu\text{m}$ and thus the workpieces used in the experiments had $180\text{ }\mu\text{m}$ square cross-sections (S_{profile}).

4.4.2 Experimental design

As it was already stated one of the objectives of this research is to investigate the influence of five set-up parameters, spindle speed, flushing pressure, discharge intervals, open circuit voltage and pulse ON time, on the resulting surface roughness after WEDG. Figure 4.5 depicts the differences between the machining “footprints” of conventional μWEDM and WEDG after performing one main and three trim cuts. For this test, both tungsten carbide pieces were produced using the same technological parameters (Table 4.3) as those applied for performing conventional μWEDM , and thus did not take into account the specific process conditions arising from the test piece rotation.

Table 4.3. Set-up parameters for conventional μ WEDM

Parameter	Main cut	Trim cut 1	Trim cut 2	Trim cut 3
Flushing pressure [MPa]	1.2	1.2	1.2	1.2
Discharge intervals [μs]	40	2	2	2
Open circuit voltage [volts]	200	120	150	120
Pulse ON time	20 [μ s]	500 [ns]	300 [ns]	200 [ns]

The comparison of the machining results shows clearly that an improved surface roughness was obtainable by performing μ WEDM. Approximately, Ra 0.20 μm , compared to Ra 0.51 μm is achieved by WEDG. Based on these experimental results, it was not difficult to conclude that by using the same processing parameters for both WEDG and μ WEDM there would be significant differences in the resulting surface roughness due to the rotation of the workpiece. Therefore, to improve the surface roughness resulting after WEDG the factors affecting the process performance were studied.

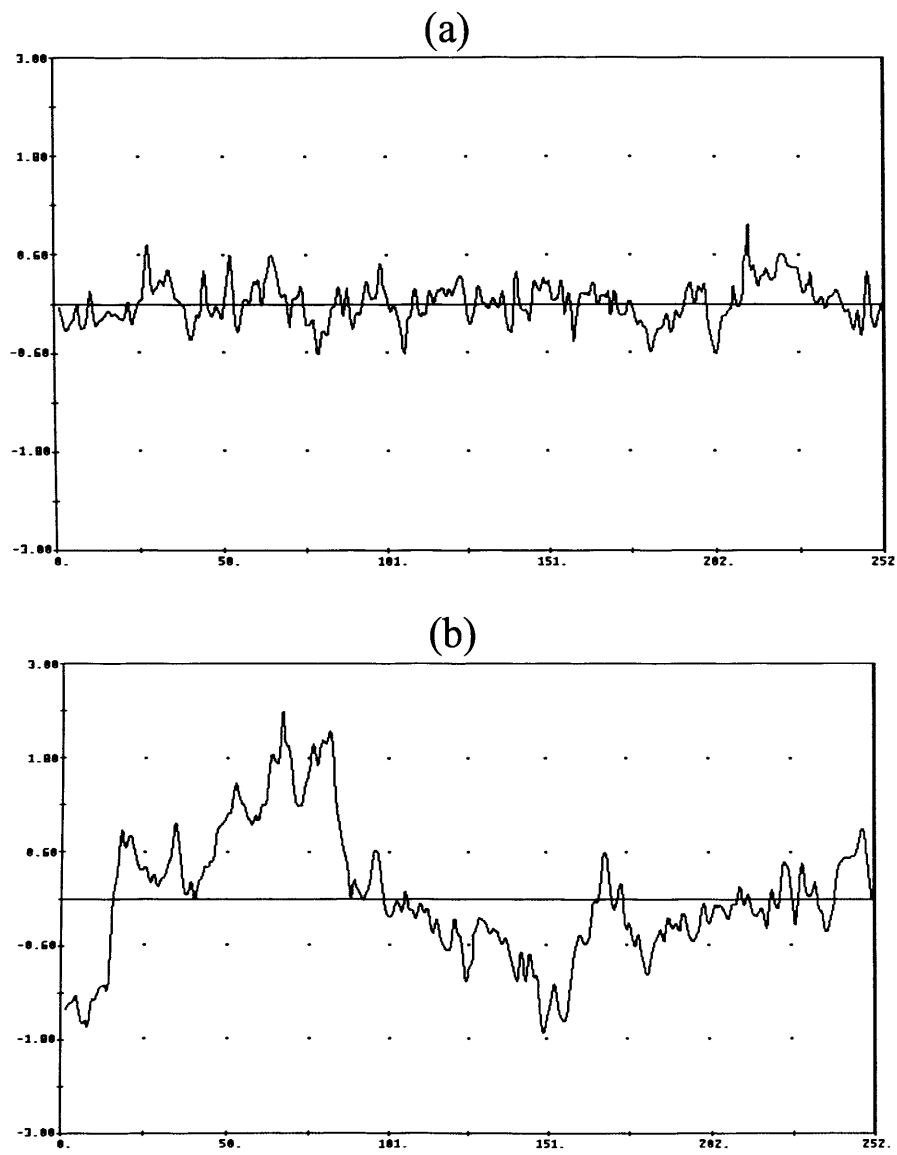


Figure 4.5. Surface profiles resulting after (a) conventional μ WEDM and (b) WEDG

The set-up parameters and their levels investigated in this research are listed in Table 4.4. The levels for each parameter were selected in order to achieve a stable WEDG process, and also to obtain consistent results. Given that five parameters at three levels each were investigated, for a full factorial analysis it will be required to perform 243 experiments. However, by assuming that the control parameters were independent, it was possible to employ the basic Taguchi L_{27} orthogonal array OA (Roy, 1990; Taguchi, 1987) and thus to reduce the number of experiments to 27.

Table 4.4. Machining parameters and their levels

Parameter	Code	Level 1	Level 2	Level 3
Spindle speed [rpm]	A	500	1000	1500
Flushing pressure [MPa]	B	0	0.1	0.2
Discharge intervals [μs]	C	12.5	27.5	42.5
Open circuit voltage [volts]	D	100	150	200
Pulse ON time [μs]	E	4.5	28.55	52.4

Table 4.5 shows the 27 combinations of set-up parameters used in the experimental runs, together with the surface roughness achieved for each of them. To minimise the influence of possible stochastic factors on the resulting surface finish after WEDG, the experiments were carried out in a random order. Also, due to time and cost constraints, the experiments were not repeated and thus, only one run was performed for each combination of control parameters.

Table 4.5. L27 orthogonal array

Run	A	B	C	D	E	Ra (μm)
1	1	1	1	1	1	1.32
2	1	1	1	1	2	1.09
3	1	1	1	1	3	0.64
4	1	2	2	2	1	1.66
5	1	2	2	2	2	1.70
6	1	2	2	2	3	2.12
7	1	3	3	3	1	1.27
8	1	3	3	3	2	1.58
9	1	3	3	3	3	1.70
10	2	1	2	3	1	1.09
11	2	1	2	3	2	3.20
12	2	1	2	3	3	2.09
13	2	2	3	1	1	1.34
14	2	2	3	1	2	0.89
15	2	2	3	1	3	1.14
16	2	3	1	2	1	1.02
17	2	3	1	2	2	0.80
18	2	3	1	2	3	1.54
19	3	1	3	2	1	1.05
20	3	1	3	2	2	1.17
21	3	1	3	2	3	1.04
22	3	2	1	3	1	0.87
23	3	2	1	3	2	0.96
24	3	2	1	3	3	1.18
25	3	3	2	1	1	1.51
26	3	3	2	1	2	1.05
27	3	3	2	1	3	0.93

4.4.3 Machining Response Evaluation

To evaluate the effects of the control parameters on the WEDG process, an analysis of variance (ANOVA) was conducted. The results are presented in Table 4.6. To apply the ANOVA analysis several assumptions have to be satisfied based on a 95% confidence interval. All P -values are lower than 0.05 and thus the effects of the respective factors were considered significant. Especially, it can be seen in Table 4.6 that discharge intervals, $P = 0.019$, has the highest significance in regard to the resulting surface roughness, while open circuit voltage, $P = 0.137$, and spindle speed, $P = 0.161$, have a lesser effect. The other two studied factors, flushing, $P = 0.792$, and pulse ON time, $P = 0.743$, have the least significance. In Table 4.6, the total degrees of freedom and error are 26 and 16 respectively.

Table 4.6. ANOVA for Surface Roughness						
Source	D.F.	Seq SS	Adj SS	Adj MS	F	P
Spindle Speed	2	0.8239	0.8239	0.4120	2.05	0.161
Flushing	2	0.0950	0.0950	0.0475	0.24	0.792
Discharge Intervals	2	2.0612	2.0612	1.0306	5.13	0.019
Open circuit voltage	2	0.9045	0.9045	0.4523	2.25	0.137
Pulse ON time	2	0.1216	0.1216	0.0608	0.30	0.743
Error	16	3.2134	3.2134	0.2008		
Total	26	7.2195				

Note: D.F. - degrees of freedom; Seq SS - sequential sum of squares; Adj SS - adjusted sum of squares; Adj MS' - adjusted mean square; F - F-value, P - P-value.

A normal probability plot shown in Figure 4.6 was used to check the assumption that the raw data test had a normal distribution of errors. In addition, the experiment results satisfy a further two assumptions as shown in Figure 4.7. The residuals vs. the fitted values' plot does not indicate any correlation between residuals, and does not suggest any error dependencies or violations of the constant variance assumption (Montgomery, 2000; Mason, 2003). Only two outliers were detected in Figures 4.6 and 4.7 for the following experimental setting: spindle speed 1000 [rpm], flushing 0 [MPa], discharge interval 27.5 [μ s], open circuit voltage 200 [volts] and pulse ON time 28.55 [μ s]. It is worth noting that the underlying error normality assumption is well satisfied because the plot in Figure 4.6 resembles a straight line.

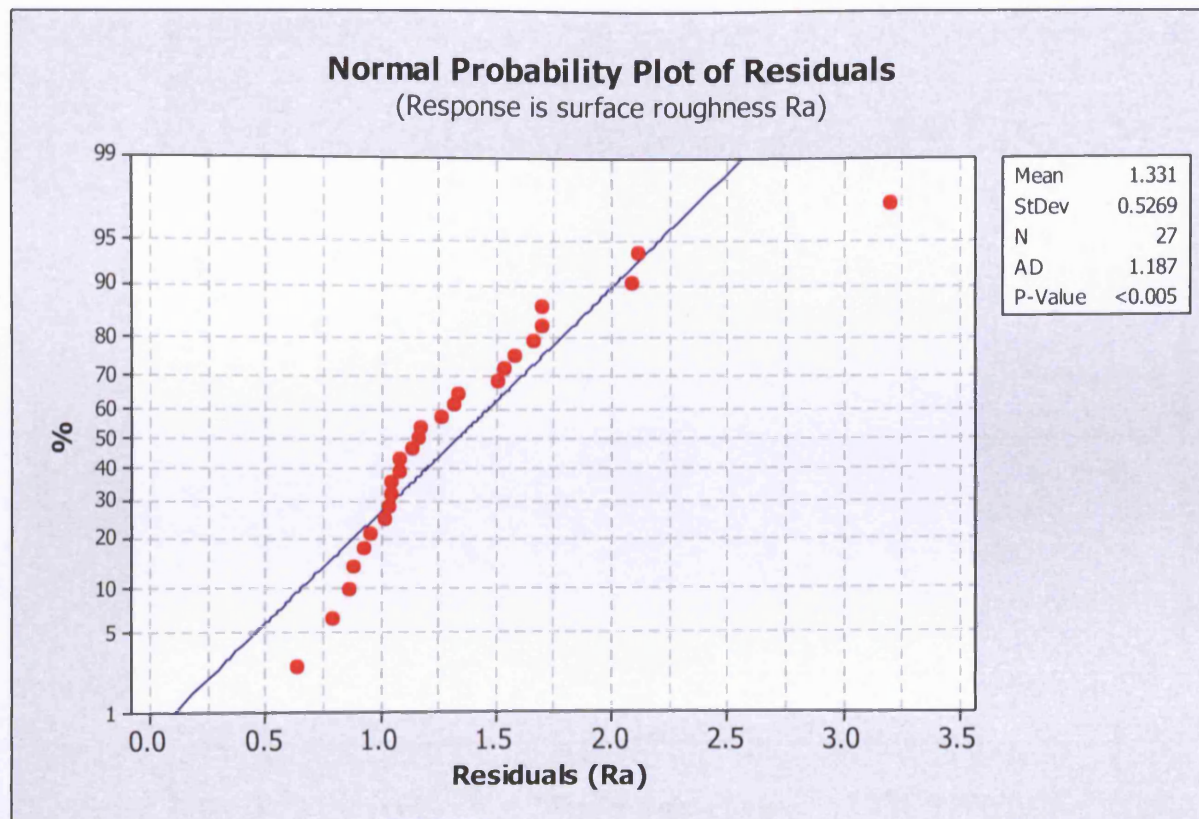


Figure 4.6. Normal plot of residuals

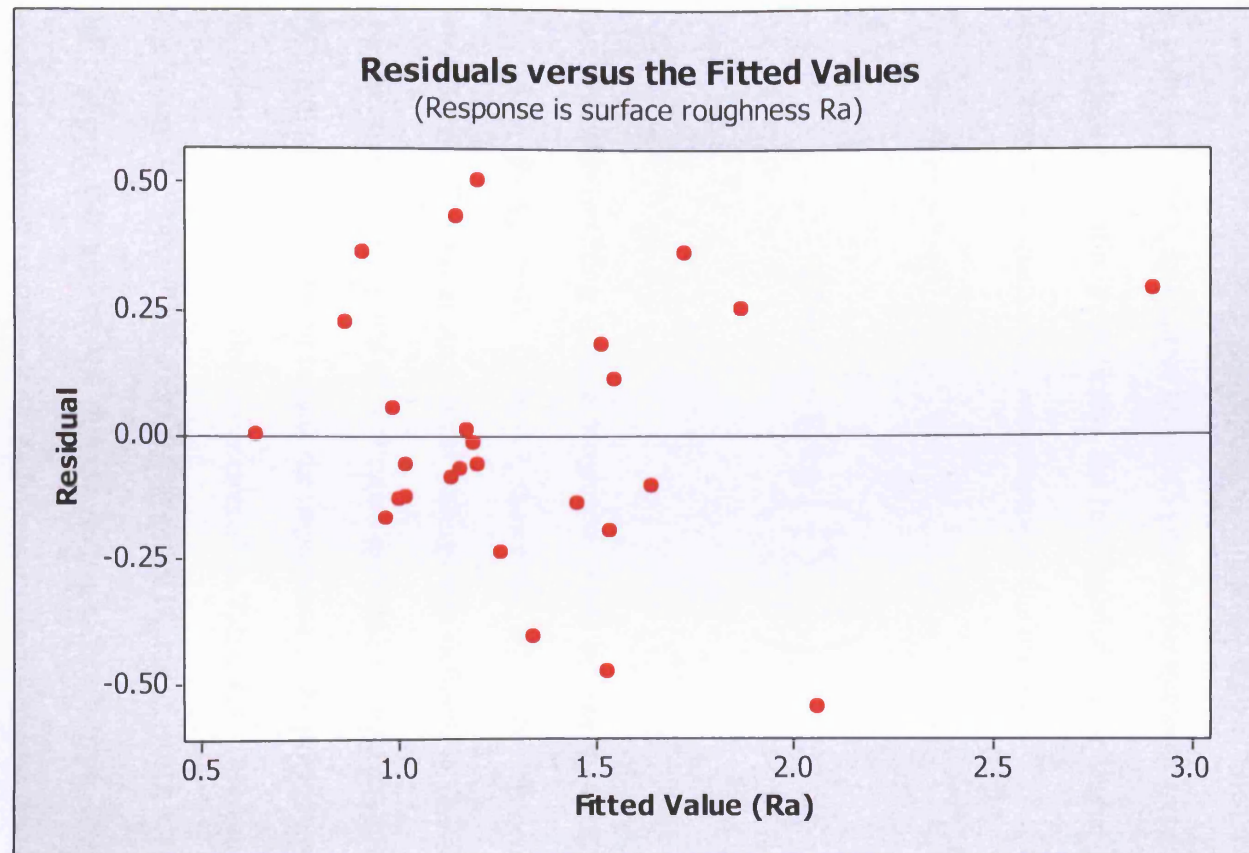


Figure 4.7. Residuals versus fitted values

4.4.4 Optimal parameters

A loss function was employed to measure response deviations from the desired value and also used to calculate optimal parameter values. The loss function values were further transformed into signal-to-noise (S/N) ratios and higher ratios indicated a better process response. Thus, an optimal level of a process parameter corresponded to a level with the highest S/N ratio. In particular, the loss function for the higher-the-better (HB) response expressed in equation (2) was adopted in this research.

$$S/N_{HB} = -10 \log \left(\frac{1}{r} \sum_{i=1}^r \frac{1}{y_i^2} \right) \quad (2)$$

Where y_i was the resulting surface roughness, while r - the number of replications (Phadke, 1989; Ross, 1998). Table 4.7 shows the S/N ratios obtained for process parameters levels. The optimum process settings was defined, as shown in Table 4.8, based on the main effects plots of S/N ratios provided in Figure 4.8. In addition, the ANOVA method was employed to rank the importance of the process parameters based on their effects on the S/N ratios, as presented in Table 4.9. The results showed that discharge interval, P and F values of 0.019 and 5.13, respectively, was the parameter with the highest influence on the process response, while open circuit voltage and spindle speed, p -values less than 0.05, had a lesser effect. Flushing and pulse ON time, p -values in excess of 0.05, did not have a significant effect on the process.

The relatively high percentage contribution of error witnessed in Table 4.8 would

generally indicate the absence of a significant processing parameter from the experimental investigation or a degree of interaction between process input parameters. Figure 4.9 shows the relatively strong interaction between processing parameters which can explain the resulting high percentage contribution of error.

Table 4.7. Response Table for Signal to Noise Ratios Larger is better					
Level	Spindle Speed	Flushing	Discharge Intervals	Open circuit voltage	Pulse time ON
1	2.8311	2.0740	0.1268	0.5916	1.6829
2	2.4341	2.0088	4.0184	2.1834	1.9907
3	0.5972	1.7795	1.7172	3.0873	2.1887
Delta	2.2339	0.2945	3.8916	2.4957	0.5058
Rank	3	5	1	2	4

Table 4.8. Optimum factor levels		
Factor	Level	Value
Spindle Speed	3	1500 (RPM)
Flushing	3	0.2 (MPa)
Discharge Intervals	1	12.5 (μsec)
Open circuit voltage	1	100 (volts)
Pulse time ON	1	4.5 (μsec)

Table 4.9. ANOVA for S/N ratios							
Source	D.F.	Seq SS	Adj SS	Adj MS	F	P	PCR
Spindle Speed	2	25.566	25.566	12.7831	1.90	0.181	11.3
Flushing	2	0.431	0.431	0.2154	0.03	0.969	0
Discharge Intervals	2	68.907	68.907	34.4535	5.13	0.019	9.6
Open circuit voltage	2	28.738	28.738	14.3692	2.14	0.150	14.2
Pulse time ON	2	1.170	1.170	0.5848	0.09	0.917	0
Error	16	107.511	107.511	6.7194			22.9
Total	26	232.323					

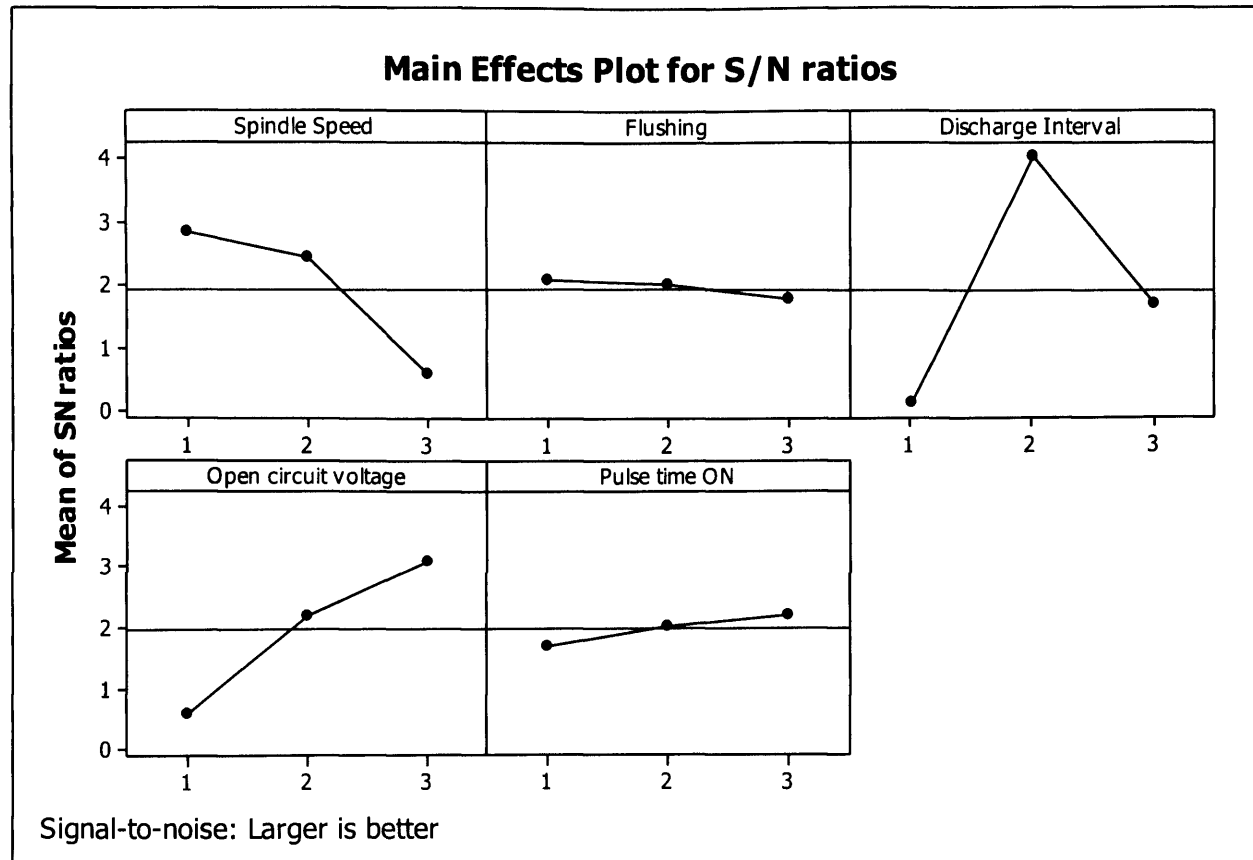


Figure 4.8. Main effects on the S/N ratio

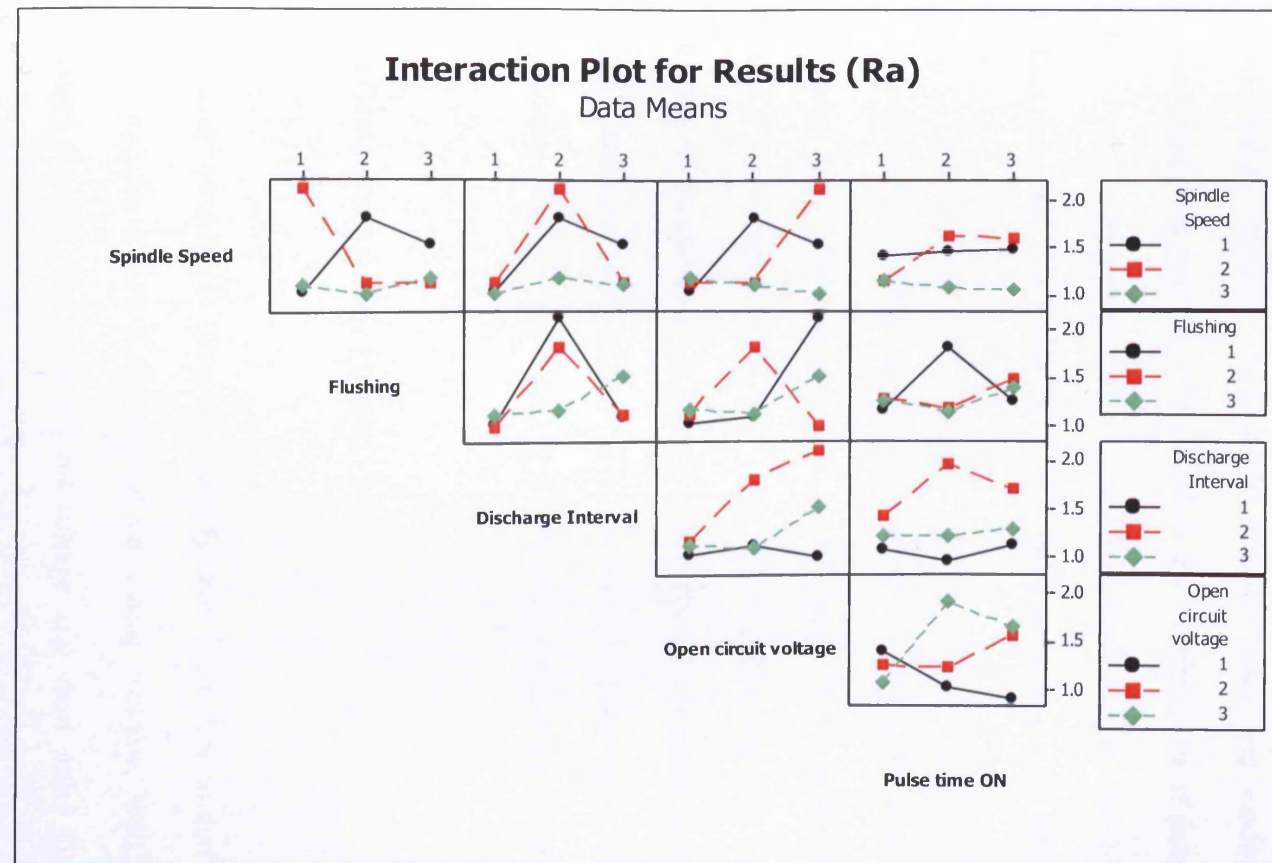


Figure 4.9. Interaction plot

4.4.5 Confirmation experiment

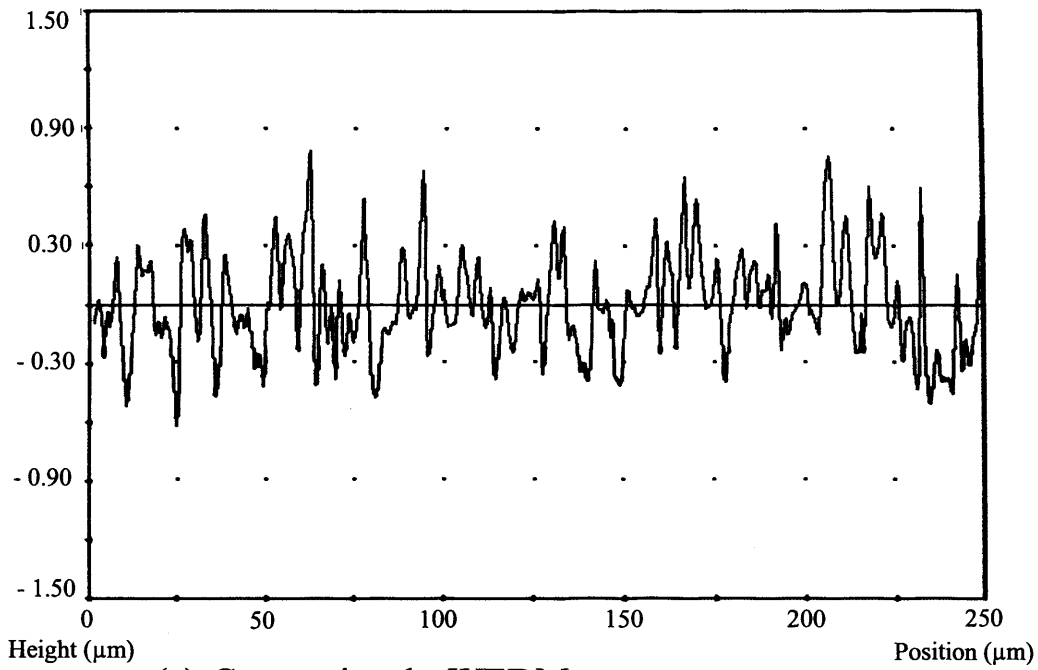
Given that the identified optimum combination of parameters did not correspond to any of the 27 experimental runs, one more trial was conducted in order to confirm that it represented an optimum setting for the considered processing window. In particular, the surface roughness that was achieved with this combination of parameters' values was $R_a 0.57 \mu\text{m}$. In comparison to other results in Table 4.5, it is evident that the achieved surface finish was better than those obtained in any of the other 27 experimental runs.

In addition, three subsequent trim cuts (see Table 4.3) were performed on the workpiece and further improvements to the surface finish down to $R_a 0.21 \mu\text{m}$ were obtained. This result was comparable with $R_a 0.20 \mu\text{m}$ achieved with the conventional μWEDM by applying an optimised technology as discussed in Section 4.4.4. These results demonstrate that after a thorough process optimisation, the surface finish of components produced by WEDG can match conventional μWEDM .

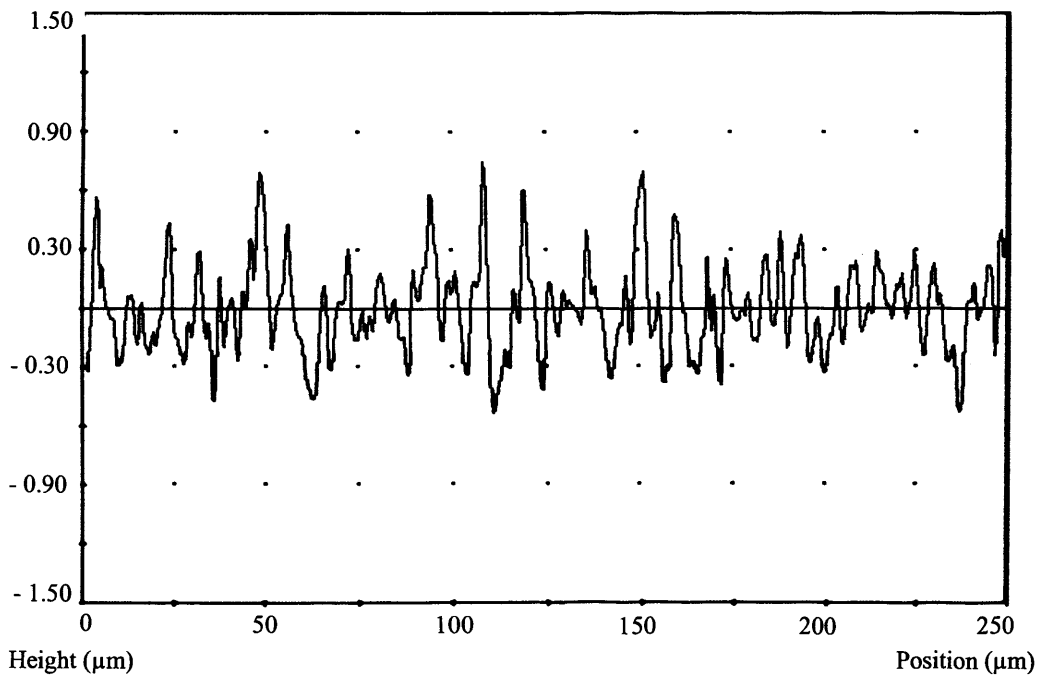
4.4.6 Comparison with μWEDM

The carried out process optimisation in Section 4.4.4 showed that to achieve the best surface roughness within the studied processing window, WEDG required a long discharge interval, low open circuit voltage and short pulse ON time, hence low discharge energy. At first, such a conclusion might seem obvious and also applicable to the μWEDM process. To verify whether such a reduction in discharge energy to the level used in WEDG would also lead to surface roughness improvements in

conventional μ WEDM, an additional experiment was conducted. In particular, the surface roughness of two test pieces machined by μ WEDM using the optimal process settings for WEDG (Table 4.8) and μ WEDM (Table 4.3), respectively, followed with three trim cuts (Table 4.3) was compared as shown in Figure 4.10. From the obtained results it was evident that a reduction of discharge energy to the level required in WEDG could bring only negligible improvements to the surface finish in conventional μ WEDM. Thus, a reduction of discharge energy is only effective when the test piece rotates as in the case of WEDG. A plausible explanation of this is that the static discharge channels cannot be maintained over long pulse ON time periods due to the test piece rotation. Thus, the discharge channels are interrupted above a particular rotational speed of the workpiece, and hence the discharge energy remained unchanged. This hypothesis was also supported by the ANOVA analysis which suggests that statistically the pulse ON time had no significant effect on the process response.



(a) Conventional μ WEDM set-up parameters
 $R_a = 0.20 \mu\text{m}$



(b) Optimised WEDG set-up parameters
 $R_a = 0.19 \mu\text{m}$

Figure 4.10. Surface roughness comparison of two test pieces machined by μ WEDM

In addition, to the four process parameters gathered by the data acquisition system voltage pulse waveforms were captured also using a digital oscilloscope, Tektronix DPO7254, with a band width of 2.5Ghz. Figure 4.11 depicts an example of voltage “footprints” that were displayed on the oscilloscope screen during μ WEDM and WEDG.

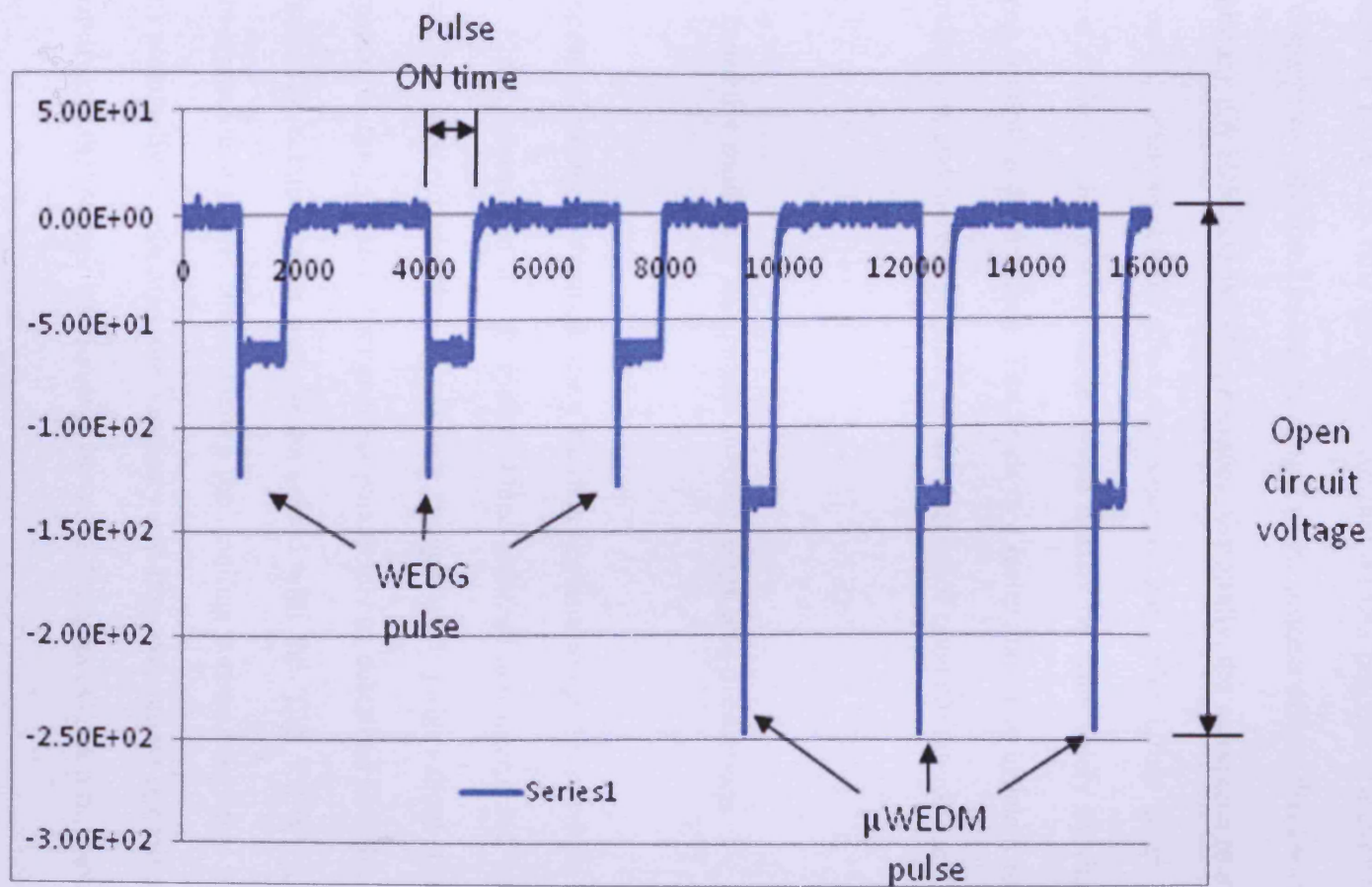


Figure 4.11 Voltage profiles of WEDG and conventional μ WEDM

The contrast in pulse profiles is depicted in Figure 4.11 and it shows clearly the distinct differences between the fundamentals of optimised μ WEDM and WEDG process footprints. Open circuit voltages are typically much higher during μ WEDM while the real values of pulse ON time are longer for the WEDG process. An explanation for such a disparity of pulse profiles can be sought in the process effects that are introduced by combining μ WEDM and WEDG processes. Especially, the workpiece rotation leads to increased variations of the discharge channel gap. The effect is an amplified retraction of the electrode wire which would usually be done solely by the adaptive servo gap control on the machine. This leads to a faster and more efficient recovery of the working gap, and thereby resulting in a reduction of open circuit voltage required.

4.5 Inductive model for in-process surface roughness predictions

The process information obtained using the data acquisition system provides an insight into the EDM process and its “footprint”. Once gathered and interpreted this process data can be used to develop predictive models and judge about the process performance. In this research, four process parameters as described in Table 4.2 were monitored. The acquired data was pre-processed with the ‘Lab VIEW’ software to generate a predictive model for estimating the resulting surface roughness in WEDG, and thus potentially to minimise the necessary and time consuming optimisation tasks and identifying the causal relationship between the process footprint and surface quality.

Many machine learning techniques are available for the creation of such predictive models. However, few attempts have been made to employ such techniques in the field of EDM. One such study was described by Tsai et al. (2001) where satisfactory results were reported in applying neural networks to estimate the surface finish of parts produced by EDM. In particular, their research compared the capabilities of various neural networks for creating models for predicting the resulting surface finish as a function of the work material and electrode polarity.

However, the drawback of applying neural networks is that the created models represent a “blackbox” and are therefore almost impossible to interpret by human experts. It would be beneficial for machine operators to be able not only to estimate the resulting surface roughness but also to understand the logic of the underlying model, and thus to allow them to comprehend the causal relations between process parameters and the resulting process performance. In this research, the suitability of applying an inductive learning algorithm to generate such predictive models in the form of rule sets is investigated. Particularly, the RULES-F algorithm (Pham and Dimov, 1997) was employed to create a predictive model in the form of fuzzy rules that can be readily interpreted by experts.

4.5.1 Data pre-processing

The first step in successfully creating a predictive model is the pre-processing of relevant data, especially its selection and formatting into training examples for follow-up rule induction.

The four monitoring parameters as described in Table 4.2 were used to generate this predictive model. As it was already mentioned five data points per second for each monitoring parameter were collected during the experiments. Figure 4.12 illustrates the steady state machining regime along the x-axis used to gather the training data. To generate the model the mean and standard deviation (STD) of each monitoring parameter were used as input attributes to form a training set. In this way, each instance in the training set was composed of 8 input attributes and the corresponding Ra value output. In Table 4.10 an example of such an instance is provided.

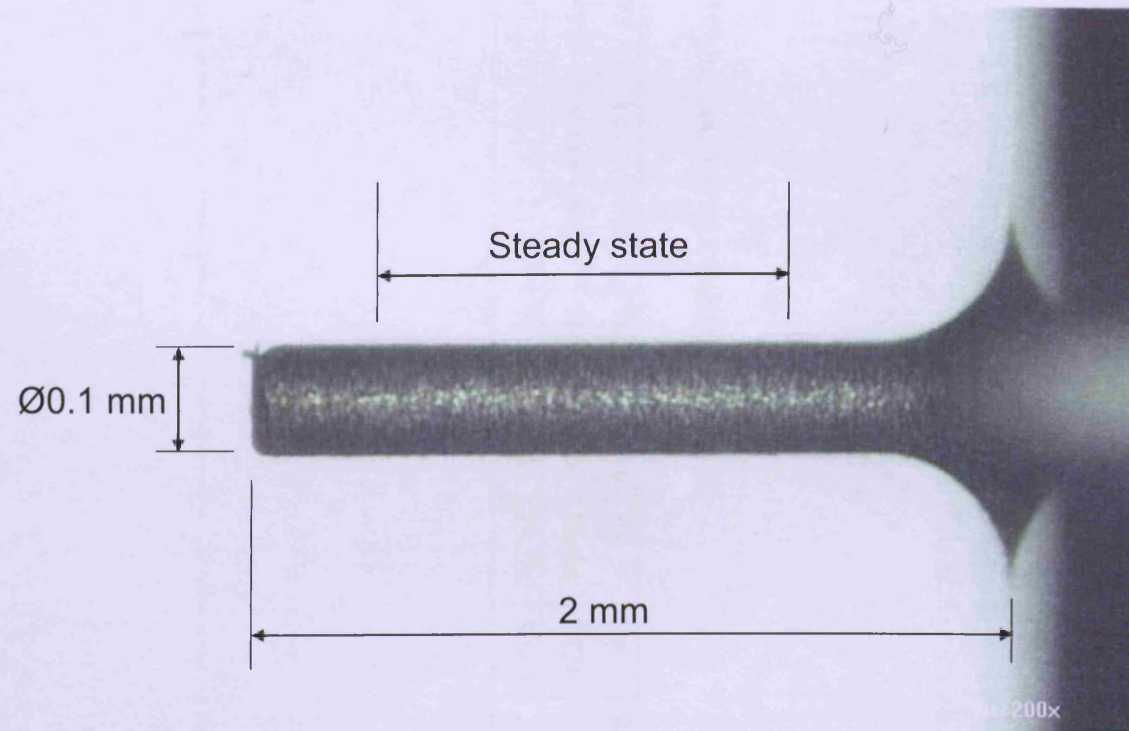


Figure 4.12 Illustration of steady state machining regime

Table 4.10. An example of a training instance

Vx	Vx	Ufs	Ufs	Servo	Servo	Pw	Pw	Ra
Mean	STD	Mean	STD	Mean	STD	Mean	STD	
0.54	37.765	20.12	11.317	24.547	6.654	29.232	3.803	1.32

In addition to the 27 experiments in Table 4.5, 5 (APPENDIX E) more machining trials were performed using a combination of controlled parameters' values not used previously. Only 5 additional process settings were analysed due to time and cost constraints. Thus, the total number of available instances to generate the predictive model was 32.

It was not possible to apply typical model validation methods that require the available instances to be split into training and testing sets, because there would not have been a sufficient number of instances to adequately represent the searched space. Therefore, all examples were used for training.

4.5.2 Model generation and discussion

In order to generate rules with RULES-F, it is necessary first to specify the number of membership functions for the output (N_f). To study the effect of this number on the performance of the generated rule sets, the algorithm was run 31 times by varying the number of membership functions from 2 to 32 during the training. Each rule set was then used to predict the R_a value of the 32 training instances. Next, the absolute error between the predicted and the measured R_a values was computed for each instance. Figure 4.13 shows the number of rules obtained for each number of fuzzy sets together with their corresponding absolute mean error.

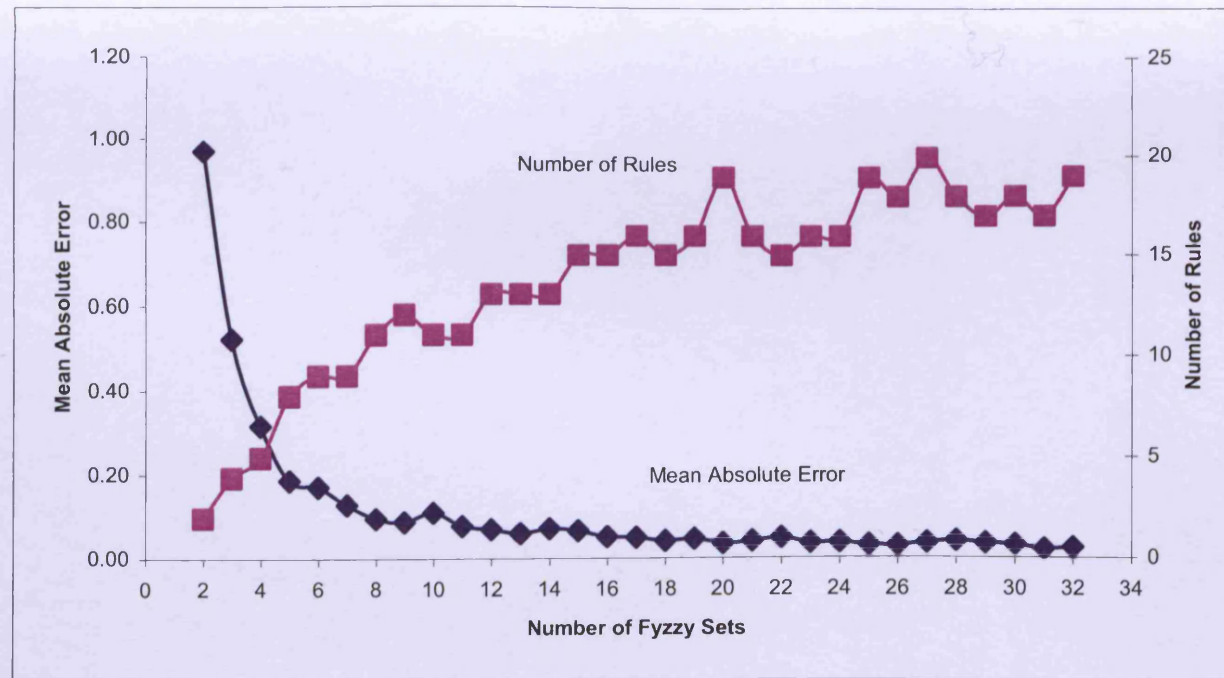


Figure 4.13. Prediction accuracy of the generated models

The increase of the number of membership functions generally results in more accurate models. However, this also increases the number of rules created and also their complexity. Thus, the models become more difficult to interpret. An example of a very generic rule set generated with only three membership functions (low, medium and high) is given in Table 4.11.

Table 4.11. An example of a generic rule set

Examples covered	Fuzzy Rules including their interpretation by an expert
19	<p><i>IF</i> VxMean is Tr(11.25, 73.57,+ ∞) & Ufs mean is Tr(-∞,0, 0.23) <i>THEN</i> Ra is Tr(0.64,1.92,3.2)</p> <p><i>IF</i> [Mean of cutting speed along the x-axis] is medium high & [the mean of the voltage between the electrode wire and the work piece] is low <i>THEN</i> Ra is medium</p>
17	<p><i>IF</i> UfsSTD is Tr(-∞,2.18, 6.36) <i>THEN</i> Ra is Tr(0.64,1.92,3.2)</p> <p><i>IF</i> [the STD of the voltage between the electrode wire and the work piece] is low <i>THEN</i> Ra is medium</p>
13	<p><i>IF</i> VxSTD is Tr(-∞,2.56, 11.83) & UfsMean is Tr(19.19, 30.48,+ ∞) <i>THEN</i> Ra is Tr(-0.64, 0.64,1.92)</p> <p><i>IF</i> [the STD of cutting speed along the x-axis] is low & [the mean of the voltage between the electrode wire and the work piece] is medium high <i>THEN</i> Ra is low</p>
13	<p><i>IF</i> UfsSTD is Tr(6.64, 28.10,+ ∞) <i>THEN</i> Tr(-0.64, 0.64,1.92)</p> <p><i>If</i> [the STD of the voltage between the electrode wire and the work piece] is medium high <i>THEN</i> Ra is low</p>
1	<p><i>IF</i> VxSTD is Tr(3.43, 29.18,+∞) & VxMean is Tr(-∞,10.25, 12.5) & PwSTD is Tr(-∞,2.31, 2.43) <i>THEN</i> Ra is Tr(1.92,3.2,4.48)</p> <p><i>IF</i> [the STD of cutting speed along the x-axis] is medium high & [Mean of cutting speed along the x-axis] is low & [the STD of the pulse frequency] is low <i>THEN</i> Ra is high</p>

As shown in Figure 4.14, the terms $Tr(a,b,c)$ represent triangular fuzzy sets, a being the base of the triangle and b the location of its apex. They were replaced by linguistic terms (low, medium and high) to facilitate the interpretation of the rules.

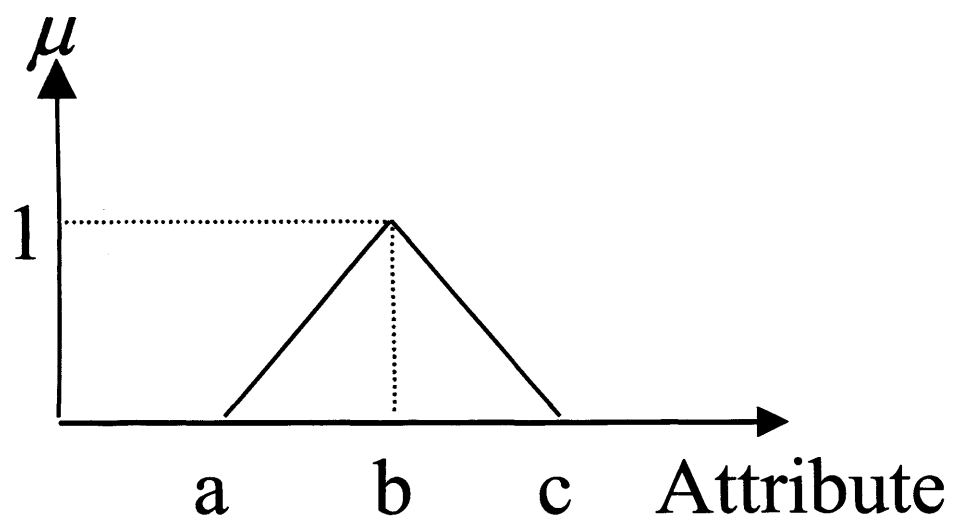


Figure 4.14. Triangular fuzzy set

With a mean absolute error of 0.52, the accuracy of this model is relatively poor as illustrated in Figure 4.15. However, this does not mean that the created rules are inaccurate. In fact, each individual rule has been created with 100% accuracy, but the output fuzzy sets used (low, medium, high) are too broad to lead to an accurate prediction during the defuzzification process. This suggests that there is a need to increase the number of fuzzy sets (N_f). In addition, to take advantage from the use of fuzzy sets it is necessary for the rules created to be meaningful and logical in order to gain some understanding of the underlining process behaviour. However, when only 3 fuzzy output sets were applied the resulting rules were formed using one or two of the output variables and their corresponding values in linguistic terms. Following on from the experiments carried out in Section 4.4.2 the results showed that for the WEDG process the resultant output, the surface roughness, is governed by the interactions of several input variables. Therefore, the rules generated by using only 3 fuzzy rule sets are not interpretable.

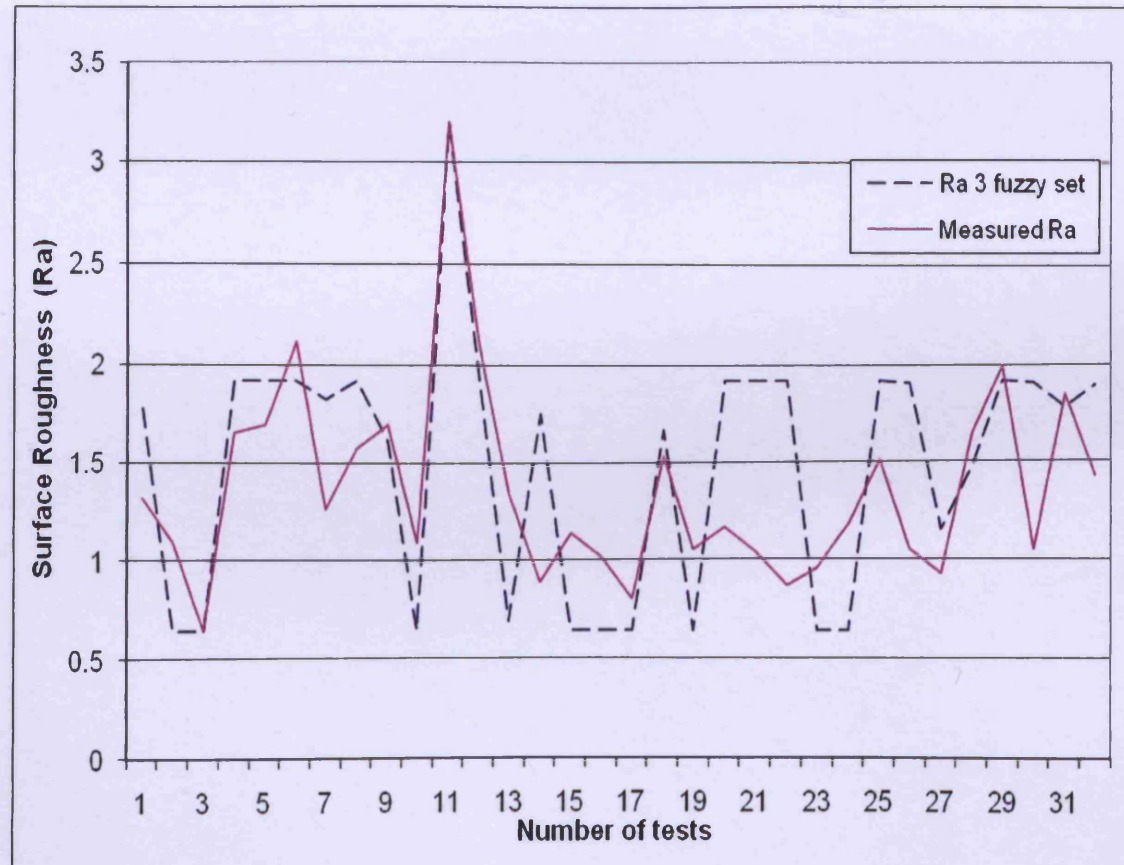


Figure 4.15. Predicted and measured Ra when 3 fuzzy output sets were used

By increasing the number of fuzzy sets, the number of rules increases and more specific rules are formed. Consequently, it is possible to identify patterns in process behaviour and more importantly, draw upon some logical interpretation of the process response. For instance, with $N_f = 9$ (Figure 4.16), 9 rules were created with a mean absolute error of only 0.08. A comparison of predicted and measured roughness is provided in Figure 4.17.

Fuzzy Sets

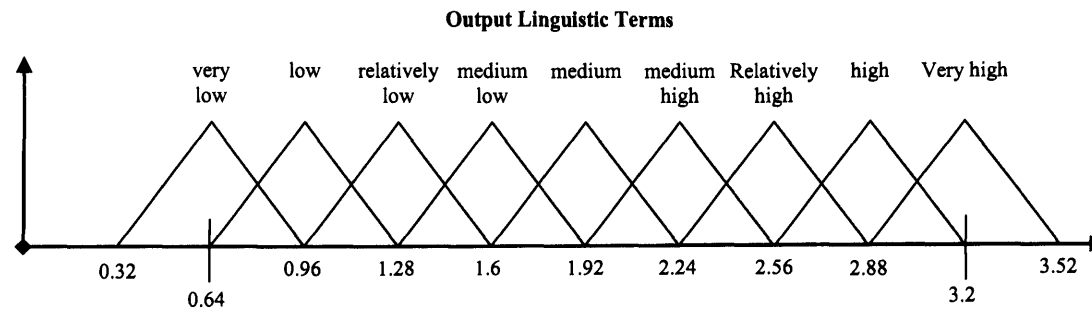


Figure 4.16. Nine membership functions for the output

Table 4.12. The rule set when 9 membership functions were used for the output

Examples covered	Fuzzy Rules including the interpretation by an expert
10	<p><i>IF</i> PwSTD is Tr($-\infty$, 2.31, 5.72) & PwMean is Tr(26.08, 42.65, $+\infty$) & UfsSTD is Tr(6.64, 28.1, $+\infty$) <i>THEN</i> Ra is Tr(0.64, 0.96, 1.28)</p> <p><i>IF</i> [the STD of the pulse frequency] is medium low & [the mean of the pulse frequency] is medium high & [the STD of the voltage between the electrode wire and the work piece] is medium high <i>THEN</i> Ra is Low</p>
9	<p><i>IF</i> PwSTD is Tr(2.62, 4.10, 5.59) & PwMean is Tr(27.28, 42.65, $+\infty$) & UfsSTD is Tr(2.18, 28.1, $+\infty$) & S.istSTD is Tr($-\infty$, 2.46, 8.25) <i>THEN</i> Ra is Tr(0.96, 0.32, 1.6)</p> <p><i>IF</i> [the STD of the pulse frequency] is medium & [the mean of the pulse frequency] is medium high & [the STD of the voltage between the electrode wire and the work piece] is medium high & [the STD of the real value of the servo control parameter] is Low <i>THEN</i> Ra is relatively Low</p>
5	<p><i>IF</i> PwMean is Tr($-\infty$, 26.04, 28.32) <i>THEN</i> Ra is Tr(1.6, 1.92, 2.24)</p> <p><i>IF</i> [the mean of the pulse frequency] is Low <i>THEN</i> Ra is medium</p>
5	<p><i>IF</i> VxSTD is Tr(2.57, 7.2, 11.83) & VxMean is Tr(11.25, 73.58, $+\infty$) & PwSTD is Tr($-\infty$, 2.31, 4.02) & PwMean is Tr(28.51, 42.65, $+\infty$) & UfsSTD is Tr(2.18, 28.09, $+\infty$) <i>THEN</i> Ra is Tr(0.64, 0.96, 1.28)</p> <p><i>IF</i> [the STD of cutting speed along the x-axis] is relatively low & [Mean of cutting speed along the x-axis] is Medium high & [the STD of the pulse frequency] is medium low & [the mean of the pulse frequency] is medium high & [the STD of the voltage between the electrode wire and the work piece] is medium high <i>THEN</i> Ra is low</p>
4	<p><i>IF</i> VxMean is Tr(11.29, 73.58, $+\infty$) & PwMean is Tr(38.84, 42.65, $+\infty$) & S.istSTD is Tr($-\infty$, 2.46, 9.57) <i>THEN</i> Ra is Tr(1.28, 1.6, 1.92)</p> <p><i>IF</i> [Mean of cutting speed along the x-axis] is medium high & [the mean of the pulse frequency] is high & [the STD of the real value of the servo control parameter] is low <i>THEN</i> Ra is medium low</p>
3	<p><i>IF</i> UfsSTD is Tr($-\infty$, 2.18, 11.42) & S.istSTD is Tr(9.57, 25.54, $+\infty$) <i>THEN</i> Ra is Tr(0.32, 0.64, 0.96)</p> <p><i>IF</i> [the STD of the voltage between the electrode wire and the work piece] is low & [the STD of the real value of the servo control parameter] is medium high <i>THEN</i> Ra is very low</p>
1	<p><i>IF</i> VxSTD is Tr(10.52, 29.18, $+\infty$) & VxMean is Tr($-\infty$, 10.26, 33.41) <i>THEN</i> Ra is Tr(1.6, 1.92, 2.24)</p> <p><i>IF</i> [the STD of cutting speed along the x-axis] is medium high & [Mean of cutting speed along the x-axis] is low <i>THEN</i> Ra is medium</p>
1	<p><i>IF</i> VxSTD is Tr(3.43, 29.18, $+\infty$) & VxMean is Tr($-\infty$, 10.26, 12.50) & PwSTD is Tr($-\infty$, 2.31, 2.43) <i>THEN</i> Ra is Tr(2.88, 3.2, 3.52)</p> <p><i>IF</i> [the STD of cutting speed along the x-axis] is medium high & [Mean of cutting speed along the x-axis] is low & [the STD of the pulse frequency] is low <i>THEN</i> Ra is very high</p>

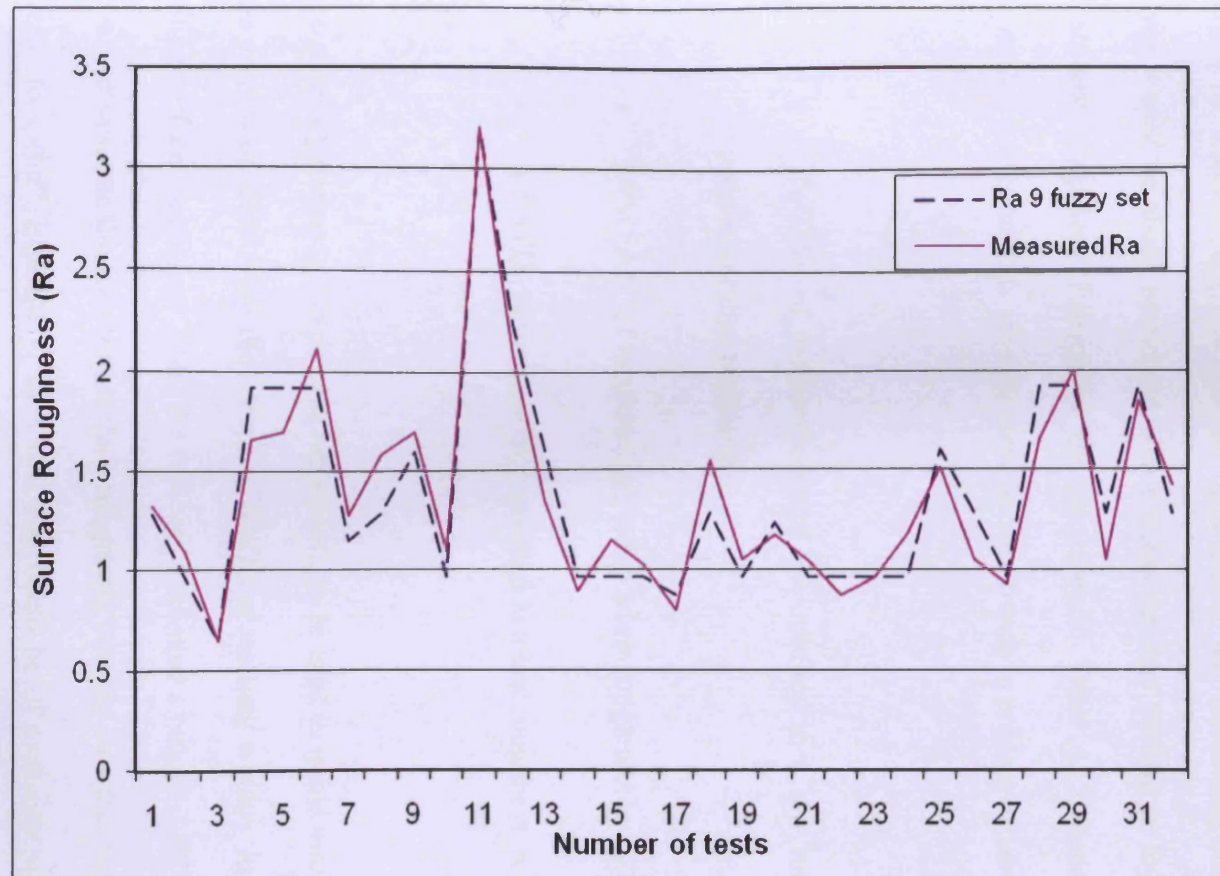


Figure 4.17. Predicted and measured Ra when 9 fuzzy output sets were used

Once again in order to facilitate the interpretation of the rules, the triangular fuzzy sets have been replaced by linguistic terms as in Table 4.11. Also for simplicity, similar linguistic terms were used for different sets. For instance, the low linguistic term in Table 4.11, was divided up further into very low, low and relatively low as it shown in Figure 4.16. Considering this specific application, the interesting rules for further analysis would be those associated with process settings leading to low & relatively low surface roughness. Especially, for the rules in Table 4.12 some interpretable patterns that can be used to identify some generic trends in process behaviour are:

- ‘PwSTD’ of medium/medium low resulted in a low roughness in 26 process settings (examples).
- ‘PwMEAN’ of medium high led to a low roughness in 24 examples.
- ‘UfsSTD’ of medium high resulted in a low roughness in 19 examples.

These generic patterns in the process behaviour can be used to guide machine operators in the process of identifying the optimum WEDG processing window in regards to the resulting surface roughness. Thus, the rule sets generated using RULES-F can be used not only to estimate the resulting surface roughness but also as a tool for analysing the process “footprint”. Especially, such rule sets could be of particular relevance when machining parts that have varying cross-sectional areas. Figure 4.18 presents an machining approach that could be adopted to ‘search’ for optimum processing window if low surface roughness was required.

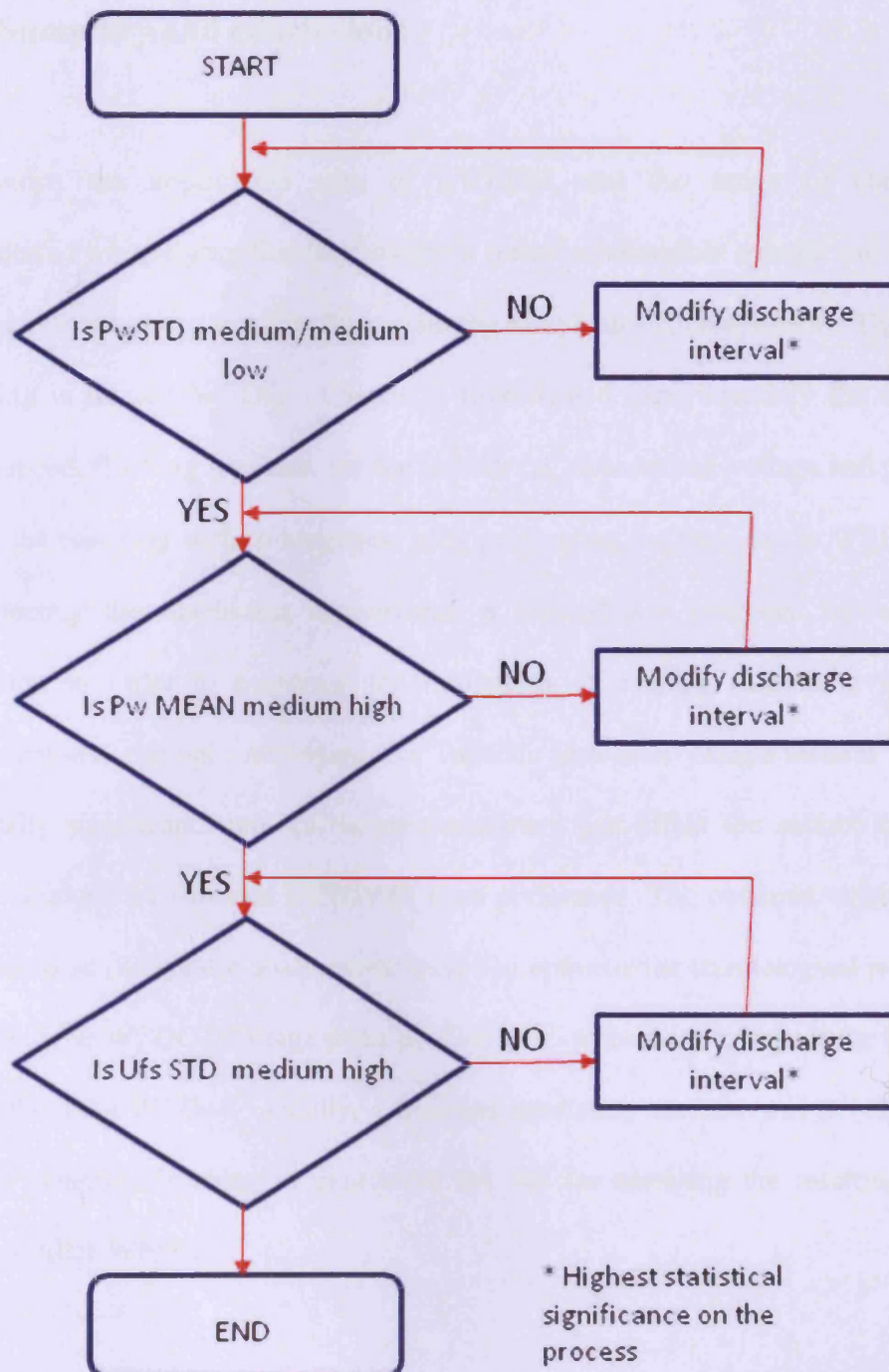


Figure 4.18. An approach for searching on the machine for an optimum processing window

4.6 Summary and conclusions

To broaden the application area of μ WEDM and the range of components manufactured by applying this technology, a rotary submergible spindle can be added to the equipment set-up to allow the machining of cylindrical components. This type of machining is termed WEDG. Chapter 4 investigated experimentally the effects of spindle speed, flushing pressure, discharge interval, open circuit voltage and pulse ON time on the resulting surface roughness after performing the main cut in WEDG. Prior to conducting the machining experiments, a method was proposed for workpiece preparation in order to overcome the limitations of existing machining strategies. Experimentally, through employing the Taguchi parameter design method the most statistically significant main cut set-up parameters that affect the surface roughness through analysis of variance (ANOVA) were performed. The obtained results from a signal-to-noise (S/N) ratio analyses were used to optimise the technological parameters for performing WEDG. Voltage pulse profiles were gathered to compare the processes of WEDG and μ WEDM. Finally, a machine prediction method was developed that employs inductive learning to generate a rule set for assessing the resulting surface roughness after WEDG.

To conclude this chapter the experimental results focus on advancing this technology through the development of:

- A machining strategy for workpiece preparation was proposed in order to create processing conditions during WEDG as close as possible to those in “conventional”

μ WEDM. By applying this strategy, it is possible to minimise the effects of the inherent concentricity errors associated with the use of submergible spindles.

- A Taguchi DOE was conducted to assess the statistical significance of the discharge interval with regard to resulting surface roughness after WEDG on a μ WEDM setup.
- The optimum process window for performing WEDG on a μ WEDM machine were identified, in particular spindle speed of 1500 RPM, flushing 0.2 MPa, discharge interval - 12.5 μ s, open circuit voltage - 100 volts and pulse ON time - 4.5 μ s.
- The comparison between voltage pulse shapes in “conventional” μ WEDM and those during WEDG on a μ WEDM machine showed fundamental differences in the process behaviours that can be explained with the combined effect of these two processes. Especially, the workpiece rotation leads to increased variations of the discharge channel gap and as a result an amplified retraction of the electrode wire. Ultimately, this results in a reduction of open circuit voltage required during the machining due to a faster and more efficient recovery of the working gap.
- For “conventional” μ WEDM, the reduction of the discharge energy to levels required in WEDG brought only negligible improvements in regards to the resulting surface roughness.
- A simple and cost-effective method for on-the-machine prediction of the surface roughness was demonstrated. The method employs rule-based models generated by inductive learning. For example, by applying this method it was possible to identify

patterns, combinations of process parameters, in the process “footprint” that led to a low or relatively low surface roughness, in particular the STD of cutting speed along the x-axis need to be medium/medium low, the mean of cutting speed along the x-axis - medium high and the STD of the pulse frequency - medium high.

CHAPTER 5

THE EFFECTS OF MATERIAL GRAIN STRUCTURE ON SURFACE INTEGRITY OF COMPONENTS PROCESSED BY μ WEDM

5.1 Motivation

The characterisation of the resulting surface integrity after machining with various micro manufacturing technologies is becoming a very important factor in broadening their application areas, and especially in satisfying the constantly growing requirements for miniaturisation, function integration, longevity and reliability of existing and new emerging MST based products. Particularly, it is very important to study the influence of materials' microstructure and processing conditions on the mechanical properties of machined surfaces. When processes such as micro milling have been applied to refined aluminium alloys with a sub-micron crystalline microstructure, results have shown an almost three times improvement of surface finish when compared with the response of the same materials but in its unrefined state (Popov et al., 2006c). The research reported in this chapter investigates and characterises the effects of material crystalline microstructure on the resulting surface integrity of samples machined by μ WEDM.

This chapter is organised as follows. In Section 5.2 a description of the μ WEDM is provided, and some of inherent effects on the surface integrity of components produced

through the process are described. Then, the experimental procedures and method used to modify the material microstructure of the material used in the research is described in Section 5.3. The next, section 5.4 investigates and characterises the process-material effects on the resulting micro hardness, phase content changes, HAZ, surface roughness, micro cracks, recast layers formation, MRR and element spectrum after both rough and finishing μ WEDM cuts were investigated. Finally, Section 5.5 summarises the carried out research and gives conclusions.

5.2 μ WEDM process

μ WEDM is a widely used material removal technology for manufacture of precision micro components incorporating intricate features and complex profiles with wire electrodes down to 0.02mm, and achieving high levels of surface finish down to Ra 0.07 μ m (Rees et al., 2008). Unlike traditional cutting and grinding processes, which rely on a processing energy generated by cutting with a harder tool or abrasives to machine softer workpieces, by employing as tools wire electrodes the EDM process utilises electrical sparks or the thermal energy of plasma channels to erode the unwanted material and generate the desired shape (Ho et al., 2004). To perform the WEDM operation, both the workpiece and the wire electrode are submerged in either de-ionised, de-mineralised water or hydrocarbon oil (Kunieda et al., 2005).

The sparks and plasma channels generated during the EDM process creates craters on the surface, and a thermal wave propagates through the material resulting in a HAZ on the sub surface and the formation of a recast layer on the surface of the components

(Qu et al., 2002a).

This re-solidification/recast layer is typically very fine grained and subjected to a surface tensile stress regime, localised hardening, micro cracking, porosity and grain growth and may be alloyed with carbon as a side product of dielectric ionisation during the sparks or with the material transferred from the tool (Ramasawmy et al., 2005; Cusanelli et al., 2004). Generally, the recast layer that is formed on the surface as a result of WEDM is considered to have a detrimental effect on workpiece surfaces, thus preventing the use of WEDM for some critical applications, such as the machining of aerospace components (Aspinwall et al., 2008). Immediately beneath the recast or white layer as it is sometimes referred to is the resulting HAZ on the machined workpiece. This is the material layer where the heat is not high enough to cause melting but is sufficiently high to induce micro-structure transformation in the material (Rebelo et al., 1998).

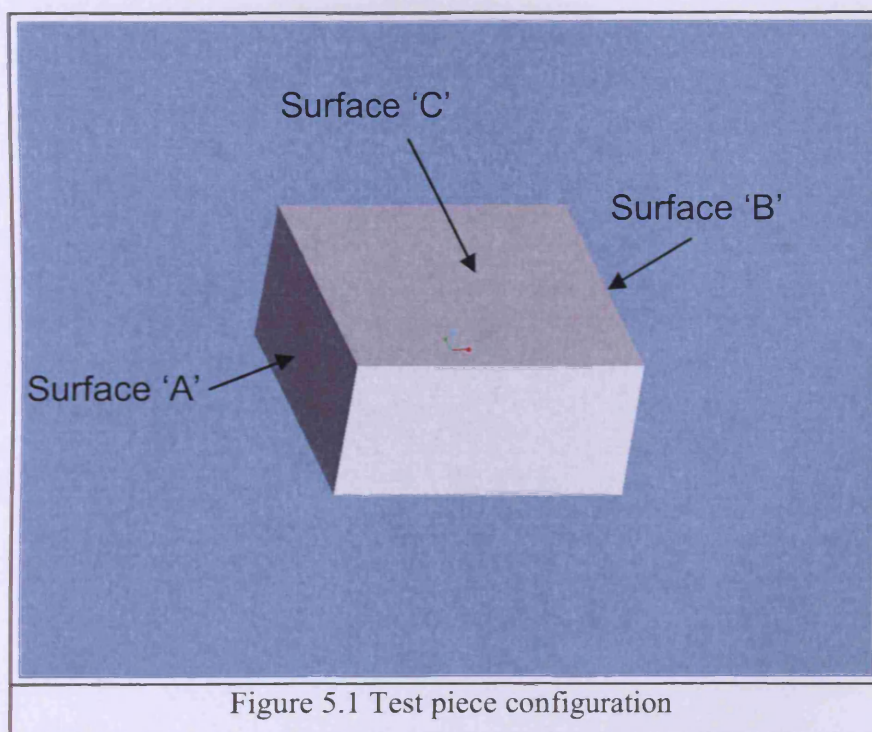
Jawahir et al. (2011) conducted a comprehensive investigation on the correlations and interactions between different machining processes, by evaluating process surface integrity parameters such as surface roughness, hardness and the associated residual stresses in a range of machining operations such as turning, milling, grinding and EDM. Although the experimental investigation analysed 5 different workpiece materials, the study did not evaluate the effect of varying the material microstructure on the resulting surface integrity.

The aim of this research is to investigate and characterise the effects of material

crystalline microstructure on the resulting surface integrity of samples machined by μ WEDM. In particular, the machining response of an “as received” aluminium alloy were analysed and compared against the results obtained on samples processed through extrusion strain hardening and severe plastic deformation. Especially, the process-material effects on the resulting micro hardness, phase content changes, HAZ, surface roughness, micro cracks, recast layers formation, MRR and element spectrum after both rough and finishing μ WEDM cuts were investigated.

5.3 Material, Equipment and Experimental Design

In this research three different test workpieces of AlMg4.5Mn aluminium alloy, with ISO designation Al 5083, were used to investigate the effects of material microstructure on surface integrity after μ WEDM. The material is a non-heat treatable alloy which can only be hardened by plastic deformation and can be used for producing micro injection moulding inserts where multi machine process chains are required. Prior to μ WEDM, the crystalline microstructure of two Al 5083 workpieces was modified by extrusion strain hardening and severe plastic deformation. Then, to investigate the process-material interactions two surfaces of the test workpieces were machined using an AGIE Vertex μ WEDM machine (APPENDIX D), and then analysed. A 50 μ m diameter wire with a steel core coated in brass was employed during the experiments. As shown in Figure 5.1, surfaces ‘A’ and ‘B’ of the test workpieces were machined with distinctly different technological parameters, in particular, rough and finishing μ WEDM cuts were used for surfaces ‘A’ and ‘B’, respectively. Table 5.1 lists the technological parameters chosen to carry out the tests.



After the completion of the μ WEDM operation, the test workpieces were cleaned in an ultrasonic bath with light degreaser to preserve the topology of the machined surfaces. To assess the roughness, micro hardness and phase content of surfaces 'A' and 'B', the samples were prepared using acrylic embedding resin and surface 'C' (see Figure 5.1) was polished with diamond paste and colloidal silica. Metallographic images were taken using a Leica DHLM microscope in polarised light in order to analyse the material crystalline microstructure and phase content. The micrographs were processed using erosion and grain separation morphology filters.

Table 5.1. Finish and rough machining parameters

Parameter	Rough Machining	Finish Machining
Flushing pressure (MPa)	0.2	0.2
Pulse OFF time (μs)	12.5	42.5
Open circuit voltage (V)	300	100
Pulse ON time (μs)	25	4.5

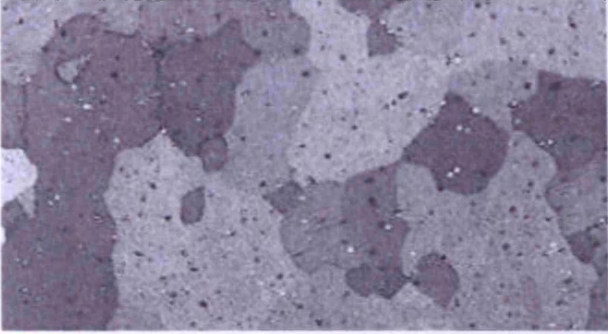
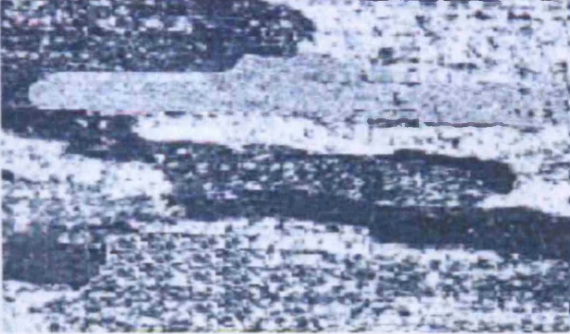
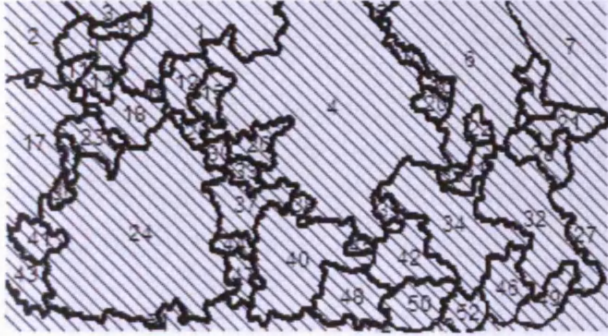

Table 5.2 Mechanical properties of the Al5083 samples

Sample Number	Al5083 samples processing	Yield Stress MPa	Ultimate Tensile Strength MPa	Elongation %
1 – As received sample (AR)	Annealed	152	315	18.8
2 – Conventionally processed sample (CP)	Forward Extruded	228	379	12.9
3 – Ultrafine grained (UFG) sample	After four ECAP passes	433	472	6.1

The three test workpieces used in this research together with their material microstructure are described below:

1. 'As received' (AR) Al5083. In its initial state the material was in the form of a 20mm diameter bar. The bar was produced through hot extrusion and then annealed at 540°C. Figure 5.2a shows a micrograph of the AR Al5083 used during this investigation that depicts the grain structure of the analysed area. The microstructure of the annealed material was non-uniform across the bar with an average grain size of approximately 80µm. The statistical analysis of the micrograph was performed employing the SIS 'Scandium' software according to ASTM E-112 96. In Figure 5.2b, a print out of this analysis is provided that includes calculations of the number of grains, their maximum and minimum grain sizes, the standard deviation of the grain sizes and the grains' aspect ratio.
2. 'Conventionally Processed' (CP) Al5083. The second test workpiece was strain hardened to $\varepsilon = 0.9$ by reducing the diameter of the AR bar from a diameter of 20mm to diameter of 13mm through forward extrusion at room temperature. After the extrusion process, the same area of the bar cross-section as in the AR sample was inspected. As can be seen in Figures 5.2c and 5.2d, the size of the grains was similar to that of the AR material but elongated along the extrusion axis with a significant change of the grains' aspect ratio, from 1.8 to 2.6. The material microstructure was almost uniform across the core of the bar.
3. 'Ultrafine Grained' (UFG) Al5083. The third test workpiece material underwent the following processing. Square samples with dimensions of 8 x 8 x 46 mm were cut out from the CP bar, lubricated and subjected to Equal Channel Angular Pressing (ECAP) at 180°C. Plastic strain generated during one ECAP pass was

approximately $\varepsilon = 1.15$. The process was repeated four times, with samples being rotated around the extrusion axes by 90° between consecutive passes (Popov et al., 2006). After four ECAP passes the size of the grains was reduced to approximately 200nm, as shown in the micrograph in Figure 5.3 and the transmission electron microscopy (TEM) image in Figure 5.4, which represented a size reduction in the order of 400 times.

As received (AR)	Conventionally processed (CP)
(a)	(c)
	
	
(b) Max. grain size = 361 μm Mean grain size = 78 μm Standard Deviation (mean grain size) = 78 μm Aspect ratio = 1.8 Grains measured = 72	(d) Max. grain size = 321 μm Mean grain size = 55 μm Standard Deviation (mean grain size) = 75 μm Aspect ratio = 2.6 Grains measured = 65
Figure 5.2. Micrographs of AR (a) and CP (c) samples and their corresponding statistical analysis	

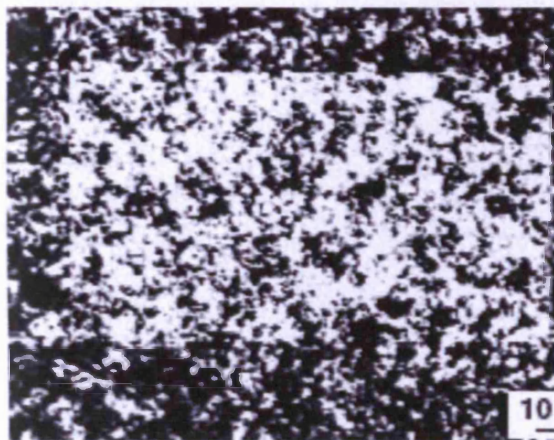


Figure 5.3. 'Ultrafine Grained'(UFG)
Al5083 sample morphology

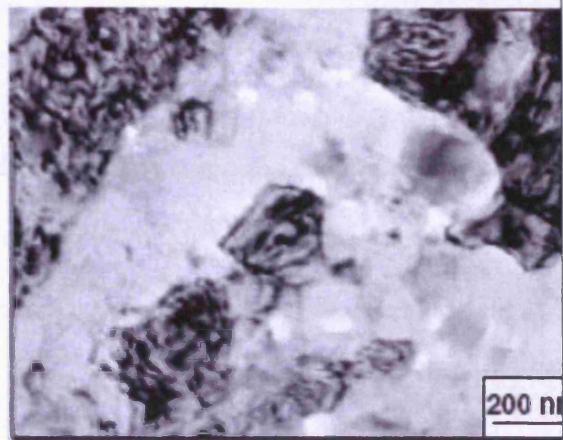


Figure 5.4. 'Ultrafine Grained' (UFG)
Al5083 TEM micrograph

The mechanical properties of the three test workpieces used in this research are compared in Table 5.2.

To ensure that the machining results on surfaces 'A' and 'B' of the AR, CP and UFG test pieces are representative, the rough and finish cuts were performed at three different cross-sections, in particular at a distance of 3.5, 3 and 2.5mm from the centre of the sample, respectively.

After the experiments, the surface roughness of each machined component was measured employing a white light interferometer microscope. The parameter used to evaluate the surface roughness was the arithmetic mean roughness (R_a) because relative heights in micro topographies are more representative. In particular, R_a measurements were obtained by analysing the scanned profiles along a sampling length of 250 μm and by applying a high-pass filter to eliminate their waviness characteristics.

To investigate MRR all three test pieces were machined using the roughing machining regime (Table 5.1). For each material, three runs were performed randomly to average out any extraneous factors that may be present. In addition to machining times, voltage pulse data were captured using a digital oscilloscope, Tektronix DPO7254, with a bandwidth of 2.5Ghz. To analyse process stability a pulse discrimination technique was applied similar to the technique employed by other researchers (Rajurkar et al., 1997; Yan and Chien, 2007). Pulses were characterised into three categories namely, normal, arc and short pulses. An illustration of the pulse classification is given in Figure 5.5. The normal and short pulses can be identified by detecting pulse voltage levels during on-time (t_i), while Arc pulses typically display no evidences of pulse voltage during t_i .

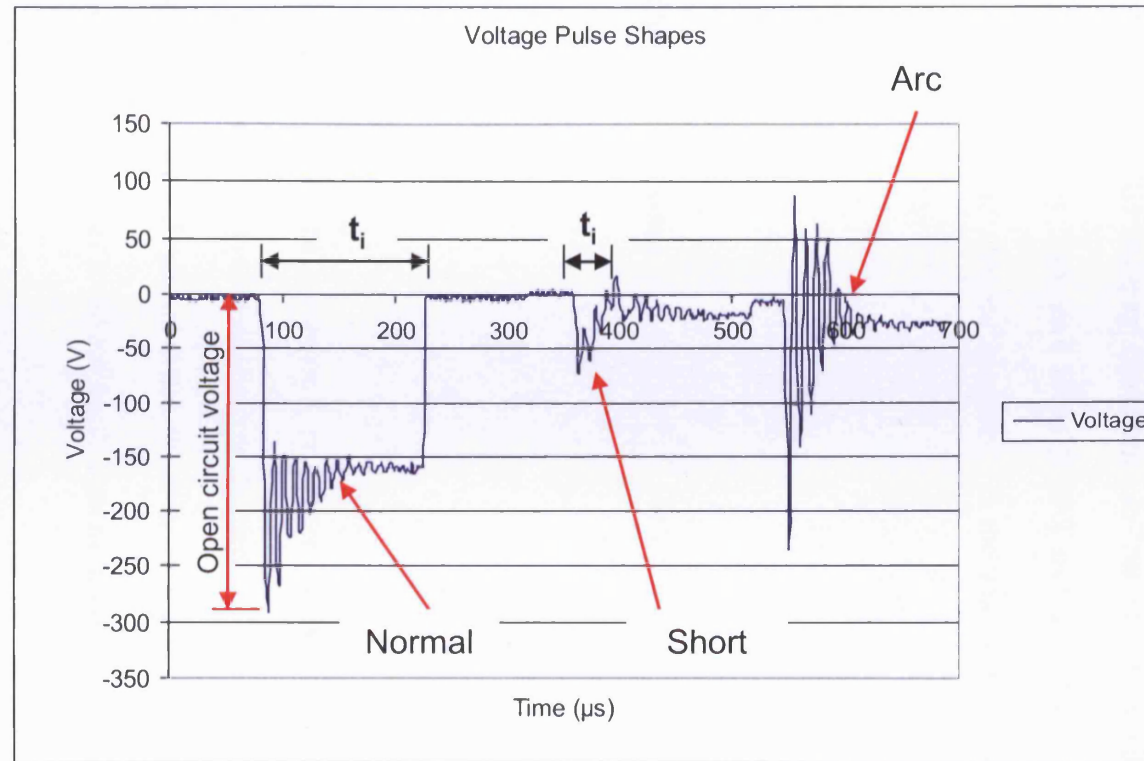


Figure 5.5. Pulse discrimination system showing three voltage pulse states

Finally, the recast layers formed on the μ WEDM machined surfaces of the test workpieces were analysed employing a focus ion beam/scanning electron microscopy (FIB/SEM) system (Carl Zeiss 1540XB). Cross-sectional cuts were made by FIB using high probe current of 2nA. Then, the machined surfaces were developed by a short ion exposure with low probe current of 200 pA to reveal the recast layer. The images were taken employing the FIB imaging mode with in-lens and back scattering electron detectors (BSED). Energy dispersive X-ray (EDX) analysis was carried out on each sample to investigate the element spectrum on the machined surfaces of the test workpieces.

5.4 – Results and Discussion

5.4.1 Micro Hardness

In order to characterise the mechanical properties of each sample material after μ WEDM, a depth hardness profile has been performed as displayed in Figure 5.6 using a micro hardness pyramidal imprint tester. From this test it is evident that all samples undergo structural changes up to 30 μ m depth from the machined surface.

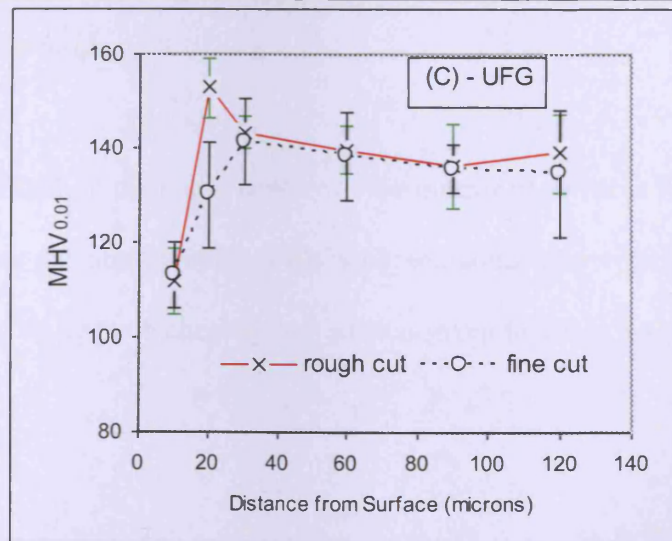
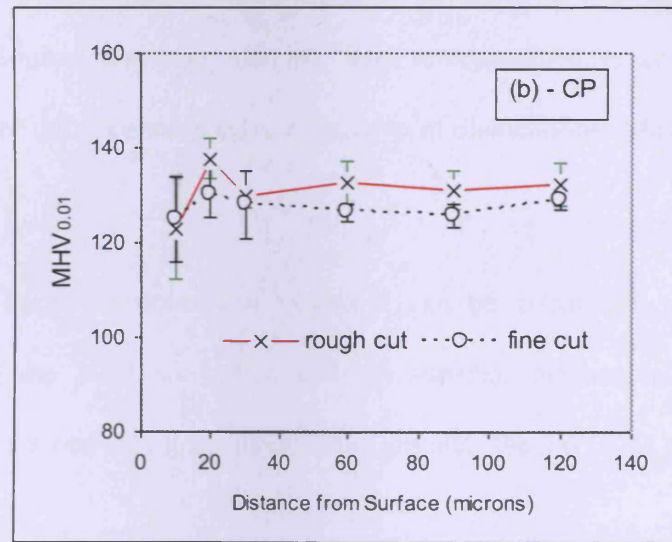
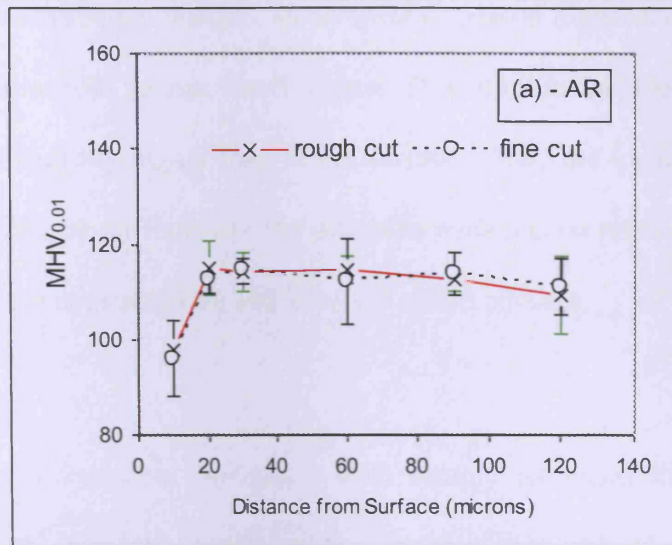


Figure 5.6. Micro hardness of the AR (a), CP (b) and UFG (c) samples

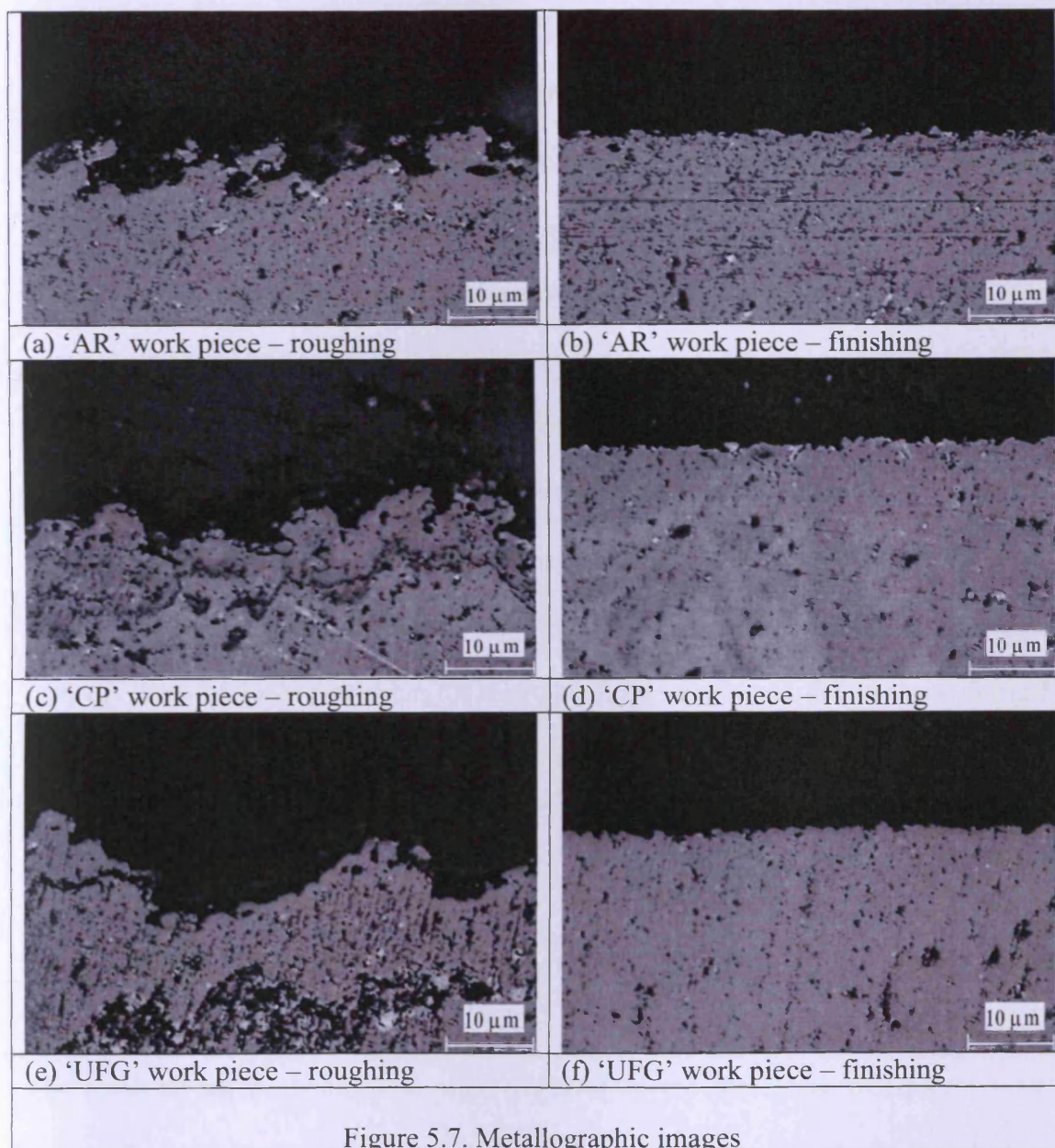
As a result of these structural changes, all samples displayed higher hardness values at approximately 20 μm from the machined surface. This suggests that the cooling rates at this depth are significantly higher than at the surface. Thus, the local increase of the micro hardness could be attributed to the intensive coalescence processes in the zone causing non-homogeneous structure and localised micro-stresses.

The micro hardness variation throughout each sample remained the same for all materials. Therefore, it can be concluded that the materials utilised in the tests had experienced continuous dynamic recovery and re-crystallization controlled by the dynamic balance of the generation and annihilation of dislocations (May et al., 2005).

Based on these micro hardness test results it can be concluded that the refined microstructure of the UFG workpiece with its superior mechanical properties has undergone some changes only up to depth of 30 μm after the μWEDM process.

5.4.2 Surface morphology

The effect of μWEDM on the phase content of the machined surfaces was investigated. Figure 5.7 presents the micrographs of the analysed areas after typical roughing and finishing μWEDM using the technology parameters given in Table 5.1.

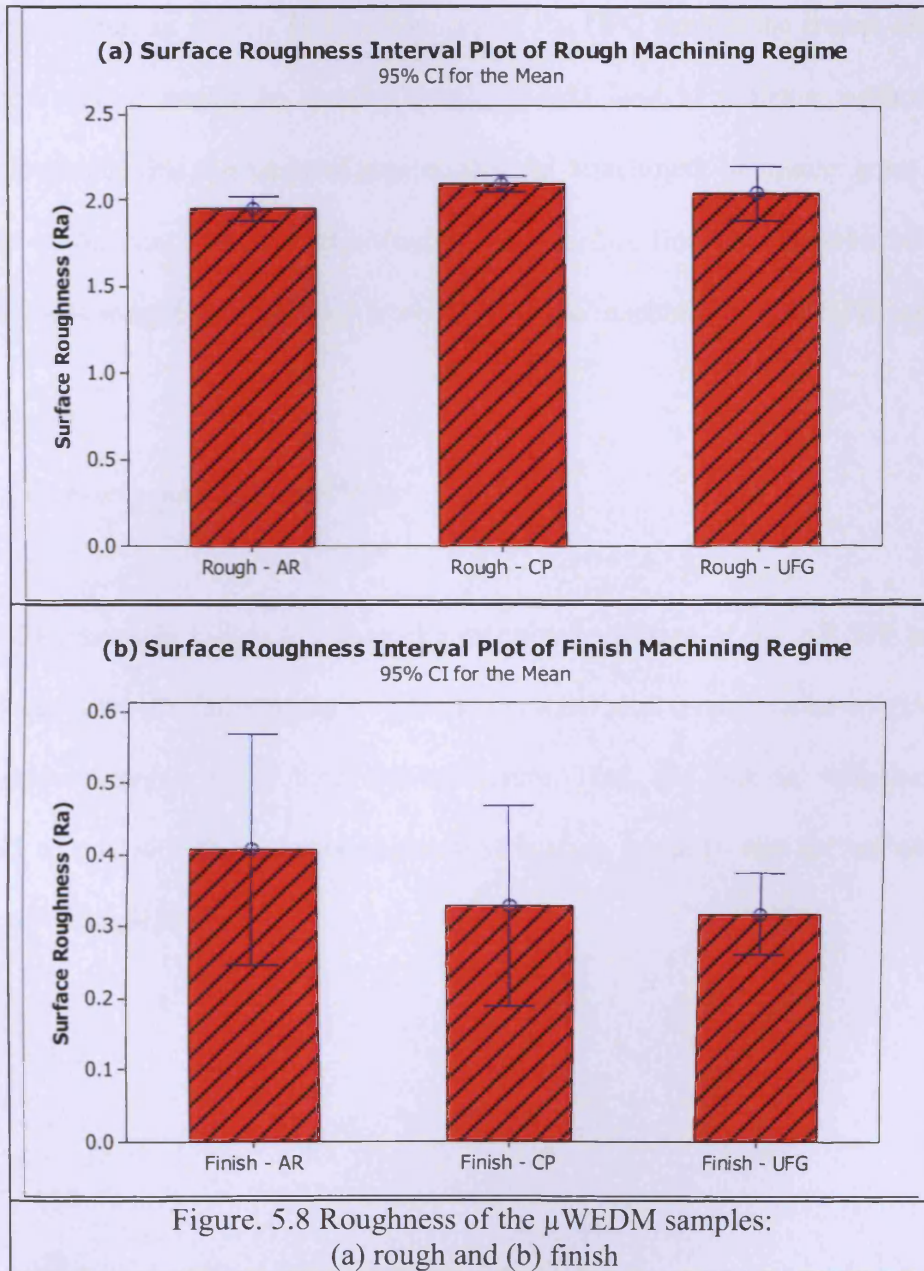


The extent of the material morphology change between the roughing and finishing machining regimes can be witnessed clearly. The difference can be explained with the structural changes that the test pieces undergo, especially the re-crystallisation of the extrusion strain hardened samples, CP and UFG. The clear sign of this re-crystallisation is the 5 to 10 μm deep HAZ as shown in Figures 5.7c and 5.7e. In the roughing regime the discharge energy (1.7 μJ) is significantly higher, approximately 20 times, than that applied during the finishing one (0.09 μJ). As a result of this the surfaces of the workpieces are subjected to very high thermal loads followed by a rapid cooling. The relatively high cooling speed of the workpiece surface impedes the stress relaxation and advanced stages of the re-crystallization process with corresponding uniform grain formation. Thus, the resulting non homogeneous material microstructure in the as-formed sub-zone is characterised with higher stress levels. Further evidences of such material morphological changes were also witnessed in the carried out micro hardness tests (Section 5.4.1). In particular, the micro hardness values recorded in the as-formed sub-zone, up to 30 μm depth, display high levels of variations which indicate a non homogeneous material microstructure.

5.4.3 Surface roughness

The resulting surface roughness after μWEDM of the three test workpieces were measured employing a white light interferometer microscope. The results are given in Figure 5.8. After the roughing machining regime all test workpieces displayed surface roughness that are comparable to each other. Although, the material refinement of the CP and UFG samples did not lead to a better surface quality after the roughing cuts (see Figure. 5.8(a) the roughness improved significantly after the finishing ones. The

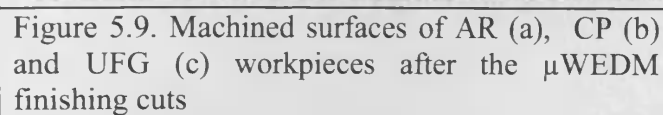
surface finish values achieved on the UFG sample after the finishing cut were marginally better than those on the other two samples. Also, it is worth noting that the surface roughness, R_a , of the UFG sample improved almost 6 times after the finishing cut.



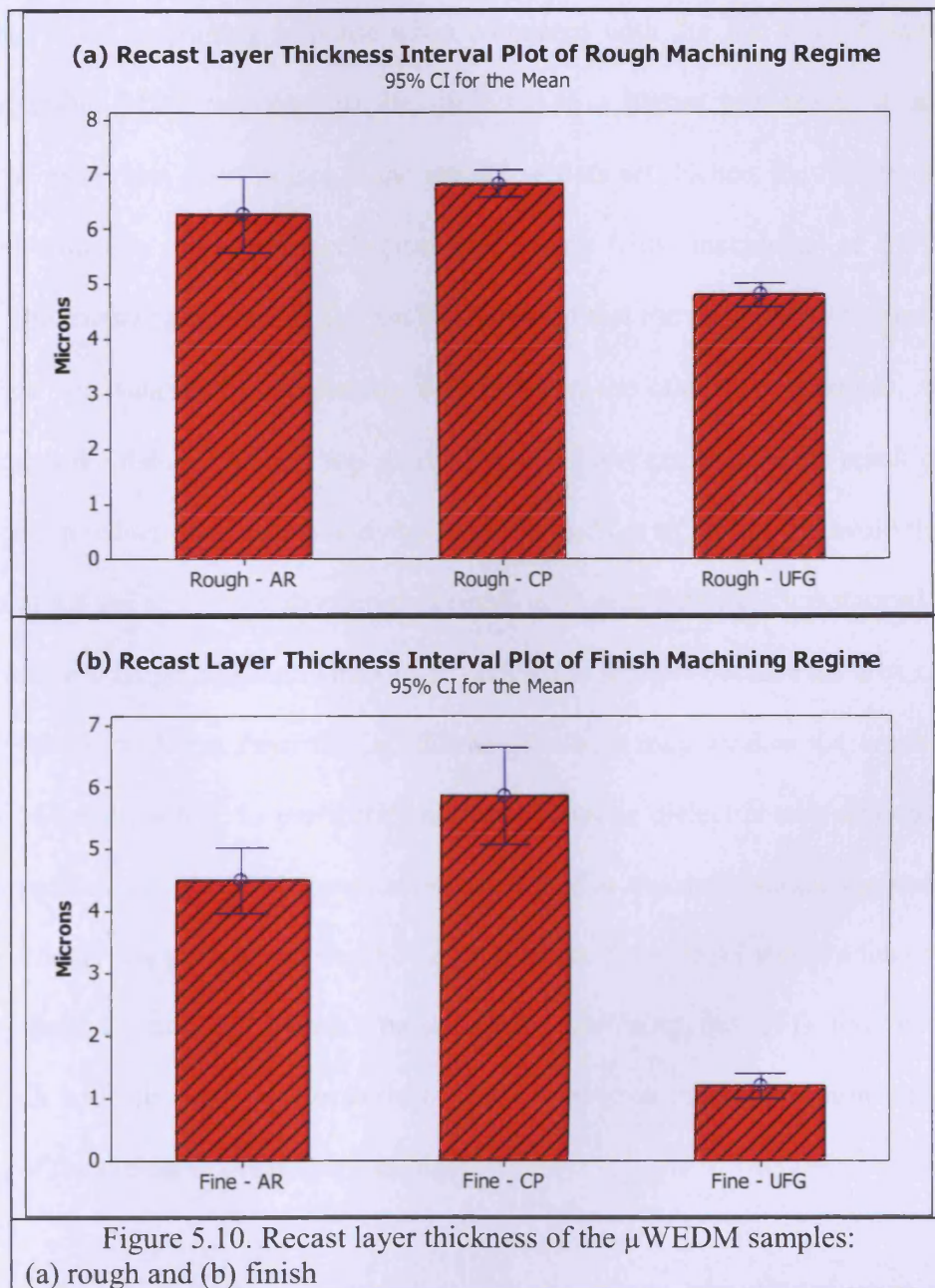
The marginally better results achieved on the UFG sample together with the high level of improvement between the roughing and finishing cuts should be attributed to the material microstructure refinement. μ WEDM is an electro thermal process, and by creating plasma channels between the wire and the workpiece the material is eroded by detaching clusters of grains. Thus, in the case of the UFG sample the craters left on the machined surface would be smaller, which should lead to a better surface finish. Further evidence that this removal mechanism, the detachment of smaller grain clusters from the workpiece, leads to improvements of the surface finish can be witnessed in the relatively low roughness variations recorded after the machining of the UFG samples.

5.4.4 Micro cracks and recast layer

The SEM images in Figure 5.9 show the machined surfaces of the AR, CP and UFG workpieces after the finishing cuts. The results show that micro cracks are present on all workpieces regardless of their microstructure. Thus, the material refinement does not lead to any significant improvements of surface integrity that are necessary for some critical applications.



Generally, the recast layer that is formed on the surfaces of WEDM components has a detrimental effect and limits the application areas for this technology. Figure 5.10 compares the thickness of the recast layers formed on the three different samples after applying the rough and finish machining regimes. The UFG sample has a recast layer that is considerably thinner than that formed on the other samples especially after the finishing cuts. Considering the material removal mechanism, this can be explained with the refined material microstructure of the UFG workpiece. The recast layers are typically composed of material that fails to be evacuated from the gap between the electrode and the workpiece through flushing, and is thereby re-solidified onto the machined surface. As the workpiece has an ultra-fine grain structure the debris generated during μ WEDM are much finer, which improves the efficiency of the evacuation process and thus results in a thinner recast layer. However, it is worth noting that the recast layer thickness on the AR and CP samples did not differ significantly from one another after both roughing and finishing cuts.



5.4.5 Material Removal Rates

By analysing pulse shape variations in the data sets the pulses are clustered in three categories as illustrated in Figure 5.5. The results show that the UFG material has a favourable EDM machining response when compared with the AR and CP samples. This favourable EDM response can be attributed to a higher proportion of normal pulses and much less short pulses in the respective data set. Hence, the results can be explained with the improved mechanism of flushing when machining of the UFG sample. The results presented in Section 5.4.4 showed that the recast layer formed onto the surface was smaller in comparison with those on the other two materials, which suggests that the debris flushing was more efficient. Short circuits are the result of the minimum gap reduction to below a given value (Kunieda et al., 2005). To avoid them it is essential for the next pulse discharge to occur in an area sufficiently distanced from the previous discharge location. This can be difficult to achieve because the area can be contaminated with debris from the last discharge, which may weaken the breakdown strength of the dielectric. In particular, failure to achieve dielectric recovery strength between pulses through debris evacuation can result in thermal overheating and non uniform erosion due to the occurrence of short circuits. Figure 5.11 shows a lower ratio between short circuits and normal pulses when machining the UFG test piece in comparison with the other two materials. This observation indicates a more efficient recovery of the dielectric breakdown strength.

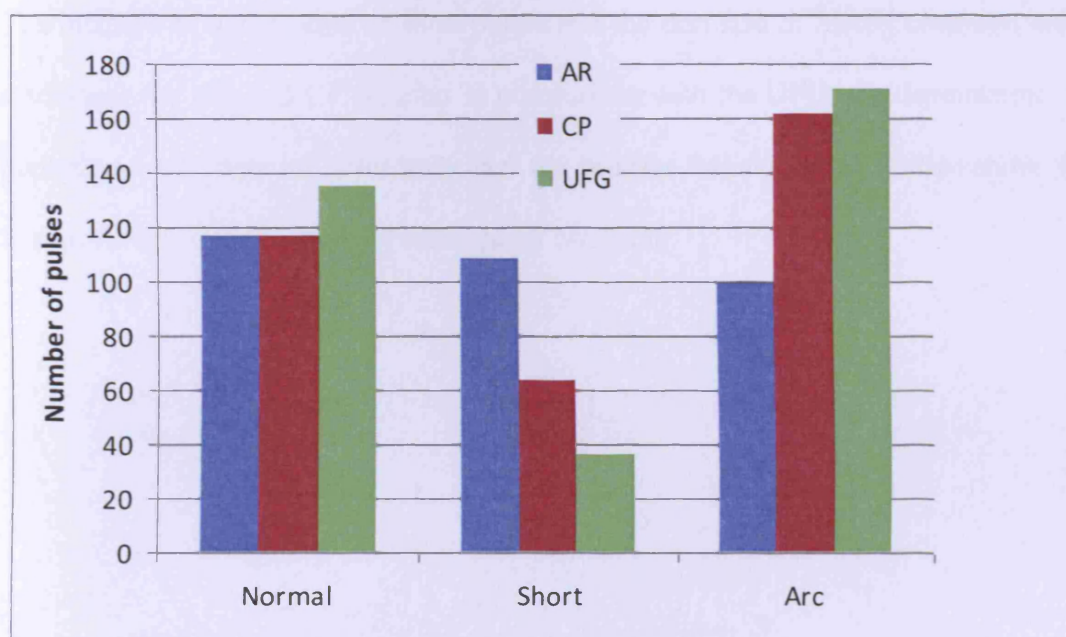


Figure 5.11. Pulse characteristics for the three studied materials

Figure 5.12 presents MRR of the three test materials. MRRs are given in machined volumes per minutes. The highest removal rates were achieved on the UFG sample, which demonstrates an improvement of EDM efficiency when machining materials with finer material micro structure. Again, this improvement can be attributed to the more effective recovery of the dielectric strength.

The increase of the number of short pulses and the decrease of MRRs observed when machining the AR and CP samples in comparison with the UFG one demonstrate the importance of material microstructure on process behaviour and also show the improvements that the material refinements can bring.

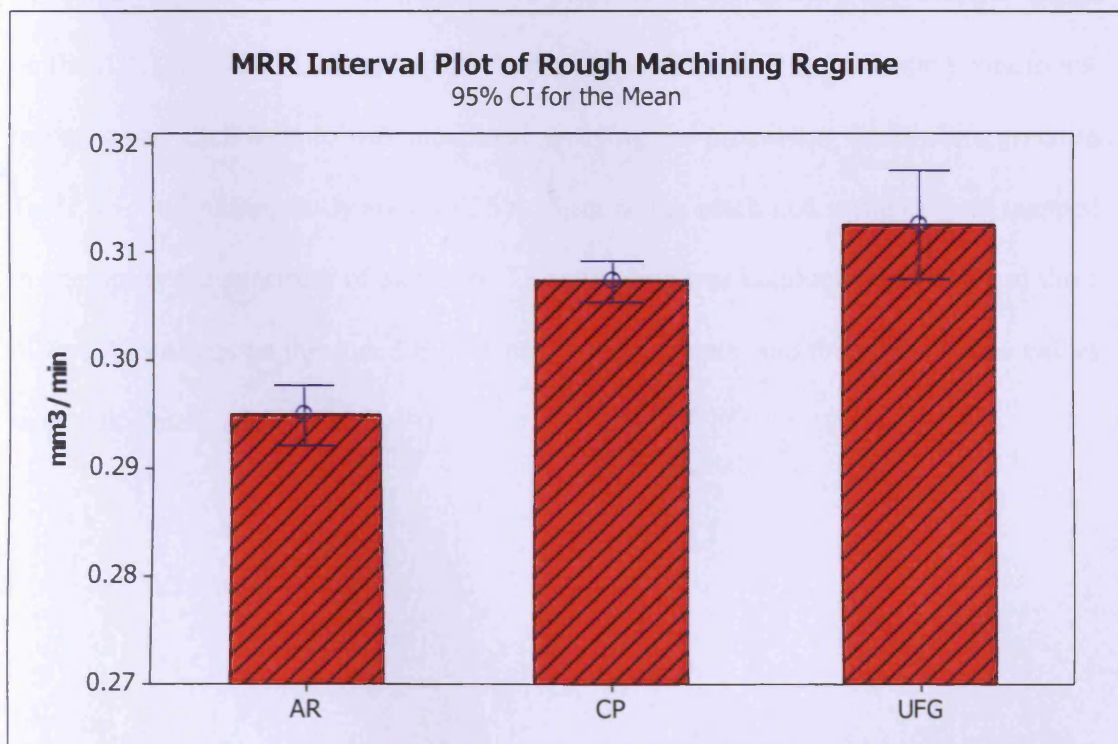


Figure 5.12. MRR of the μ WEDM samples

5.4.6 Material composition

As a result of μ WEDM the element spectrum of the machined surface may not be solely composed of atoms originated from the workpiece. Changes in the composition may occur due to contaminations from the wire electrode or dielectric fluid. To study the spectrum of the main elements present on the machined surfaces after μ WEDM, an EDX analysis was carried out. Figure 5.13 presents typical element spectrums obtained on the AR, CP and UFG samples after μ WEDM under different processing conditions. In particular, each sample was machined applying the processing parameters given in Table 5.1, and subsequently areas of $25 \times 15 \mu\text{m}$ on the machined surfaces were mapped to exemplify the spectrum of elements. The sampling was conducted randomly at three different locations on the A and B surfaces of each sample, and then the average values were calculated.

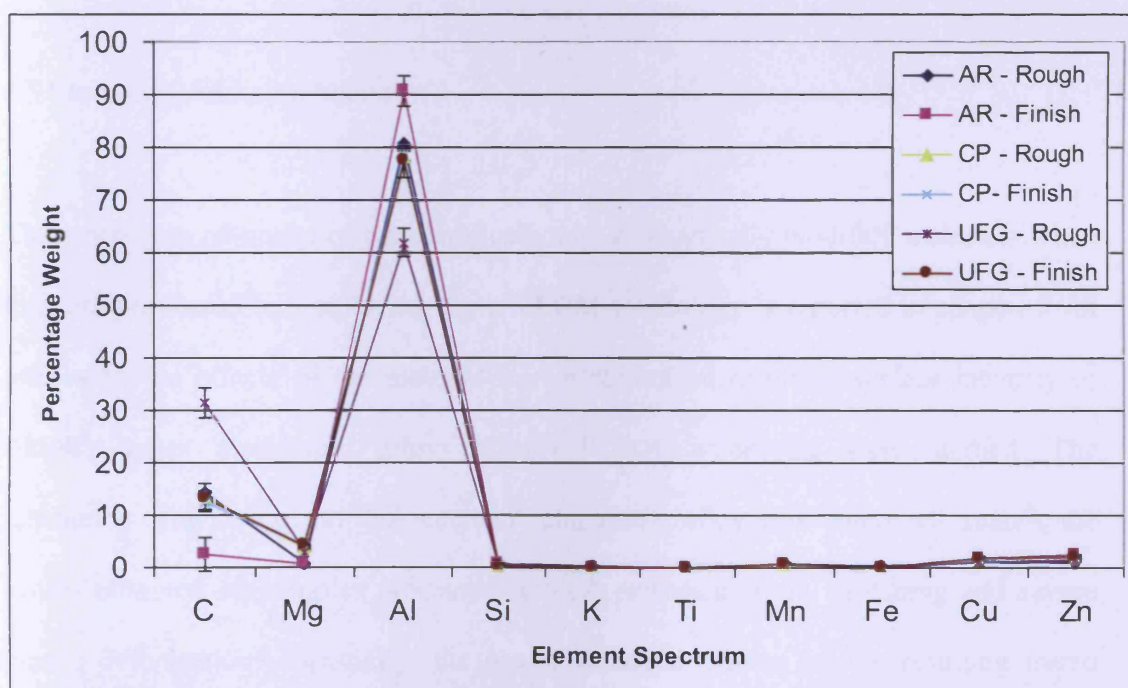


Figure 5.13. The EDX spectra of the workpiece surfaces after μ WEDM

It is not difficult to notice that the spectrum of elements is relatively uniform throughout the inspected samples. Some variations of the carbon and aluminium content were observed on the CP and UFG samples under different μ WEDM regimes. The highest degree of carbon content variation was measured on the UFG workpiece. The increase of the carbon content is usually associated with bi-products of the dielectric ionisation during the erosion process, and also as a result of C atom transfer from the wire electrode. To compensate for the increase of the carbon content in the UFG sample a reduction in the aluminium content was observed.

5.5 Summary and conclusions

The machining response of metallurgically and mechanically modified materials when they are processed by employing the μ WEDM technology is reported in chapter 5. In particular, the effects of the material microstructure on resulting surface integrity of Al5083 series aluminium alloys after μ WEDM processing were studied. The machining response of an “as received” aluminium alloy was compared against the results obtained on samples processed through extrusion strain hardening and severe plastic deformation. Especially, the process-material effects on the resulting micro hardness, phase content changes, heat affected zone, surface roughness, micro cracks, recast layer, material removal rate and element spectrum after both rough and finishing μ WEDM cuts were investigated.

Based on the obtained experimental results the following conclusions could be drawn:

- The micro hardness analysis showed that there were structural changes within all samples up to 30 μm depth. In addition, the refined microstructure of the UFG test workpiece with its superior material hardness is maintained after the μWEDM process. Localised hardening was observed in the as-formed sub-zone on the machined surface and the micro hardness values recorded up to 30 μm depth display high levels of variations which indicate un-homogeneities in the material microstructure.
- The surface roughness achieved on the UFG sample after the finishing cut was only marginally better than those on the other two samples. However, the surface roughness, R_a , of the sample improved almost 6 times in comparison with that obtained after the roughing cut.
- All test samples displayed some evidences of micro crack formation regardless of the microstructure.
- The recast layer formed on the UFG sample was considerably thinner than those on the other samples especially after the finishing cuts.
- The decrease of the number of short pulses and the increase of MRRs observed when machining the UFG sample in comparison with the other two materials demonstrated the importance of material microstructure on process behaviour and also showed the improvements such material refinements could bring.

- Variations of the carbon and aluminium composition content were observed on the CP and UFG samples after μ WEDM under different machining regimes.

CHAPTER 6

CONTRIBUTIONS AND FUTURE WORK

This chapter summarises the main contributions to knowledge accomplished in this work. It also provides suggestions for future work.

6.1 Contributions

The main contributions to existing knowledge in micro electrical discharge machining (μ EDM) are presented below:

1. The choice of electrode material used when applying the process of wire electro-discharge grinding (WEDG) has a significant effect on achievable aspect ratio and surface roughness. This is attributed to the different Young's Modulus of elasticity and contrasting material microstructures of different electrode materials. For example, to produce electrodes of higher aspect ratios tungsten carbide is more appropriate than tungsten, while the use of tungsten electrodes provides a higher level of surface finish.
2. The application of specially developed dressing strategies has a major effect on the quality of the electrode. In particular, a high number of machining passes applied in the dressing process leads to a higher standard of surface finish.
3. Due to the inherent process errors related to machine accuracy and repeatability of the WEDG process, specialised "adaptive control" systems need to be developed and implemented to increase the process accuracy. Such systems

should counter act any time-varying or uncertain process characteristics that are machine specific, such as positional accuracy and repeatability of the dressing unit, and any dimensional variations when the electrodes are brought into contact with the running wire.

4. When applying the process of WEDG in combination with micro wire electrical discharge machining (μ WEDM), specially designed strategies have to be applied for workpiece preparation and thus to minimise the material removal volume and its variations prior to starting the workpiece rotation and WEDG. At the same time, it is necessary when such strategies are applied, measures to be taken to compensate the inherent run-out of submergible spindles.
5. Technological parameters that are optimised for conventional μ WEDM are not directly applicable for use with the WEDG process as they do not provide comparable results in respect to surface finish. The introduction of test piece rotation prevents a static discharge channel being maintained over relatively long pulse ON times as the discharge channels are broken up above a particular rotational speed. Thus, the WEDG process requires a reduction in discharge energy in order to achieve surfaces roughness comparable with that of μ WEDM. At the same time, such a reduction of discharge energy brings negligible improvements to the surface roughness if applied to conventional μ WEDM.
6. The application of inductive learning algorithms is a simple and cost-effective method for identifying patterns in the process behaviour and thus to create models for on-the-machine prediction of the surface roughness. Once gathered and interpreted the developed predictive models benefit machine operators in allowing them to understand the causal relationships between process parameters and the resulting process performance, and thus the logic of the underlying model.

7. Material microstructure refinement does not only provide superior mechanical properties to workpiece materials but also leads to favourable machining “footprints” during μ WEDM machining and a lower surface roughness. The reduction of recast layer thickness witnessed in materials with microstructure refinements facilitate the flushing of debris. Thus, this leads to a faster dielectric recovery, a decrease of the number of short pulses and thus to an increase of the material removal rates. In addition, the material refinement facilitates the removal of smaller grain clusters detached from workpiece, and thus leads to improvements in the resulting surface finish.
8. Surface contamination due to the alloying of the tool electrode with the workpiece material is always present regardless of material microstructure, and thus can limit the application areas of this technology.

A list of publications that have been generated through the completion of the thesis are displayed in APPENDIX F

6.2 Future work

To further develop the electrical discharge machining process possible directions for future research are presented below:

1. By employing “adaptive control” systems many of the inherent process errors can be compensated. Thus, the use of such “adaptive control” systems should not be limited to just increasing the accuracy and repeatability of the dressing process. For example, they could be used to monitor and take corrective actions in regards to the electrode wear during milling and drilling operations. Having a fully integrated system with such

functionality would also reduce substantially the time necessary to investigate material/process interactions of new electrode/workpiece combinations.

2. Material refinement that leads to a favourable machining response during μ EDM will be critical in overcoming some process limitations and challenges associated with the process functionality and performance. Especially, advances in material engineering and processing technologies are expected to lead to a reduction of achievable minimum feature sizes, higher material removal rates and a better surface finish. Therefore, it is necessary to study the process/material interactions of more electrode/workpiece combinations. Research in this area should not be focused only on workpiece materials. Development of new and improved electrode materials will be also critical in order to limit some inherent processing issues such as secondary discharging. Potentially, such material developments could lead to improved machining efficiency, reduction of electrode wear and feature sizes, and a better surface finish.

3. The use of dielectric fluids with suspended powder is another area of research that is highly promising for improving the surface finish in μ EDM die-sinking. However, these improvements may not be just limited to this process and the resulting surface roughness. Therefore, it is necessary also to investigate how the use of such dielectric fluids affects other process characteristics, such as the surface integrity as a whole, electrode wear and material removal rates and whether such improvements can be obtained in μ WEDM and WEDG, too.

APPENDIX A

Wire electro discharge grinding device design

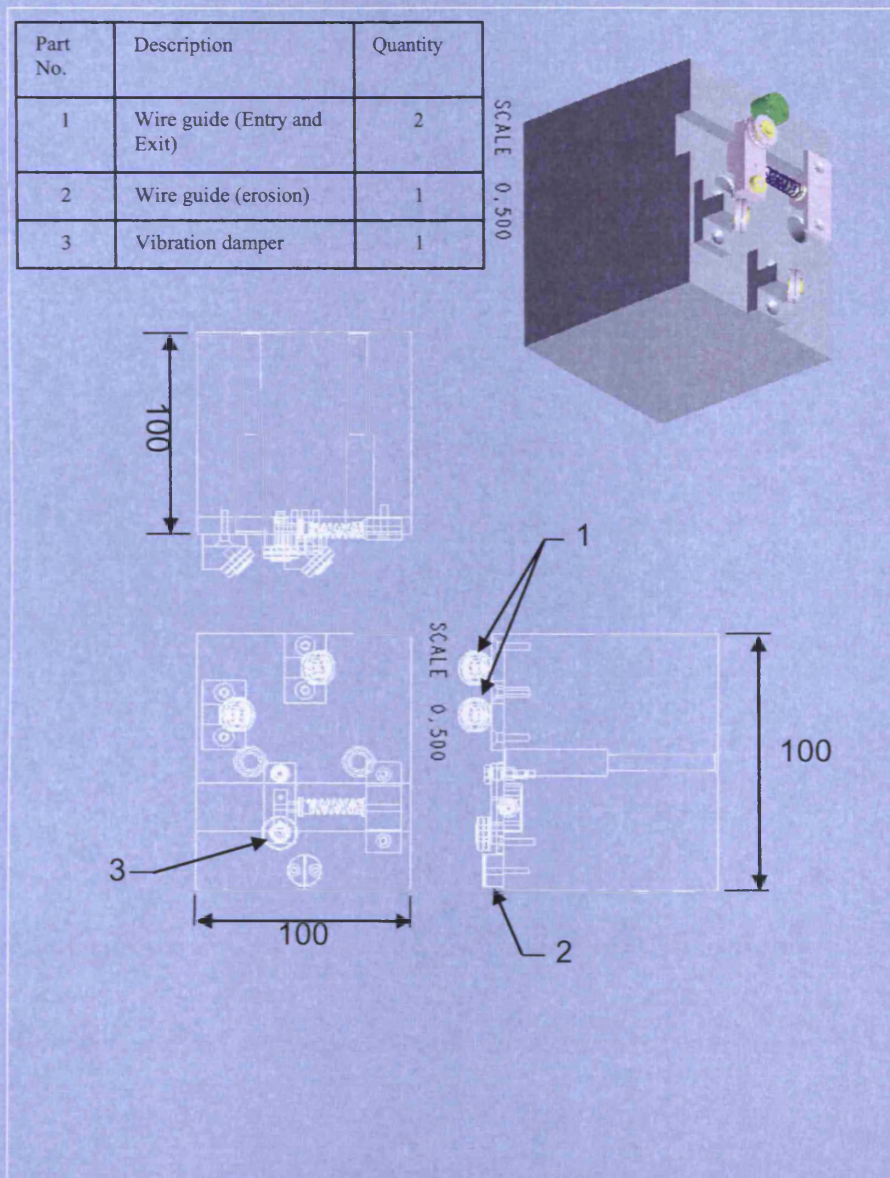


Figure A1. Wire electro discharge dressing device

APPENDIX B

Agietron Compact 1 Micro die sink

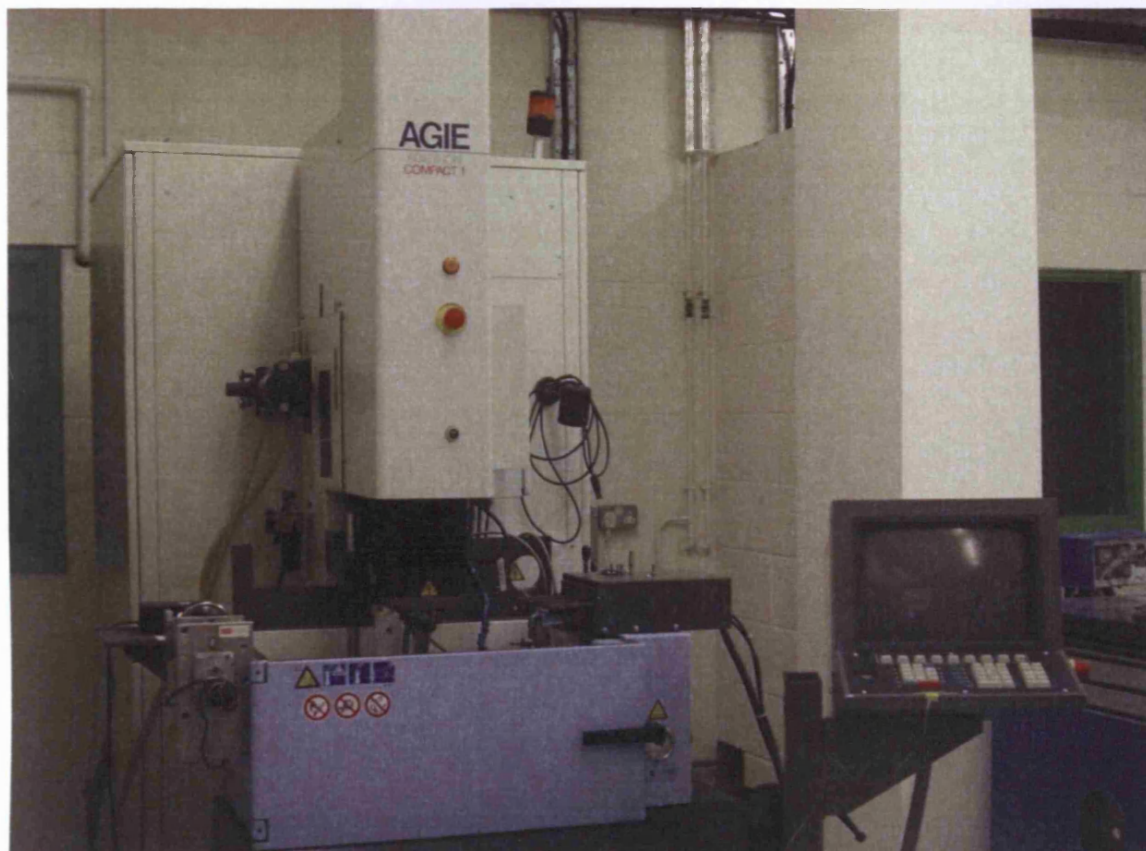


Figure B1. Agietron Compact 1 Micro die sink

Table B1. Technical Specification of Agietron Compact 1

High speed spindle	100 to 2500 RPM
Standard electrodes	Ø0.12 to Ø0.90mm
Polarity	Positive/negative
Idle voltage	60 to 250 volts
Charging current	0 to 5.8 Amps
Charging pulse length T	1 to 24 μ s
Pause	1 to 7500 μ s
Flushing	5 to 20 bar
Capacitance	0.2nF to 1320nF
Working area (X/Y/Z)	300 x 200 x 150 mm
Dielectric	Oil (Hedma 111)
Precision of positioning	+/- 6 μ m

APPENDIX C
SARIX micro EDM drilling machine

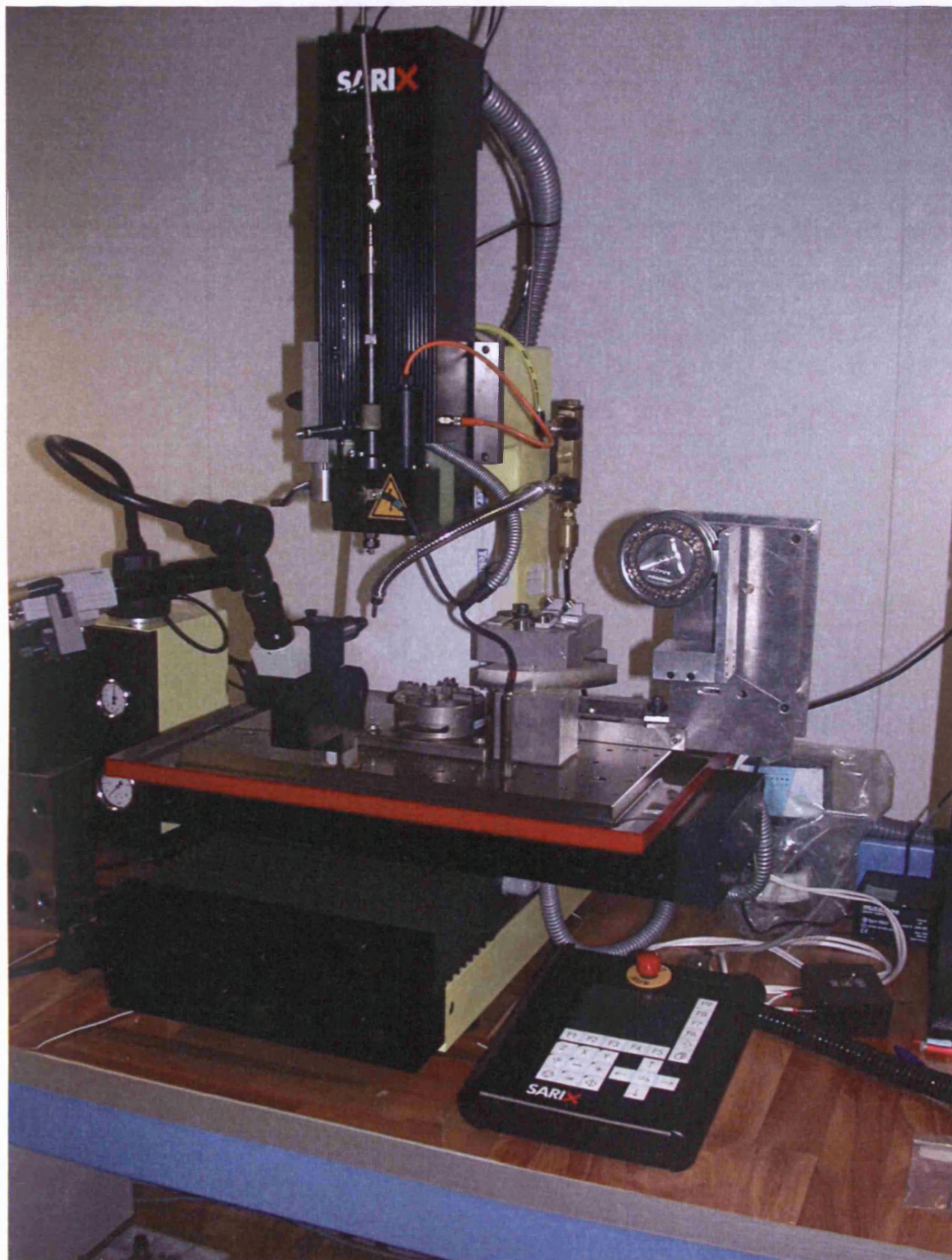


Figure C1. SARIX micro EDM drilling machine

Table C2. Technical Specification Sarix SX-100 HPM

Work table size	530 x 270 mm
Travel X axis	200 mm
Travel Y axis	150 mm
Travel Z axis	150 mm
Z axis feed rate	650mm/min
X/Y axis feed rate	800mm/min
Precision of positioning	+/- 2 μ m
Resolution	0.1 μ m
Maximum workpiece weight	20 kg
Electrode sizes	Ø0.09 to Ø0.3mm
Idle voltage	60 to 110 volts
Pulse ON time	1 to 5 μ s
Pulse frequency	110 to 150 KHz
Dielectric	Oil (Hedma 111)

APPENDIX D
AGIE Vertex wire electrical discharge machine

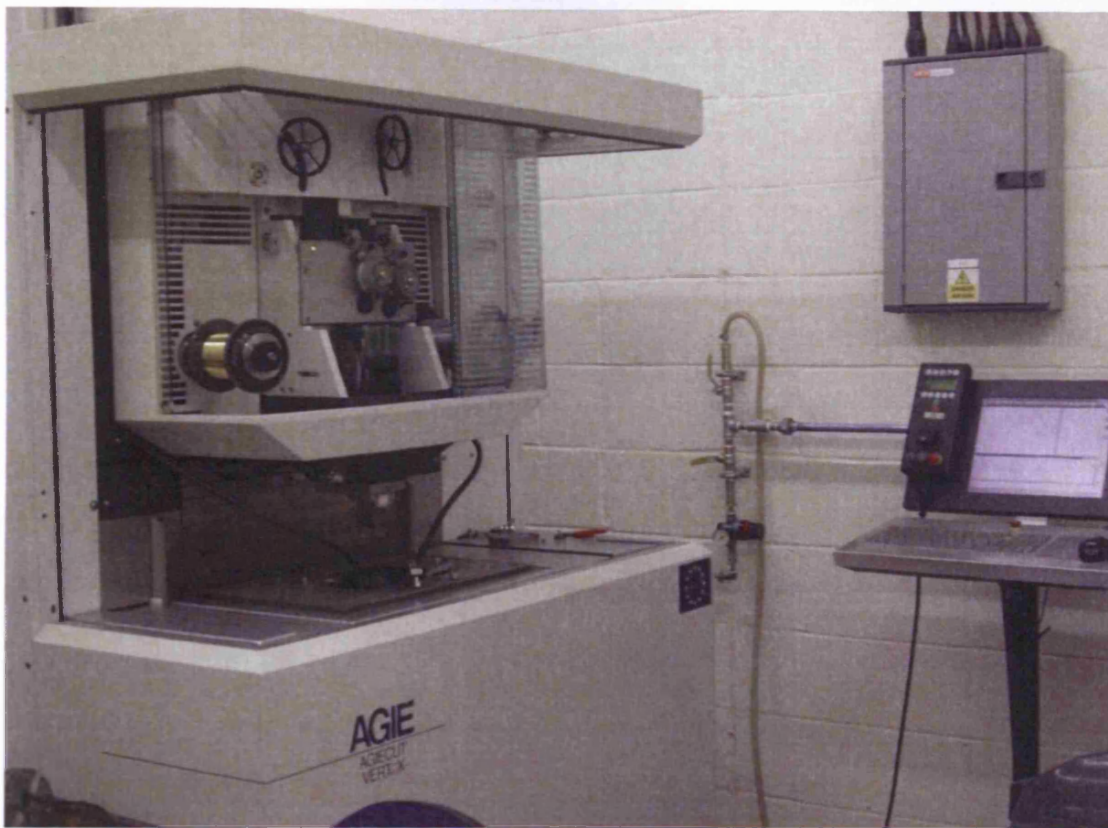


Figure D1. AGIE Vertex Micro Wire Electrical Discharge Machin

Table D1. Technical Specification Vertex wire electrical discharge machine

Maximum workpiece dimensions	Length x width x height	300 x 200 x 80 mm
Maximum workpiece weight		15 kg
Travels	X/Y/Z axis	220/160/100 mm
	U/V axis	40 mm
	Minimum taper/height	2°/ 80 mm
High-speed motion	X/Y/U/V/Z axis	3 m/min
Drives	X/Y/U/V/Z axis	Brushless AC servomotors
Geometrical tolerances	Linearity U/V axis	1µm
	Linearity U/V/Z axis	2µm
	Squareness X/Y axis	2µm
	Squareness U/V axis	2µm
Wire threading system	Input element	Alphanumeric push-button keyboard/mouse
	Threadable height	Up to 100 mm
Wire guide system	“V” guides, wire diameters	0.03mm
	Wire spool	Up to 8kg
	Wire tension	0.1 + 25N
Flushing	Pressure flushing	0.1 to 18 bar
	Combined flushing	Coaxial flushing/pressure/suction
DA unit	Pre-deionised water	10µS/cm
Wire diameters		0.03 to 0.3 mm

APPENDIX E

Training instances for tests 28 to 31

APPENDIX E. Five additional training instance performed using a combination of controlled parameters not used previously

Test 28				Test 29			
Vx	Ufs	S.ist	Pw	Vx	Ufs	S.ist	Pw
85.2	55	11	30	36.6	20	26	40
86.4	24	16	30	37.2	19	26	40
76.8	17	48	30	37.2	21	27	40
79.8	20	59	30	37.2	21	26	40
81	40	58	30	37.2	21	26	40
79.2	62	45	30	37.8	22	24	40
81.6	46	32	30	37.8	21	22	40
87.6	21	19	30	37.2	19	24	40
82.2	13	17	30	37.8	20	24	40
81	51	13	30	37.2	20	24	40
82.2	27	17	30	37.8	19	24	40
75	13	40	30	38.4	21	26	40
73.2	16	59	30	39	18	22	40
79.2	47	59	30	39	19	24	40
78.6	61	53	30	39.6	19	24	40
79.8	43	28	30	39	21	21	40
79.8	25	24	30	39	20	22	40
78.6	13	15	30	39.6	20	22	40
77.4	44	10	30	39	19	22	40
79.8	21	21	30	39	19	24	40
74.4	13	43	30	39.6	20	24	40
76.8	22	54	30	40.2	18	22	40
80.4	44	57	30	39.6	20	24	40
77.4	64	54	30	41.4	20	22	40
78.6	42	39	30	41.4	18	22	40
84	17	15	30	41.4	19	22	40
81	57	18	30	40.8	18	27	40
76.2	49	15	30	42	20	26	40
80.4	20	15	30	41.4	19	22	40
77.4	8	39	30	41.4	18	22	40
72	23	56	30	41.4	20	26	40
72.6	27	31	20	41.4	19	24	40
60.6	40	38	20	41.4	17	24	40
46.2	36	34	20	41.4	18	22	40
34.2	30	27	20	41.4	17	21	40
25.2	23	23	20	41.4	17	22	40
16.2	20	20	20	42	15	21	40
17.4	22	23	20	41.4	17	22	40
18	27	28	20	40.8	16	21	40
18.6	19	36	20	41.4	18	22	40
19.8	19	37	20	40.8	18	22	40
21	30	37	20	40.8	18	21	40
22.8	37	27	20	40.8	18	21	40
24.6	31	23	20	41.4	17	22	40
25.2	23	17	20	41.4	17	21	40
25.2	16	16	20	41.4	15	20	40

25.8	18	16	20	41.4	17	21	40
25.8	22	25	20	41.4	16	20	40
25.8	13	31	20	41.4	16	20	40
26.4	14	35	20	42	18	20	40
28.2	26	33	20	42	17	20	40
29.4	36	29	20	42.6	18	21	40
30	31	18	20	42.6	18	21	40
31.8	18	15	21	42.6	18	21	40
33	10	11	21	42.6	17	20	40
33.6	33	15	22	43.2	18	20	40
34.8	18	19	22	42	17	21	40
36.6	10	35	22	42	17	21	40
39	14	39	23	42.6	16	20	40
42	29	38	23	41.4	16	22	40
38.4	48	37	24	41.4	16	22	40
36	39	33	24	42.6	17	24	40
34.2	28	23	24	42.6	18	24	40
31.8	49	18	25	42	19	24	40
30.6	40	24	25	42.6	16	20	40
36	23	29	25	42.6	17	20	40
40.2	15	41	26	34.2	11	32	30
46.2	14	48	26	28.2	23	27	30
53.4	39	44	26	22.2	22	31	30
58.2	47	36	26	15.6	21	28	30
56.4	45	31	27	9	20	27	30
55.8	25	23	27	10.8	23	31	30
54	17	17	27	10.8	22	31	30
50.4	38	16	27	10.8	24	26	30
49.2	22	23	28	11.4	20	26	30
52.2	20	53	28	12	22	28	30
54.6	23	55	28	12	20	24	30
56.4	42	52	28	12	21	24	30
58.8	52	39	28	12	19	24	30
63	36	30	29	12	23	24	30
63	26	22	29	12	20	24	30
63	58	18	29	12	21	24	30
63.6	45	20	29	12	20	24	30
63	19	31	29	12.6	20	24	30
61.8	11	38	29	12.6	19	22	30
69.6	13	53	30	12.6	20	24	30
69.6	54	59	30	12.6	20	24	30
72.6	59	41	30	13.2	18	24	30
74.4	33	27	30	12.6	21	24	31
78.6	53	16	30	13.2	21	24	31
				13.8	20	24	32
				14.4	21	22	32
				14.4	20	24	32
				16.2	21	24	33
				16.2	21	26	33
				16.8	21	26	34
				18	23	28	34

				18.6	20	24	34
				19.2	21	24	35
				20.4	19	26	35
				21.6	19	27	35
				22.2	22	28	36
				24	21	27	36
				23.4	20	26	36
				24.6	21	26	36
				25.2	23	30	37
				25.8	23	27	37
				26.4	20	27	37
				27.6	19	26	37
				28.2	19	24	37
				28.2	20	26	38
				29.4	17	22	38
				29.4	21	26	38
				30	22	24	38
				31.2	22	21	38
				32.4	21	24	39
				32.4	20	24	39
				34.2	22	24	39
				35.4	22	24	39
				34.8	22	24	39
				35.4	20	24	40
				36.6	20	24	40
				36	20	24	40
				36.6	20	24	40
				37.2	21	24	40
				37.8	21	24	40
				37.2	20	26	40
				38.4	21	24	40
				38.4	19	21	40
				38.4	19	22	40
				38.4	18	24	40
				38.4	19	24	40
				37.8	18	27	40
				37.8	18	24	40
				37.8	15	24	40
				38.4	18	24	40
				38.4	18	24	40
				39	19	24	40
				39	19	24	40
				39	18	24	40
				39	18	21	40
				39	19	24	40
				38.4	17	18	40
				37.8	17	21	40
				39	17	24	40
				38.4	15	21	40
				39.6	17	22	40
				39	19	22	40

				39.6	18	21	40
				39.6	20	18	40
				39.6	20	18	40
				39	18	20	40
				39.6	17	18	40
				40.2	18	20	40
				40.2	16	20	40
				40.8	16	18	40
				43.2	29	36	40

Test	Test 28				Test 29			
Name	Vx	Ufs	S.ist	Pw	Vx	Ufs	S.ist	Pw
Nb data	90	90	90	90	157	157	157	157
Mean	55.4200	30.4778	31.3556	26.0778	32.9732	19.1975	23.5987	37.7389
Stdeviation	22.5876	14.7223	14.0827	4.2087	10.7401	2.1793	2.8213	3.7265

Test 30				Test 31			
Vx	Ufs	S.ist	Pw	Vx	Ufs	S.ist	Pw
50.4	25	31	40	75	34	12	30
50.4	28	26	40	73.2	12	13	30
49.8	23	26	40	74.4	35	18	30
51.6	28	29	40	70.8	15	13	30
52.2	24	23	40	73.8	32	24	30
52.8	26	26	40	72.6	17	17	30
54	27	27	40	75.6	31	31	30
54.6	23	24	40	72.6	20	25	30
54	27	27	40	73.2	17	28	30
54.6	22	24	40	73.2	18	20	30
54	24	23	40	72	12	29	30
54	25	26	40	74.4	19	14	30
55.2	25	24	40	74.4	15	24	30
55.8	24	24	40	76.8	21	15	30
55.8	26	25	40	75	15	16	30
57	23	24	40	76.2	16	16	30
56.4	24	23	40	73.8	17	19	30
55.8	25	25	40	74.4	14	15	30
56.4	25	24	40	75	25	23	30
56.4	22	23	40	75	13	15	30
56.4	24	25	40	77.4	31	34	30
57.6	24	23	40	72.6	31	28	30
58.2	21	22	40	68.4	47	51	30
58.2	25	24	40	62.4	43	50	30
57.6	21	24	40	63	29	30	30
57.6	24	23	40	57.6	30	46	30
57	22	23	40	63.6	45	15	30
57	23	20	40	64.2	24	35	30
57	22	23	40	70.8	40	17	30
57.6	24	23	40	67.2	22	23	30

57	20	20	40	72.6	39	25	30
57	24	23	40	67.2	16	17	30
57.6	22	24	40	68.4	62	55	30
57	23	21	40	64.2	31	31	30
57	23	24	40	65.4	33	48	30
58.8	23	19	40	60.6	18	5	20
59.4	23	19	40	52.2	27	29	20
58.2	21	24	40	45.6	32	36	20
58.8	22	19	40	38.4	24	34	20
58.8	20	22	40	31.8	28	28	20
58.2	23	23	40	24.6	25	27	20
58.2	20	22	40	28.2	31	27	20
59.4	21	23	40	28.8	27	23	20
60	22	24	40	28.2	26	24	20
60.6	22	19	40	29.4	29	28	20
60	18	18	40	30	19	20	20
55.8	15	16	30	30	25	22	20
50.4	15	14	30	29.4	25	28	20
43.8	15	15	30	30.6	26	26	20
38.4	16	15	30	30	28	31	20
33	13	13	30	29.4	20	30	20
31.2	16	16	30	30	27	28	20
30.6	16	15	30	30	28	34	20
31.2	15	14	30	29.4	29	31	20
30.6	18	16	30	30	26	24	20
30.6	15	15	30	30.6	28	28	20
30.6	18	15	30	30.6	31	23	20
30	15	18	30	31.2	27	20	21
29.4	18	16	30	32.4	23	16	21
29.4	17	18	30	33	32	18	21
29.4	18	18	30	33.6	26	21	22
29.4	17	16	30	34.2	26	22	22
29.4	18	16	30	36	22	23	23
28.8	17	19	30	36	19	27	23
28.8	16	16	30	37.8	21	31	23
28.2	17	17	30	40.2	16	24	24
28.2	17	18	30	41.4	18	26	24
28.2	18	17	30	42	17	34	25
28.8	19	20	31	45	14	21	25
28.8	18	17	31	45.6	17	24	25
29.4	16	18	32	45.6	20	21	25
29.4	21	20	32	48	27	19	26
30	18	17	32	50.4	35	18	26
30	20	18	33	50.4	27	18	26
30.6	18	20	33	52.2	34	17	26
30.6	20	20	34	54.6	33	23	27
31.2	19	21	34	55.2	35	29	27
33	21	21	34	55.8	33	26	27
34.2	21	21	35	58.2	31	28	27
35.4	20	19	35	60.6	25	25	28
37.2	20	23	35	61.8	24	30	28

38.4	20	20	36	63	22	33	28
38.4	23	22	36	64.8	21	30	28
39.6	19	22	36	65.4	21	27	28
40.2	23	19	36	66.6	22	20	29
40.2	20	22	37	67.2	18	17	29
42	25	24	37	67.8	17	15	29
43.2	22	19	37	69	17	15	29
43.8	24	24	37	69.6	16	15	29
43.8	22	23	37	68.4	21	17	29
45.6	25	23	38	72.6	25	25	30
45.6	21	24	38				
46.2	25	25	38				
46.2	22	20	38				
47.4	21	24	38				
47.4	22	21	39				
48	21	21	39				
49.2	28	22	39				
50.4	22	23	39				
51.6	24	21	39				
51.6	21	26	40				
52.8	25	22	40				
53.4	22	23	40				
54	25	24	40				
54	19	19	40				
55.2	24	22	40				
54.6	24	25	40				
54	22	19	40				
55.2	25	27	40				
69	45	54	40				

Test	Test 30				Test 31			
Name	Vx	Ufs	S.ist	Pw	Vx	Ufs	S.ist	Pw
Nb data	110	110	110	110	91	91	91	91
Mean	46.6036	21.5000	21.5091	36.7727	54.6132	25.2967	24.7582	26.0440
Stdeviation	11.4773	4.0473	4.7502	4.0899	17.6608	8.4846	8.7956	4.2056

Test 32			
Vx	Ufs	S.ist	Pw
46.8	27	28	40
46.8	27	29	40
47.4	24	26	40
48	26	24	40
48.6	25	25	40
48.6	26	26	40
49.8	26	25	40
49.8	25	26	40
49.2	25	25	40
49.8	25	24	40
51	25	22	40

51	25	25	40
50.4	23	25	40
51.6	24	24	40
51.6	23	24	40
51	23	24	40
51	24	24	40
51.6	25	24	40
51.6	25	24	40
51.6	22	23	40
52.2	25	22	40
52.2	22	22	40
52.2	23	23	40
52.2	24	24	40
52.2	25	22	40
51.6	22	25	40
52.8	22	22	40
53.4	22	21	40
52.8	24	23	40
52.8	22	23	40
54	22	22	40
52.2	23	22	40
52.8	22	21	40
53.4	21	20	40
54	24	23	40
54	22	22	40
54.6	20	21	40
54	22	22	40
54.6	23	22	40
54.6	21	21	40
54	20	19	40
55.2	21	22	40
55.2	21	23	40
54	19	23	40
54	21	20	40
54.6	25	22	40
54	19	20	40
53.4	21	22	40
54	23	23	40
54.6	22	23	40
50.4	9	12	30
45.6	15	13	30
40.8	14	12	30
35.4	14	15	30
30	15	16	30
28.2	14	15	30
27.6	16	16	30
28.2	16	15	30
28.2	15	17	30
27.6	17	17	30
27.6	17	18	30
27.6	15	16	30

27	16	14	30
26.4	16	16	30
26.4	17	17	30
25.8	16	17	30
25.8	17	19	30
25.8	16	16	30
25.8	17	17	30
25.2	17	15	30
25.8	17	17	30
24.6	15	17	30
24.6	18	19	31
25.2	18	18	31
25.8	19	18	32
25.2	18	18	32
26.4	16	18	32
27	18	18	33
27	21	20	33
27.6	19	22	34
29.4	20	20	34
30	21	21	34
30.6	21	22	35
31.8	20	21	35
33	22	21	35
33.6	21	20	36
34.8	21	21	36
35.4	22	22	36
36	21	22	36
36.6	21	24	37
37.2	22	21	37
38.4	23	22	37
38.4	21	22	37
39	20	21	37
39.6	23	24	38
40.2	23	23	38
40.2	22	22	38
40.8	21	19	38
41.4	23	21	38
42	24	23	39
43.2	21	26	39
43.8	23	24	39
45	23	22	39
45.6	23	21	39
45	22	23	40
45	24	22	40
45	24	26	40
45.6	21	23	40
45.6	23	22	40
47.4	22	20	40
47.4	21	21	40
48	24	26	40
48.6	23	23	40

	49.2	22	24	40
	49.2	20	21	40
	49.2	23	21	40
	50.4	23	23	40
	50.4	22	25	40
	51	23	24	40
Test	Test 32			
Name	Vx	Ufs	S.ist	Pw
Nb data	119	119	119	119
mean	42.7765	21.0504	21.2101	37.0168
Stdeviation	10.5188	3.3493	3.3341	4.0232

APPENDIX F

Publications

Journal

Rees. A, Dimov, S.S, Ivanov. A, Herrero. A, Uriarte. L.G, (2007), "Micro-EDM: Factors affecting the quality of electrodes dressed on the machine". Proceedings of IMechE, Part B, Volume 221, Number 3, pp 409-418.

Rees. A, Dimov. S.S, Minev. R, Lalev. G, Rosochowski.A, Olejnik. L, The effect of material grain structure on the surface integrity of components processed by μ WEDM. Proceedings of IMechE, Part B, Volume 255 (In Press)

Rees. A, Brousseau. E, Dimov. S.S, Bigot. S, Development of surface roughness optimisation and prediction for the process of wire electro discharge grinding. Proceedings of IMechE, Part B (Accepted)

Conference

Rees, A., Dimov, S.S., Ivanov, A., Herrero A., and Uriarte L.G., (2006), "Micro EDM: Accuracy of on-the-machine dressed electrodes". Proceedings of International Conference 4M2006, Elsevier (Oxford).

Pham, D.T., Dimov, S.S. Brousseau, E.B., Bigot, S., Dobrev, T., Ferri, C., Gandarias, E., Hoyle, R.T., Griffiths, C.A., Kettle, J., Lalev, G.M., Li, W. Matthews, C.W., Minev, R.M., Petkov, P.V., Packianather, M.S., Petrelli, A., Popov, K., Rees, A., Sha, B., Thomas, A., and Zhao, H., (2007), "Recent advances in micro and nano manufacturing". Keynote paper, Proceedings of DET2007, 4th International Conference on Digital Enterprise Technology, Bath, United Kingdom, 19th-21st September.

Rees. A, Brousseau. E, Dimov. S.S, Gruber. H, Paganetti. L, *Wire electro discharge grinding: surface finish optimisation*, in *4th International Conference on Multi-Material Micro Manufacturing*. 2008: Cardiff, UK, p. 233-236

Rees, A., Dimov, S.S., Minev, R., Lalev, G., Rosochowski, A., Olejnik, L. The effects of surface integrity of components processed through Micro WEDM, in *4M/ICOMM International Conference on Multi-Material Micro Manufacturing/Micro-manufacture*. 2009: Karlsruhe, Germany.

REFERENCE

- Abbas N.M., Solomon D.G., Bahari Md.F. (2007). **A review on current research trends in electrical discharge machining (EDM)**. International Journal of Machine Tools and Manufacture, Volume 47, Issues 7-8, pages 1214-1228.
- Asad A.B.M.A., Masaki T., Rahman M., Lim H.S., Wong Y.S. (2007). **Tool-based micro-machining**. Journal of Materials Processing Technology, Volumes 192-193, pages 204-211.
- Allen D.M., Almond H.J.A., Bhogal J.S., Green A.E., Logan P.M., Huang X.X. (1999). **Typical Metrology of Micro-Hole Arrays Made in Stainless Steel Foils by Two-Stage Micro-EDM** CIRP Annals - Manufacturing Technology, Volume 48, Issue 1, pages 127-130.
- Amer M.S., Dosser L., LeClair S., Maguire J.F. (2002). **Induced stresses and structural changes in silicon wafers as a result of laser micro-machining**. Applied Surface Science, Volume 187, Issues 3-4, pages 291-296.
- ANSI, American National Standard on Surface Integrity (1986) Society of Manufacturing Engineers (SME), ANSI B2111.
- Aspinwall D.K., Soo S.L., Berrisford A.E., Walder G. (2008). **Workpiece surface roughness and integrity after WEDM of Ti-6Al-4V and Inconel 718 using minimum damage generator technology**. CIRP Annals – Manufacturing Technology, 57(1): pages 187-190.
- Brecher C., Rosen C.J., Emonts M. (2010). **Laser-assisted milling of advanced materials**. Physics Procedia, Volume 5, Part 2, pages 259-272.
- Bigot S., Ivanov A., Popov K. (2005). **A study of the micro EDM electrode wear**. Proceedings of First International Conference on Multi-Material Micro Manufacture, pages 355 – 358.
- Bissacco. G., Valentincic. J., Hansen. H.N., Wiwe. B.D. (2010). **Towards the effective tool wear control in micro-EDM milling**. Journal of Advanced Manufacturing Technology, vol. 47, n 1-4, pages 3 – 9.
- Campanelli S.L., Ludovico A.D., Bonserio C., Cavalluzzi P., Cinquepalmi M. (2007). **Experimental analysis of the laser milling process parameters**. Journal of Materials Processing Technology, Volume 191, Issues 1-3, pages 220-223.
- Cusanelli G., Hessler-Wyser A., Bobard F., Demellayer R., Perez R., Flukiger R. (2004). **Microstructure at submicron scale of the white layer produced by EDM technique**. Journal of Materials Processing Technology, 149(1-3), pages 289-295.
- Dimov S. (2005). **4M Network of excellence: An Instrument for Integration of European research in Multi-Material Micro Manufacture IN UK**, Proceedings of

First International Conference on Multi-Material Micro Manufacture, pages xi-xv.

Dimov S. S., Matthews C. W., Glandfield A., Dorrington P, (2006). **A roadmapping study in Multi-Material Micro Manufacture**. Proceedings of the 2nd International Conference on Multi-Material Micro Manufacture, pages xi-xxv.

Dimov S., Pham D. T., Ivanov A., Popov K., Fansen K. (2004). **Micro-Milling Strategies: Optimisation Issues**, Journal of Engineering Manufacture, Proceedings Part B, Vol 218, NoB7, pages 731-736.

Dobrev T., Pham D. T. Dimov S. S. (2005). **A simulation model for crater formation in Laser milling**. Proceedings of First International Conference on Multi-Material Micro Manufacture, pages 155-159.

Ehmann K.F. (2007). **A Synopsis of U.S. Micro-Manufacturing Research and Development Activities and Trends**. Proceedings of the 3rd International Conference on Multi-material Micro Manufacture, pages 7-13.

Eloy J.C. (2008). **Europe is Maintaining its Leadership in MEMS**, in *International magazine on smart systems technologies*, pages 14-15.

Field M, Kahles JF (1964) **The Surface Integrity of Machined and Ground High Strength Steels**. DMIC Report 210, pages 54–77.

Field M, Kahles JF (1971) **Review of Surface Integrity of Machined Components**. CIRP Annals – Manufacturing Technology, Volume 20, Issue 2, pages 153–163.

Field M, Kahles JF, Cammett JT (1972) **A Review of Measuring Methods for Surface Integrity**. CIRP Annals – Manufacturing Technology, Volume 21, Issue 2, pages 219–238.

Gandarias E., Dimov S., Pham D., Ivanov A., Popov K., Lizarralde R., Arrazola P. (2006). **New Methods for Tool Failure Detection in Micromilling**. Proceedings of the Institution of Mechanical Engineers, Part B: Journal of Engineering Manufacture, 220, pages 137-144.

Gower M. (2000). **Industrial applications of laser micromachining**. Optics Express, 7, pages 56-67.

Guirau E.B. (1997). **The EDM Handbook**, chapter 8, page 103.

Haddad M.J., Fadaei Tehrani A. (2008). **Material removal rate (MRR) study in the cylindrical wire electrical discharge turning (CWEDT) process**. Journal of Materials Processing Technology, Volume 199, Issues 1-3, pages 369-378.

Han F., Wachi S., Kunieda M. (2004). **Improvement of machining characteristics of micro-EDM using transistor type isopulse generator and servo feed system**. Precision Engineering, Volume 28, Issue 4, pages 378-385.

Heeren P. H. Reynaerts D. Van Brussel H. Beuret C. Larsen O. Bertholds A. (1997).

Microstructuring of silicon by electro-discharge machining (EDM), Sensors and Actuators A 61, pages 379-386.

Higgins R.A. (1994). **Properties of Engineering Materials, Second Edition,** Edward Arnold

Ho K.H., Newman S. T., Rahimifard S., Allen R. D. (2004). **State of the art in wire electrical discharge machining (WEDM).** International Journal of Machine Tools and Manufacture, 44(12-13), pages 1247-1259.

Ho K.H., Newman S.T. (2003). **State of the art electrical discharge machining.** International Journal of Machine Tools & Manufacture 43, pages 1287 – 1300.

Huang S.H., Huang F.Y., Yan B.H. (2004). **Fracture strength analysis of micro WC-shaft manufactured by micro-electro-discharge machining,** Journal of Advanced Manufacturing Technology, vol. 26, n 1-2, pages 68 – 77.

Jahan M.P., Wong Y.S., Rahman M. (2009). **A study on the quality micro-hole machining of tungsten carbide by micro-EDM process using transistor and RC-type pulse generator.** Journal of Materials Processing Technology, Volume 209, Issues 4, pages 1706-1716.

Janmanee P., Muttamara A. (2010). **Performance of Difference Electrode Materials in Electrical Discharge Machining of Tungsten Carbide** Energy Research Journal 1 (2), pages 87-90.

Jawahir IS, et al. **Surface integrity in material removal processes: Recent advances.** CIRP Annals - Manufacturing Technology (2011), doi:10.1016/j.cirp.2011.05.002

Juhr H., Schulze H.P., Wollenberg G., Künanz K. (2004). **Improved cemented carbide properties after wire-EDM by pulse shaping.** Journal of Materials Processing Technology, 149(1-3), pages 178-183.

Karnakis D., Rutterford G., Knowles M., Dobrev T., Petkov P., Dimov S. (2006). **High quality laser milling of ceramics, dielectrics and metals using nanosecond and picosecond lasers.** SPIE Photonics West LASE 2006, Volume 6106, San Jose CA, USA, pages 610604.1-610604.11.

Kawakami T., Kunieda M. (2005). **Study on Factors Determining Limits of Minimum Machinable Size in Micro EDM.** Annals of the CIRP 54 (1), pages 167 – 170.

Knowles M., Rutterford G., Karnakis D., Ferguson A. (2007). **Micro-machining of metals, ceramics and polymers using nanosecond lasers.** The International Journal of Advanced Manufacturing Technology, 33, pages 95-102.

Knowles M.R.H., Rutterford G., Karnakis D., Dobrev T., Petkov P., Dimov S. (2006). **Laser micro-milling of ceramics, dielectrics and metals using nanosecond and**

pico-second lasers. Proceedings of the 2nd International Conference on Multi-Material Micro Manufacture, pages 131-134.

Kruth J.P. (1980). **EDM machines and generators.** Proc. Seminar Teknik Pembuatan Cetakan dan Electro-Discharge Machining, Bandung.

Kumar S., Singh R., Singht T.P., Sethi B.L. (2009). **Comparison of material transfer in electrical discharge machining of AISI H13 die steel.** Proceedings of the Institution of Mechanical Engineers, Part C: Journal of Mechanical Engineering Science, **223**(7), pages 1733-1740.

Kunieda M., Lauwers B., Rajurkar K.P., Schumacher B.M. (2005). **Advancing EDM through fundamental insight into the process.** CIRP Annals - Manufacturing Technology, **54**(2), pages 599-622.

Lalev G., Dimov S., Kettle J., Van Delft F., Minev R. (2008). **Data preparation for FIB machining of complex 3D structures.** Proc. IMechE, Part B, Vol 222 (1), pages 67-76.

Lee H.G., Simao J., Aspinwall D.K., Dewes R.C., Voice W. (2004). **Electrical discharge surface alloying.** Journal of Materials Processing Technology, **149**(1-3), pages 334-340.

Lim H.S., Wong Y.S., Rahman M., Edwin Lee M.K. (2003). **A study on the machining of high-aspect ratio micro-structures using micro-EDM.** Journal of Materials Processing Technology 140, pages 318 – 325.

Lim H.S., Wong Y.S., Rehman M., Edwin Lee M.K. (2003). **A study on the machining of high-aspect ratio micro-structures using micro-EDM.** Journals of Materials Processing Technology, 140, pages 318-325.

Loeschner H., Stengl G., Buschbeck H., Chalupka A., Lammer G., Platzgummer E., Vonach H. (2003). **Large-field particle beam optics for projection and proximity printing and for maskless lithography.** Journal of Microlithography, Microfabrication, and Microsystems 2, pages 34-48.

Madou M. J. (2001). **Fundamentals of microfabrication**, CRC Press.

Mason R.L., Gunt R.F., Hess J.L. (2003). **Statistical Design and Analysis of Experiments.** John Wiley and Sons, Inc., New York

Masuzawa T. (2001). **Micro-EDM**, Proceedings of the 13th International Symposium for Electromachining ISEM XIII (volume 1), pages 3-19.

Masuzawa T., Fujino M., Kobayashi K. (1985). **Wire electro-discharge grinding for micro-machining.** Annals of the CIRP, volume 34(1), pages 431-434.

Masuzawa, T. (2000). **State of the art of micro machining.** Annals of the CIRP, 49(2) pages 473-488.

- Masuzawa, T., Yamaguchi M., Fujino M. (2005). **Surface finishing of micropins produced by WEDG**. CIRP Annals - Manufacturing Technology, **54**(1), pages 171-174.
- Matoorian P., Sulaiman S., Ahmad M. (2008). **An experimental study for optimization of electrical discharge turning (EDT) process**. Journal of Materials Processing Technology, Volume 204, Issues 1-3, pages 350-356.
- Matthews C., Dimov S. (2008). **Achieving Micro-manufacturing, in International magazine on smart systems technologies**, pages 11-13.
- May J., Hoppel W.H., Goken M. (2005). **Strain rate sensitivity of ultrafine-grained aluminium processed by severe plastic deformation**. Scripta Materialia, **53**(2), pages 189-194.
- Meeusen W. (2003). **Micro-Electro-Discharge: Technology, computer-aided design & manufacturing and applications**. PhD thesis, Department of Mechanical Engineering Leuven.
- Meijer J., Du K., Gillner A., Hoffmann D., Kovalenko V.S., Masuzawa T., Ostendorf A., Poprawe R., Schulz W. (2002). **Laser machining by short and ultrashort pulses, state of the art and new opportunities in the age of the photons**, Annals of CIRP, **51**(2), pages 531-550.
- Mian A. J., Driver N., Mativenga P.T. (2009). **Micromachining of coarse-grained multi-phase material**. Proceedings of the Institution of Mechanical Engineers, Part B: Journal of Engineering Manufacture, **223**(4), pages 377-385.
- Mohammadi A, Tehrani A.F., Emanian E., Karimi D. (2008). **Statistical analysis of wire electrical discharge turning on material removal rate**. Journal of Materials Processing Technology, Volume 205, Issues 1-3, pages 283-289.
- Mohri N., Suzuki M., Furuya M., Saito N. (1995). **Electrode wear process in electrical discharge machining**. CIRP Annals - Manufacturing Technology, Volume 44, Issue 1, pages 165-168.
- Mohri N., Takezawa H., Furutani K., Ito Y, Sata T. (2003). **A new process of additive and removal machining by EDM with a thin electrode**. Annals of the CIRP **49** (1), pages 123 – 126.
- Montgomery D.C. (2000). **Design and Analysis of Experiments**. John Wiley & Sons
- Narasimhan J., Yu Z., Rajurkar K.P. (2005). **Tool Wear Compensation and Path Generation in Micro and Macro EDM**. Journal of Manufacturing Processes, Volume 7, Issue 1, pages 75-82.
- Newby G., Venkatachalam S., Liang S.Y. (2007). **Empirical analysis of cutting force constants in micro-end-milling operations**. Journal of Materials Processing

Technology, Volumes 192-193, pages 41-47.

Ochiai Y., Manako S., Fujita J., Nomura E. (1999). **High resolution organic resists for charged particle lithography**. Journal of Vacuum Science & Technology B, 17, pages 933-938.

Osenbruggen C.V., Luimes G., Dijck A.V., Siekman J. (1965). **Micro spark erosion as a technique in micro miniaturisation**. IFAC-IFIP Symposium on microminiaturisation.

Petkov P.V., Dimov S.S., Minev R., Pham D.T. (2008). **Laser Milling: Pulse duration effects on surface integrity**. Proceedings of the Institution of Mechanical Engineers, Part B, 222 (1), pages 35-45.

Pham D. T., Dimov S. S., Petkov P. V., Petkov S. P. (2001). **Rapid manufacturing of ceramic parts**. Proceedings of 17th National Conference on Manufacturing Research, Cardiff University, Cardiff, pages 211-216.

Pham D., Dimov S., Petkov P., Petkov S. (2002). **Laser milling**. Proceedings of the Institution of Mechanical Engineers, Part B: Journal of Engineering Manufacture, 216, pages 657-667.

Pham D.T., Dimov S.S. (1997). **Efficient algorithm for automatic knowledge acquisition**. Pattern Recognition, 30(7), pages 1137-1143.

Pham D.T., Dimov S.S., Bigot S., Ivanov A., Popov K. (2004). **A study of the accuracy of the Micro Electrical Discharge drilling process**, Journal of Materials Processing Technology, v 149, n 1-3, pages 579-584.

Pham D.T., Dimov S.S., Petkov P.V., Dobrev T. (2005). **Laser milling for micro tooling**. 7th International Conference, Lamdamap, pages 138-143.

Piltz S, Uhlmann E. (2006). **Manufacturing of Cylindrical Parts by Electrical Discharge Machining Processes**. Proceedings of the 1st International Conference on Micromanufacturing ICOMM, pages 227 – 233.

Platzgummer E., Biedermann A., Langfischer H., Eder-kapl S., Kuemmel M., Cernusca S., Loeschner H., Lehrer C., Frey L., Lugstein A., Bertagnolli E. (2006). **Simulation of ion beam direct structuring for 3D nanoimprint template fabrication**. Microelectronic Engineering, 83, pages 936-939.

Popov K., Dimov S., Pham D., Ivanov A. (2006a). **Micromilling strategies for machining thin features**. Proceedings of the Institution of Mechanical Engineers, Part C: Journal of Mechanical Engineering Science, 220, pages 1677-1684.

Popov K.B., Dimov S.S., Pham D.T., Minev R., Rosochowski A., Olejnik L. (2006b). **Micromilling: Material microstructure effects**. Proceedings of the Institution of Mechanical Engineers, Part B: Journal of Engineering Manufacture, 220(11), pages 1807-1813.

Popov K.B., Dimov S.S., Pham D.T., Minev R., Rosochowski A., Olejnik L., Richert M. (2006c). **The effects of material micro structure in micro-milling**. Proceedings of the 2nd International Conference on Multi-Material Micro Manufacture, pages 127-130.

Qu, J., A.J. Shih, Scattergood R.O. (2002a). **Development of the cylindrical wire electrical discharge machining process, part 1: Concept, design, and material removal rate**. Journal of Manufacturing Science and Engineering, Transactions of the ASME, **124**(3), pages 702-707.

Qu, J., A.J. Shih, Scattergood R.O. (2002b). **Development of the cylindrical wire electrical discharge machining process, part 2: Surface integrity and roundness**. Journal of Manufacturing Science and Engineering, Transactions of the ASME, **124**(3), pages 708-714.

Rahnama R., Sajjadi M., Park S.S. (2009). **Chatter suppression in micro end milling with process damping**. Journal of Materials Processing Technology, Volume 209, Issue 17, pages 5766-5776.

Rajurkar K. P., Wang W. M. (1997). **Improvement of EDM performance with advanced monitoring and control systems**. Journal of Manufacturing Science and Engineering, Transactions of the ASME, **119**(4), pages 770-775.

Rajurkar K.P., Yu Z.Y. (2000). **Micro-EDM using CAD/CAM**. Annals of the CIRP, volume 49(1), pages 127-130.

Rajurkar K.P., Levy G., Malshe A., Sundaram M.M., McGeough J., Hu X., Resnick R., DeSilva A. (2006). **Micro and Nano Machining by Electro-Physical and Chemical Processes**. CIRP Annals - Manufacturing Technology, **55**(2), pages 643-666.

Ramasawmy H., Blunt L., Rajurkar K.P. (2005). **Investigation of the relationship between the white layer thickness and 3D surface texture parameters in the die sinking EDM process**. Precision Engineering, **29**(4), pages 479-490.

Ratchev S. (2008). MINAM Strategic Research Agenda - **Charting the Future of Micro- and Nanomanufacturing in Europe**, in International magazine on smart systems technologies, pages 9-10.

Rebelo J.C., Dias A.M., Kremer D., Lebrun J. L. (1998). **Influence of EDM pulse energy on the surface integrity of martensitic steels**. Journal of Materials Processing Technology, **84**(1-3), pages 90-96.

Rees A., Brousseau E., Dimov S.S., Gruber H., Paganetti L. (2008). **Wire electro discharge grinding: surface finish optimisation**, Proceedings of the 4th International Conference on Multi-Material Micro Manufacturing, pages 233-236.

Rees A., Dimov S., Ivanov A., Herrero A., Uriarte L. (2007). **Micro-electrode discharge machining: factors affecting the quality of electrodes produced on the machine through the process of wire electro-discharge machining**. Proceedings of the Institution of Mechanical Engineers, Part B: Journal of Engineering Manufacture, 221, pages 409-418.

Ross P.J. (1988). **Taguchi Techniques for Quality Engineering**. McGraw Hill, New York.

Roy R. (1990). **A primer on the Taguchi method**, ed. V.N. Reinhold, New York.

Schaller Th., Bohn L., Mayer J., Schubert K. (1999). **Microstructure grooves with a width of less than 50 μm cut with ground hard metal micro end mills**, Precision Engineering 23, pages 229-235.

Shackelford J.F., Alexander W. (2001). **'CRC Materials Science and Engineering Handbook, Third Edition'**. CRC Press.

Storr M. OEL-HELD GmbH publication.

Taguchi G. (1987) **System of Experimental Design**, 1, 2, ASI, Dearborn, MI

Tao L., Qingfa L., Fuh J.Y.H., Yu P.C., Wu C.C. (2006). **Effects of lower cobalt binder concentration in sintering of tungsten carbide**. Materials Science and Engineering: A volume 430, Issues 1-2, pages 113-119.

Toren M., Zvirin Y., Winograd Y. (1975) **Melting and Evaporation Phenomenon During Electrical Erosion**, Journal of Heat transfer, pages 576-581.

Tsai K.M., Wang P.J. (2001). **Predictions on surface finish in electrical discharge machining based upon neural network models**. International Journal of Machine Tools and Manufacture, 41(10), pages 1385-1403.

Uhlmann E., Plitz S., Doll U. (2005). **Machining of micro/minature dies and moulds by electrical discharge machining – Recent development**. Journal of Materials Processing Technology, Volume 167, Issues 2-3, pages 488-493.

Uhlmann E., Plitz S., Schauer K. (2005). **Micro milling of sintered tungsten-copper composite materials**. Journal of Materials Processing Technology, Volume 167, Issues 2-3, pages 402-407.

Valentincic J., Brissaud D. B., Junkar M. (2006). **EDM process adaptation system in toolmaking industry**, Journal of Materials Processing Technology 172, pages 291–298.

Van Vlack L.H., (1970). **'Material science for engineers'**. Addison-Wesley Publishing Company, Reading, Massachusetts.

Weng F.T., Shyu R.F., Hsu C.H. (2003). **Fabrication of micro-electrodes by multi-EDM grinding process**. Journal of Materials Processing Technology 140, pages 332 – 334.

Weule H., Hüntrup V., Tritschler H. (2001). **Microcutting of steel to meet new requirements in minitiation**, Annals of CIRP, 50 (1), pages 61-64.

Wong Y.S., Rahman M., Lom H.S., Nan H., Ravi N. (2003). **Investigation of micro-EDM material removal characteristics using single RC-pulse discharges**. Journal of Materials Processing Technology, 140(1-3), pages 303-307.

Yamazaki M., Suzuki T., Mori N., Kunieda M. (2004). **EDM of micro-rods by self-drilled holes**. Journal of Materials Processing Technology 149, pages 134 – 138.

Yan M.T., Chien H.T. (2007). **Monitoring and control of the micro wire-EDM process**. International Journal of Machine Tools and Manufacture, 47(1), pages 148-157.

Yeo S.H., W. Kurnia W., Tan P.C. (2008). **Critical assessment and numerical comparison of electro-thermal models in EDM**. Journal of Materials Processing Technology, 203(1-3), pages 241-251.

Yu Z.Y., Masuzawa T., Fujino M. (1998a). **Micro-EDM for three-dimensional cavities - development of uniform wear method**. Annals of the CIRP, 47/1, pages 169 – 172.

Yu Z.Y., Masuzawa T., Fujino M. (1998b). **3D Micro-EDM with simple shape electrode**, International Journal of Electrical Machining, 3, pages 7-12.

Yu Z.Y., Kozak J., Rajurkar K.P. (2003). **Modelling and Simulation of Micro EDM Process**, CIRP Annals - Manufacturing Technology, Volume 52, Issue 1, pages 143-146.

